FOR FURTHER TRAN

(21)

12

AD A054728

DEVELOPMENT OF A MULTIMODE LIQUID-CRYSTAL LIGHT VALVE

W.P. Bleha, J.D. Margerum, L.J. Miller, G.D. Myer,
P.G. Rief, D.S. Smythe, F.G. Yamagishi, and J. Grinberg

Hughes Research Laboratories

3011 Malibu Canyon Road

Malibu, CA 90265

May 1978

Prepared for

DEPARTMENT OF THE NAVY

Naval Sea System Command

Washington, DC 20362

D D C
RECEIVED
JUN 8 1978
B

SECURITY CLASSIFICATION OF THIS PAGE *(When Data Entered)*

REPORT DOCUMENTATION PAGE		READ INSTRUCTIONS BEFORE COMPLETING FORM
1. REPORT NUMBER	2. GOVT ACCESSION NO.	3. RECIPIENT'S CATALOG NUMBER
4. TITLE *(and Subtitle)* Development of a Multimode Liquid-Crystal Light Value		5. TYPE OF REPORT & PERIOD COVERED See Supplementery Notes
		6. PERFORMING ORG. REPORT NUMBER
7. AUTHOR(s) W. P. Bleha, J. D. Margerum, L. J. Miller, G. D. Myer, P. G. Rief, D. S. Smythe, F. G. Yamagishi, and J. Grinberg		8. CONTRACT OR GRANT NUMBER(s) ⑮ N00024-76-C-5366
9. PERFORMING ORGANIZATION NAME AND ADDRESS Hughes Research Laboratories 3011 Malibu Canyon Road Malibu CA 90265		10. PROGRAM ELEMENT, PROJECT, TASK AREA & WORK UNIT NUMBERS
11. CONTROLLING OFFICE NAME AND ADDRESS Department of the Navy Naval Sea System Command Washington D.C. 20362		12. REPORT DATE 11 May 1978
		13. NUMBER OF PAGES 103 111 p.
14. MONITORING AGENCY NAME & ADDRESS*(if different from Controlling Office)*		15. SECURITY CLASS. *(of this report)* Unclassified
		15a. DECLASSIFICATION DOWNGRADING SCHEDULE

16. DISTRIBUTION STATEMENT *(of this Report)*

Approved for public release; distribution unlimited.

17. DISTRIBUTION STATEMENT *(of the abstract entered in Block 20, if different from Report)*

18. SUPPLEMENTARY NOTES

Third Progress and Final Reports, Phase I and Interim Report Phase II
1 June 1976 through 31 December 1977

19. KEY WORDS *(Continue on reverse side if necessary and identify by block number)*

Liquid Crystal
Light Valves
Display Systems
Electro-Optic Displays

Color Symbology Displays

20. ABSTRACT *(Continue on reverse side if necessary and identify by block number)*

Three major issues in the development of a multimode liquid-crystal light valve were addressed in this phase of the continuing research;

• Liquid-crystal electro-optical effect,

• Light valve stability and lifetime, and

• Photoconductor performance.

DD FORM 1473 EDITION OF 1 NOV 65 IS OBSOLETE
1 JAN 73

172 600

JCB

We concluded that the lifetime and stability of the tilted perpendicular alignment cannot be sufficiently improved to produce a practical and useful device for a high-brightness, large screen display system. The problem is that the molecular pre-tilt angle is unstable in the presence of a high-brightness projection light. The tilted perpendicular alignment therefore was abandoned in favor of the 45° twisted nematic alignment using the hybrid field effect mode (HFE mode), by HRL. With respect to color symbology and multimode operation; however, the HFE mode was less suitable, and considerable experimentation with the goal of optimization was performed and is reported here.

A phenomenological study was made on liquid-crystal cells operated in the HFE mode. The objectives were to optimize and to determine the range and intensity of colors that can be obtained with an HFE light valve and to acquire a working knowledge of the effect of certain cell parameters (e.g., twist angle, thickness, and the match or mismatch of the polarization plane with front surface alignment). The test cells and light valves were both characterized by measuring the transmission to the screen through blue, green, and red interference filters as a function of the voltage applied to the cell.

The photochemical stability of the liquid crystal (E7 mode by BDH) and the extent to which it may limit the lifetime of the HFE mode light valve were also studied. Test cells were exposed to high-intensity light, and the effects were monitored by periodically determining the transmission versus voltage curves. Cell failure was detected by means of significant changes in these curves and was accompanied by a realignment of the liquid crystal toward a homeotropic orientation. Exposure lifetime increased when shorter wavelengths were filtered out of the incident light. A ketone was identified as one of the photochemical degradation products obviously produced by oxidation of one of the liquid crystal components. We now believe that cell failure results from a photo-induced auto-oxidation of the liquid crystal to form surface-active products that change the alignment of the liquid crystal.

The main goals in the development of the photoconductor technology are to achieve high sensitivity, switching ratio, and linearity. To achieve these goals, we evaluated two approaches:

- A three layer composited film
- A thick (50 μm) CdS layer.

Both approaches produced positive results in some parameters and not in others.

In conclusion, during this phase of the program, stable and long lifetime light valve operation was achieved, and improved color symbology was demonstrated. A promising multimode liquid-crystal effect was invented, and improved photoconductor performance was achieved.

TABLE OF CONTENTS

iii

LIST OF ILLUSTRATIONS

vii

SECTION 1

INTRODUCTION AND SUMMARY

The Hughes Research Laboratories (HRL) is pleased to submit to the Navy this report describing the work done on the follow-on contract N00024-76-C-5366 during the period 1 June 1976 through 31 December 1977. The objective of this technology program is to develop a liquid–crystal light valve (LCLV) for real-time gray scale and color symbology display applications.

In this phase of the continuing research program to develop multimode LCLVs, we attacked three major issues: liquid crystal electro-optical effects, light valve stability and lifetime, and photoconductor performance. We concluded that the lifetime and stability of the tilted perpendicular alignment cannot be sufficiently improved to produce a practical and useful device for a high-brightness, large-screen display system. The problem is that the molecular pretilt angle is unstable in the presence of a high-brightness projection light. We consider lifetime to be the most important parameter of the device. Therefore, even though the tilted perpendicular alignment is very desirable for multimode operation, we had to replace it by 45° twisted nematic alignment and to use the hybrid field-effect mode (HFE mode), invented by HRL. This change produced the required stability (see Section 4) as a result of two factors. First, the positive dielectric anisotropy liquid crystals used in the alignment are basically much more stable than the negative dielectric anisotropy materials used in the perpendicular alignment. Second, the twisted nematic alignment is much less sensitive to the pretilt angle. With respect to color symbology and multimode operation, the HFE mode is less suitable. Therefore, we went back and optimized this effect first for the color symbology display device (see Section 2). A phenomenological study was made on liquid-crystal cells operated in the HFE mode. Our objectives were to optimize and to determine the range and intensity of colors that can

1

be obtained with an HFE light valve and to acquire a working knowledge of the effect of certain cell parameters (e.g., twist angle, thickness, and the match or mismatch of the polarization plane with front surface alignment). The test cells and light valves were both characterized by measuring the transmission to the screen through blue, green, and red interference filters as a function of the voltage applied to the cell.

The transmitted light is considered to consist of a series of orders, with blue, green, and red bands in each order, and with the first-order bands found at the highest voltages. As the twist angle is increased, the transmission bands increase and then decrease in intensity. The twist angle at which the maximum intensity occurs increases on passing from the lower to the higher orders. Studies indicate that thickness has a similar effect as it is increased from 6 to 16 μm. Mismatching the plane of polarization with the nematic director at the front surface also significantly affects the intensities and the positions of the transmission peaks as a function of voltage. A certain amount of mismatch in portions of the light valve is unavoidable because of the splay in alignment that results from ion-beam etching. The mismatch is sufficient to explain the color gradients that are seen on the screen.

A null point, where the transmission is low and the color is fairly neutral, generally exists at some voltage above the threshold and below the strong transmission bands. Above the null point voltage there is a range where the transmitted light intensity is too low to be useful. Following this is the useful region, the end of which is determined by the maximum switching ratio of the light valve substrate. The colors covered by this useful, accessible region vary systematically with changes in thickness and twist.

Three parameters of a twisted nematic aligned cell, working in a reflection mode, have important influence on its color transmission:

- Cell twist angles

- Cell thickness

2

- Angle between the polarization of the read-out light and the liquid crystal optical access on the front electrode.

These parameters can be manipulated to obtain good color separation, high transmission, nice looking colors, and maximum distinguishable colors and to make trade-offs between the different requirements.

We achieved several goals during the present study. We identified some general trends in performance as a function of the parameters, found a twist-angle/thickness combination that greatly improves the performance of the device, and generated a data base that will be used to achieve further improvements. This optimization resulted in the demonstration of three to four distinguishable colors and high-brightness display (as observed on the delivered devices).

We also worked towards multimode operation. This effort led to the invention of back slope multimode operation (described in Section 3). One difficulty in HFE mode operation is the lack of broad-band (white) gray-scale transmission in the low-voltage region. Back slope multimode operation, since it provides this important feature, appears promising for use in the multimode light valve, but further optimization and evaluation are required.

We also studied the photochemical stability of the liquid crystal (E7 from BDH) and the extent to which it may limit the lifetime of the HFE light valve (see Section 4). Test cells were exposed to high-intensity light, and the effects were monitored by periodically determining the transmission versus voltage curves. Cell failure was detected by means of significant changes in these curves and was accompanied by a realignment of the liquid crystal toward a homeotropic orientation. None of the cells were sealed, and oxygen could diffuse into the liquid crystal from the edges. The test cells were compared in terms of their exposure lives, given in $W-hr/cm^2$.

Exposure life increased when the shorter wavelengths were filtered out of the incident light. Increasing the light intensity decreased

3

the exposure life. A ketone was identified as one of the photochemical degradation products; it obviously was produced by oxidation of one of the liquid crystal components. Adding this ketone to the liquid crystal also reduced exposure life. We believe that cell failure results from a photoinduced auto-oxidation of the liquid crystal to form surface-active products that change the alignment of the liquid crystal. The ketone, which was present as a contaminant in E7 as it was obtained, probably acts as a sensitizer for the photochemical reactions. The lifetime of the light valve should be prolonged by carefully purifying the liquid crystal to remove oxidation products such as the ketones, by preventing contact between the liquid crystal and oxygen, and by filtering out the shorter wavelengths of the projection light. The longest exposure life measured corresponded to a lifetime of more than 3000 hr in an operating system with a lamp intensity of 250 mW/cm^2 (GSG system).

The main goals in the development of the photoconductor technology are to achieve improved sensitivity, switching ratio, and linearity. Improved sensitivity simplifies the primary display system and improves cathode ray tube (CRT) resolution, which is presently the limiting factor in system resolution. A higher switching ratio increases the range of colors that can be reached. Better linearity minimizes the outline effect, which is of primary importance for the color symbology system. To achieve these goals, we evaluated two approaches (see Section 5): a three-layer composited film and a thick (50 µm) CdS layer. The composited film exhibited good performance before polishing, but the film degraded significantly after the polish. We were able to overcome most of the problems associated with the thick CdS. The films provide higher switching ratio and good sensitivity, but the response time was somewhat of a compromise. For multimode operations, where both symbols and TV must be displayed simultaneously, a high switching ratio and fast response are required. Also, thick CdS layers have a greater tendency to exhibit the undesired effect of negative memory. Therefore,

additional improvements in the photoconductor area have to be achieved to meet the multimode mode requirements.

In conclusion, during this phase of the program, we achieved stable and long lifetime light valve operation, demonstrated improved color symbology, invented promising multimode liquid crystal mode, and improved CdS photoconductor performance.

SECTION 2

LIQUID–CRYSTAL ELECTRO–OPTICAL STUDIES

The basic concepts of the HFE light valve were described in Ref. 1. One objective of this program was to obtain a phenomenological understanding of the factors controlling the range of colors and light intensities available from this type of display. Factors determining output undoubtedly include the liquid-crystal birefringence, thickness of the liquid-crystal layer, twist in the alignment, tilt in the alignment in the off-state, and angle between the polarization plane of the incident projection light and the liquid crystal director at the front surface of the light valve. Two of these factors were held constant in our studies. We used only the commercial liquid crystal E7, which is a mixture of cyanobiphenyl compounds available from BDH Chemicals, Ltd. Although there may be minor differences in composition from batch to batch, these differences are believed to be too small to have a significant effect on the birefringence. We also used electrodes that were overcoated with SiO_2 and shallow-angle ion-beam etched to control the liquid-crystal alignment.[2] Consequently, the tilt angle was always about 3°, the angle that is induced by this alignment technique. Our studies were therefore limited to the effects of thickness, twist, and the match or mismatch of polarization with front surface alignment.

A.   CHARACTERIZATION OF THE HFE MODE

The apparatus used in evaluating the influence of these parameters is shown in Figure 1. Vertically polarized, collimated light was passed through transparent test cells with the etch direction of the front electrode also oriented vertically. The light was reflected from an aluminum mirror fastened externally to the back of the cell. The reflected light was then passed through an analyzer and an interference filter, where it was detected with a photodiode. The cell was positioned properly by rotating it in the two planes perpendicular to the face of the cell until the light reaching the detector was maximum, with the polarizer and analyzer parallel. Then, with the analyzer crossed and a

Figure 1. Experimental apparatus for characterizing test cells operating in the HFE mode.

8

green interference filter in position, the cell was rotated in the plane parallel to the face until the detector signal was at a minimum. The light transmitted through the green filter and parallel polarizers was taken as the 100% transmission setting. Light intensity was recorded as a function of the voltage applied to the cell for each of three interference filters, with peak wavelengths of 466, 545, and 623 nm. In this way, we obtained curves such as those shown in Figures 2 through 8.

The data in these figures were derived for 0.5-mil cells with twist angles ranging from 11° to 79°. Since minimum retardation (Δnd) of the polarized light occurs at high voltages, the curves are most easily understood by considering them in terms of a series of orders with a blue, a green, and a red peak in each order, beginning from the high voltage side. In the first order, the peaks are broad and only slightly separated, although well separated from the peaks of other orders. The second order (at somewhat lower voltages) has sharper and better separated peaks, still distinct from other orders. In the third and higher orders, however, the orders overlap; thus, the blue peak of the fourth order precedes the red peak of the third (starting from the high-voltage side).

At low twist angles, the intensity of transmitted light is low at all transmission peaks. As the twist angle is increased, the intensities increase and then decrease, with the lower orders passing through the maximum at lower twist angles. This is demonstrated by the curves shown in Figure 9.

The effect of the twist angle on the voltage at which each transmission peak is obtained is not clear from the data. For the series of cells used to obtain the curves in Figures 2 through 8, there was a smooth increase in the voltages as the twist increased above 45°, as shown in Figure 10. However, this trend did not hold for the lower twist angles. Since the measured voltage included the drop in potential across the silica layer used to align the liquid crystal, the variations are probably due largely to impedance differences among the silica layers. This view is supported by the fact that the cells with the three lowest twist angles were assembled with an earlier batch of electrodes.

9
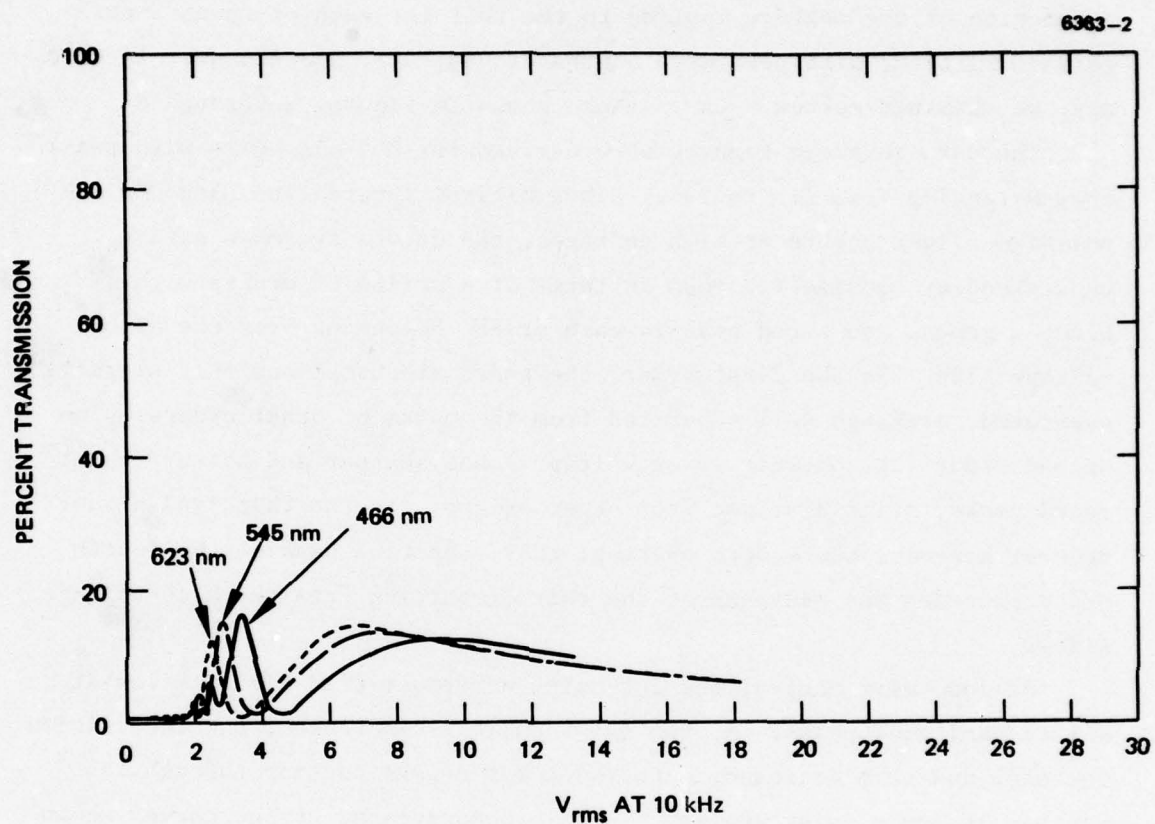
Figure 2. Voltage-transmission curves for a 0.5-mil HFE cell with 11.5° twist.
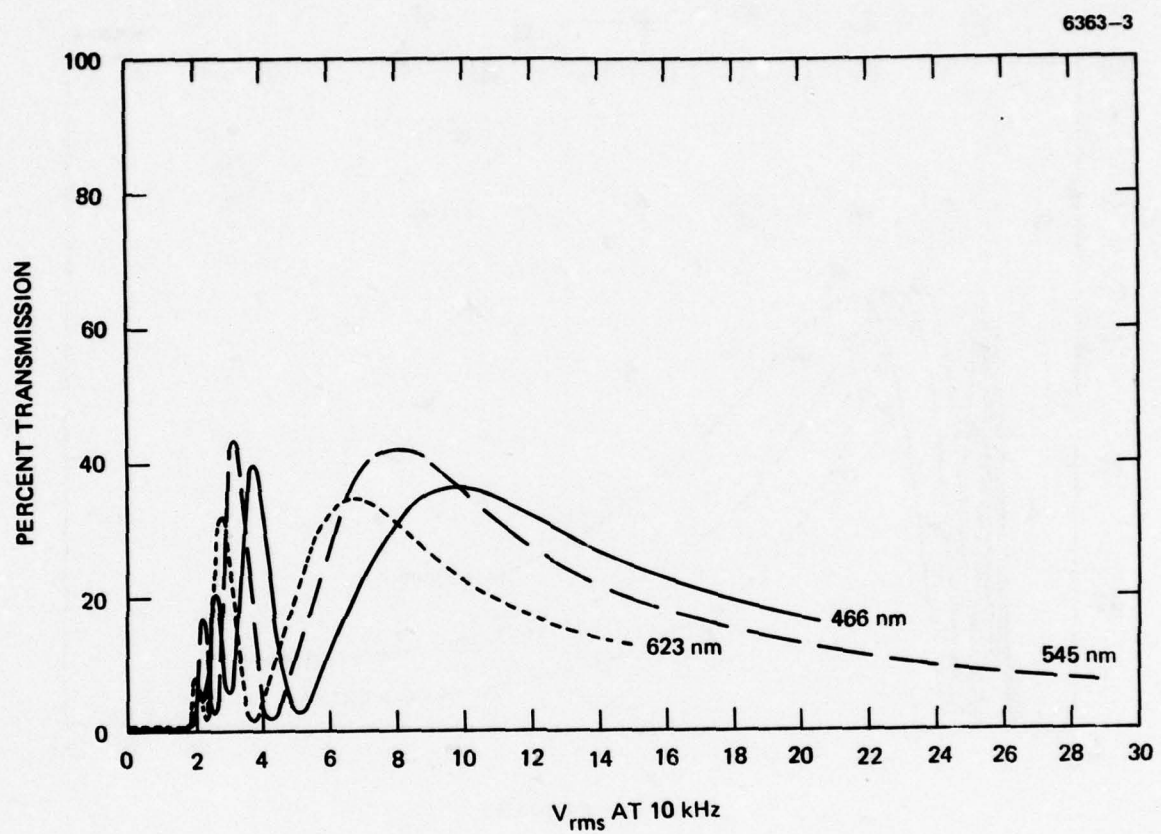
Figure 3. Voltage-transmission curves for a 0.5-mil HFE cell with 20.1° twist.

6363—4
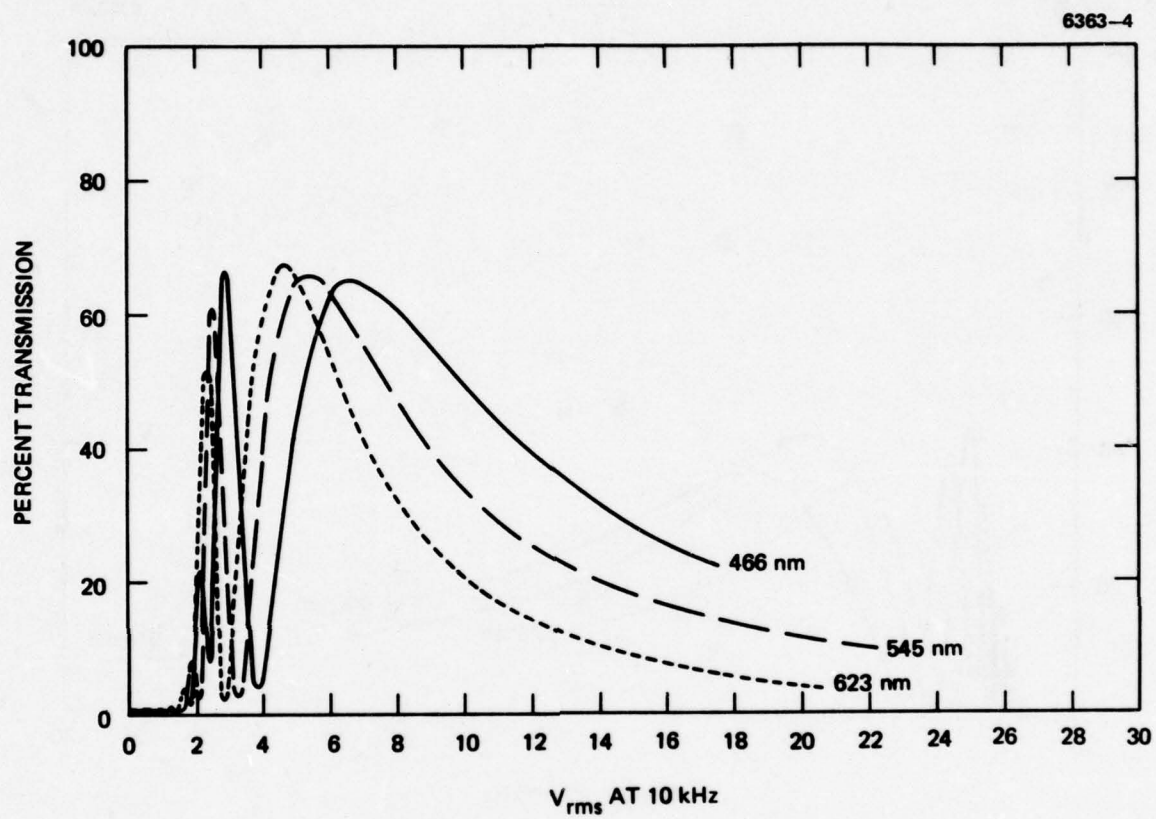
Figure 4. Voltage-transmission curves for a 0.5-mil HFE cell with 27.0° twist.

12

6363-5
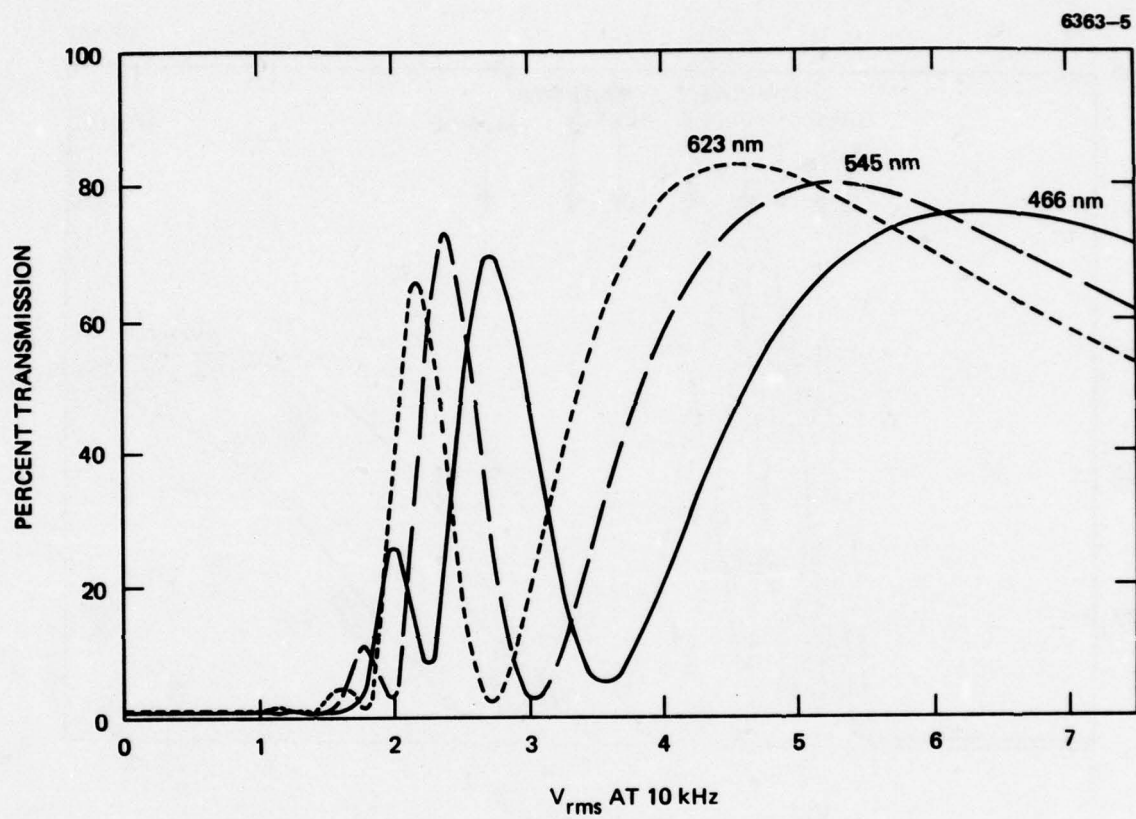
Figure 5. Voltage-transmission curves for a 0.5-mil HFE cell with 45°
twist.

13
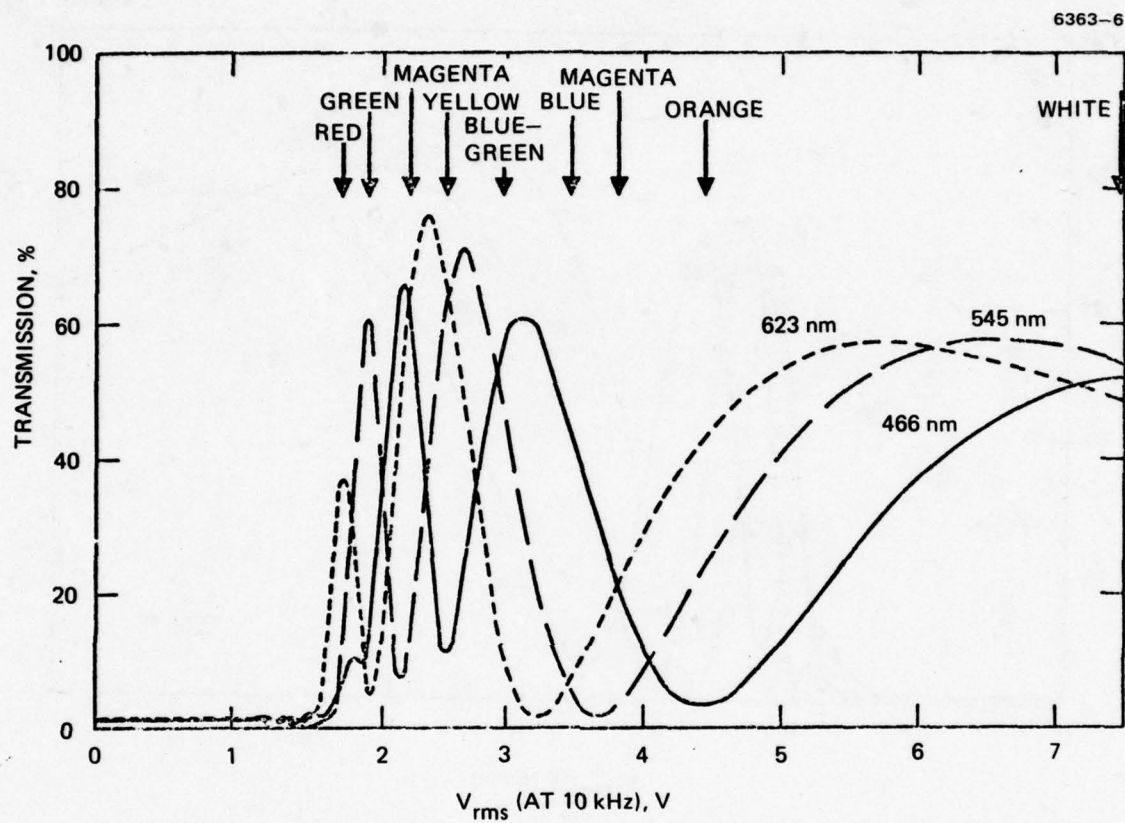
Figure 6.   Voltage-transmission curves for a 0.5-mil HFE cell with 60° twist.

14

6363–7
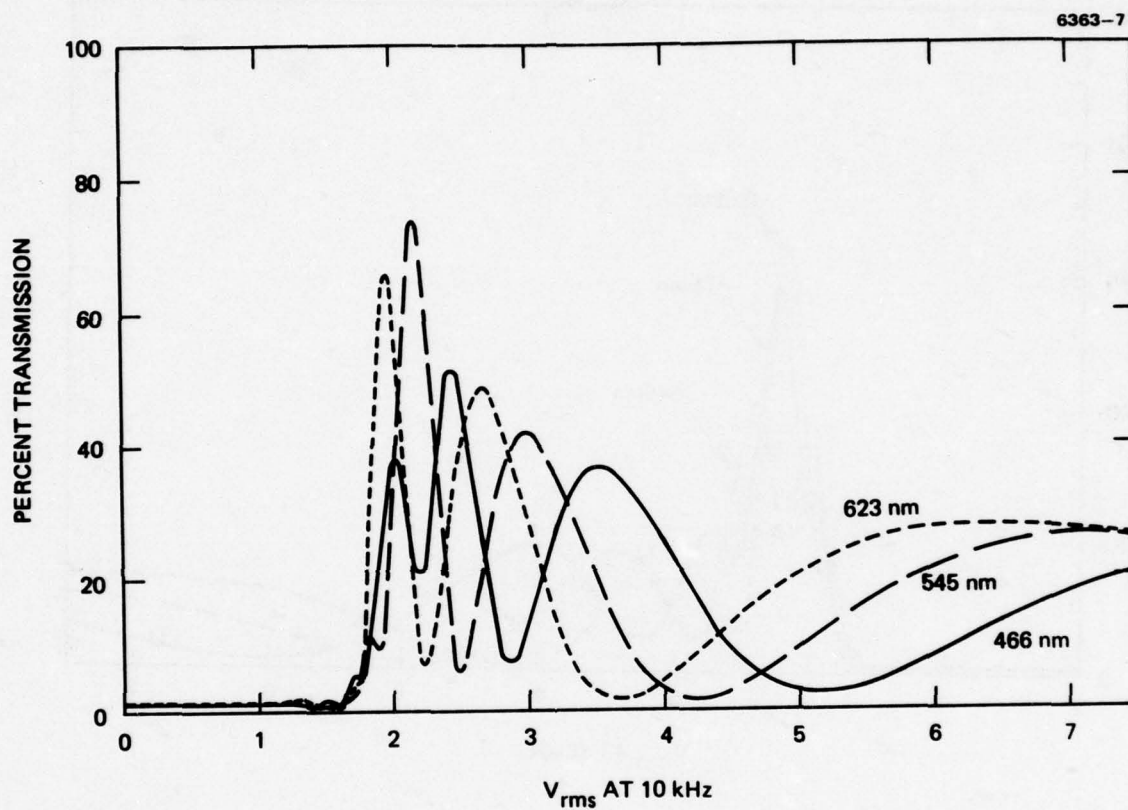
Figure 7. Voltage-transmission curves for a 0.5-mil HFE cell with 73.1°
twist.

15
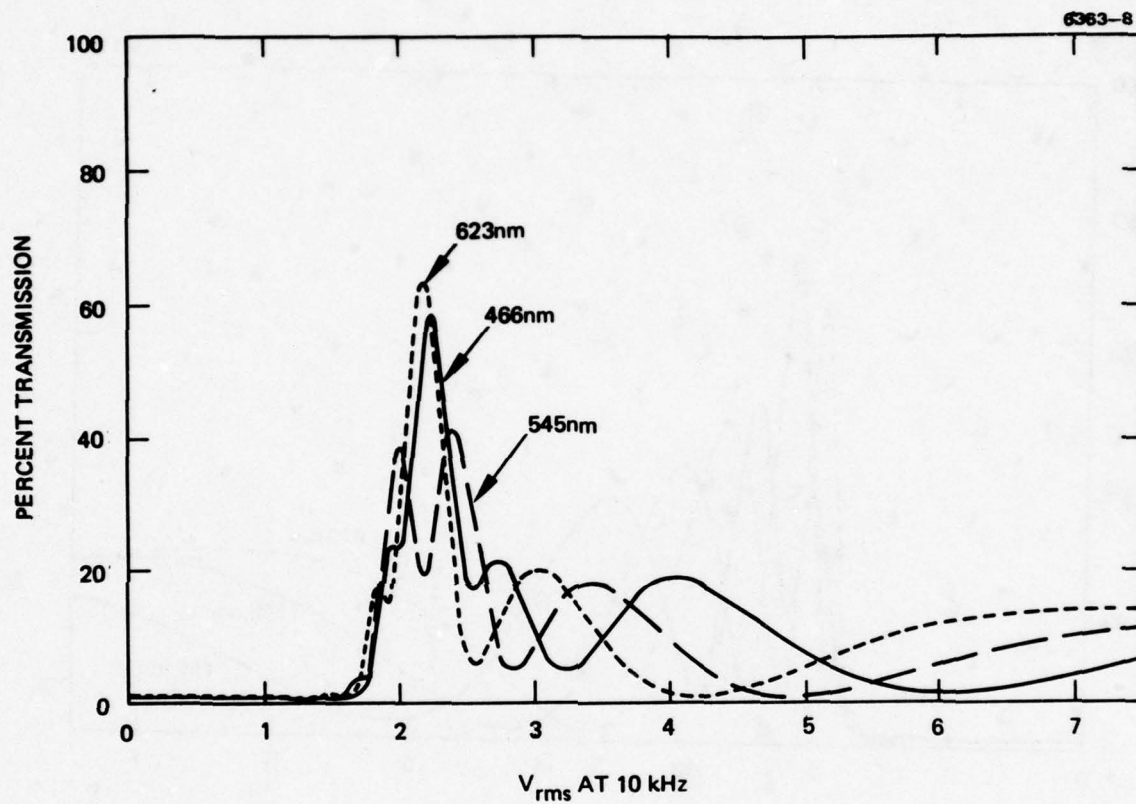
Figure 8. Voltage-transmission curves for a 0.5-mil HFE cell with 79.2° twist.

16
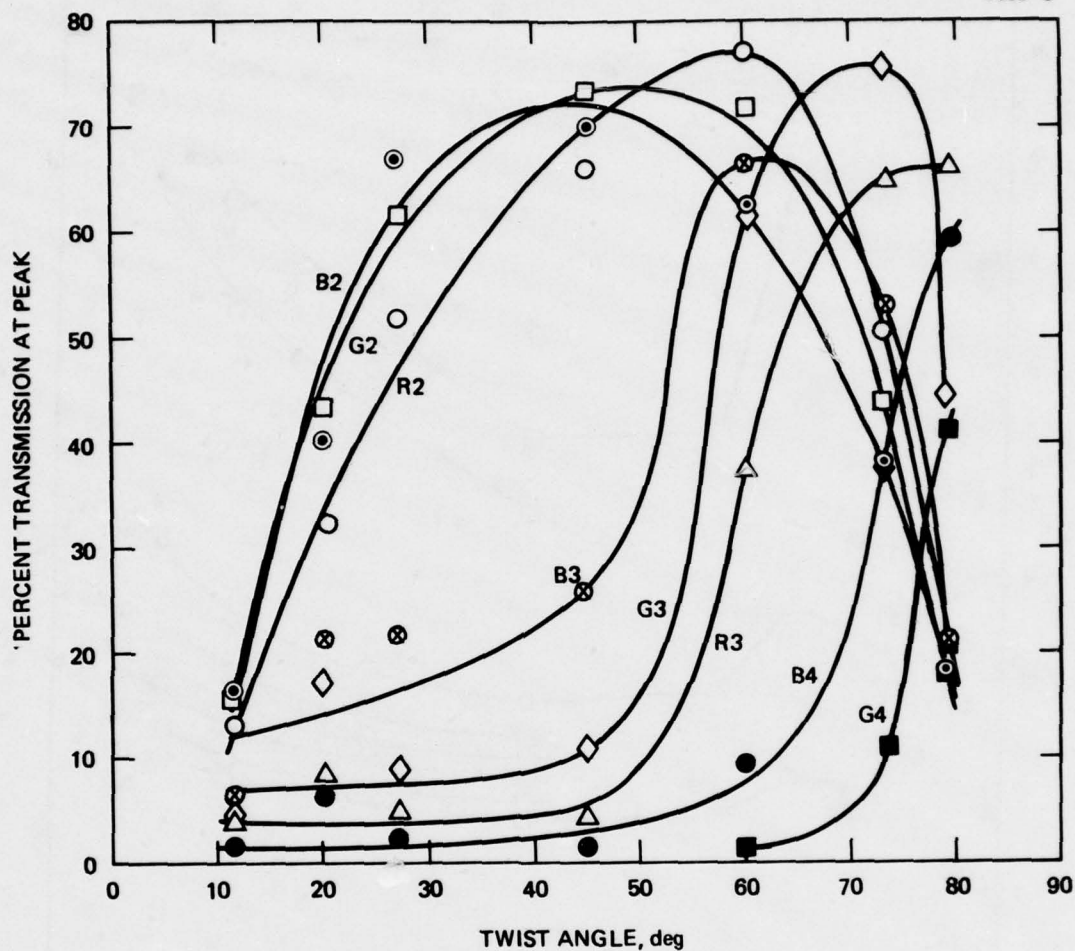
Figure 9. Peak intensity as a function of the twist angle for blue, green, and red transmission peaks of the second, third, and fourth orders in 0.5-mil HFE cells.

17
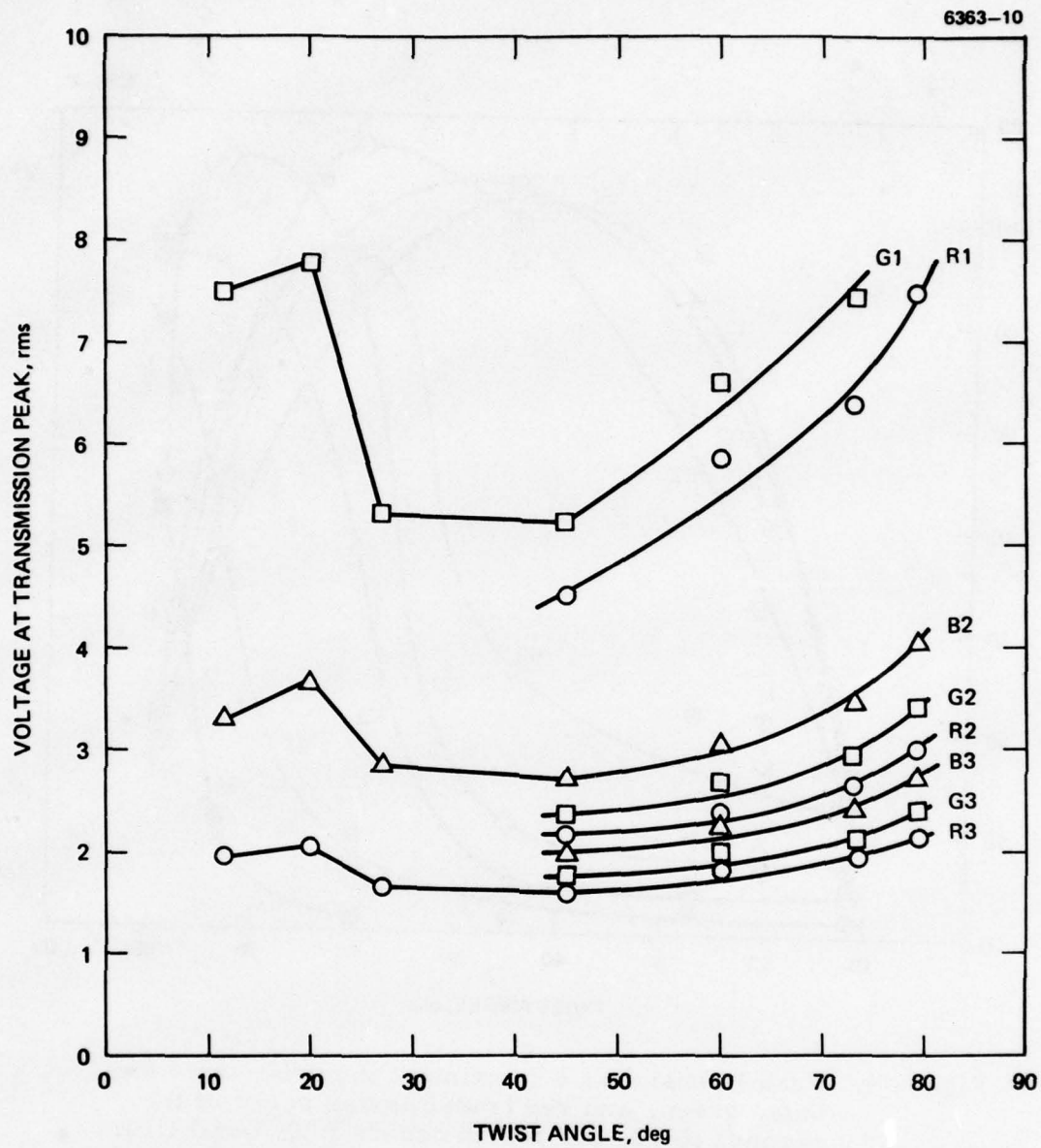
Figure 10. Voltage as a function of the twist angle for the occurrence of blue, green, and red transmission peaks of the first, second, and third orders in 0.5-mil HFE cells.

18

As noted in Ref. 1, there is generally a "null" point at which the transmission is low and almost equal for all wavelenghts. This null lies above the threshold and below the main transmission peaks. In operation, a bias voltage is applied to the cells to drive the liquid crystal to the null in the absence of activating light. Therefore, the performance of the cell is important only at voltages above the null. Furthermore, the product of the null voltage and the maximum switching ratio of a light-valve substrate determines the maximum voltage that can be applied across the liquid-crystal layer. In evaluating the performance of test cells, we assume a switching ratio of two as a practical limit, although there has been considerable variation in this property for experimental light valves.

The actual colors attainable from various cell configurations can be evaluated subjectively by projection onto a screen or by analysis of the voltage transmission curves (such as those in Figures 2 through 8). An alternative method of presenting the data is shown in Figures 11 through 15. These polar coordinate graphs are a type of chromaticity plot (not the standard chromaticity diagram) in which the percentage of transmission through the red, green, and blue interference filters is treated as three vectors separated by 120°. The magnitude of the vector sum is divided by the numerical sum of the light intensities to give an indication of color purity. This is plotted (in percent) as the radius vector and is given as a function of the vector angle in the polar coordinate graph. Key points on the original voltage-transmission curves — such as maxima, minima, and intersection points — are used to make the chromaticity plots. Each point is marked with the voltage and the average percent transmission for the three color-bands at that point. Although these plots appear complex, they offer another way of analyzing the usefulness of the cell in presenting color symbology. To aid in this analysis, the curves are dotted between the null and a point at which the average transmission is approximately 15%; this portion of the curve represents a region where the light intensity is generally not high enough for optimal symbology projection. Beyond the point at which the voltage is approximately two times that of the null, the curve is given

19
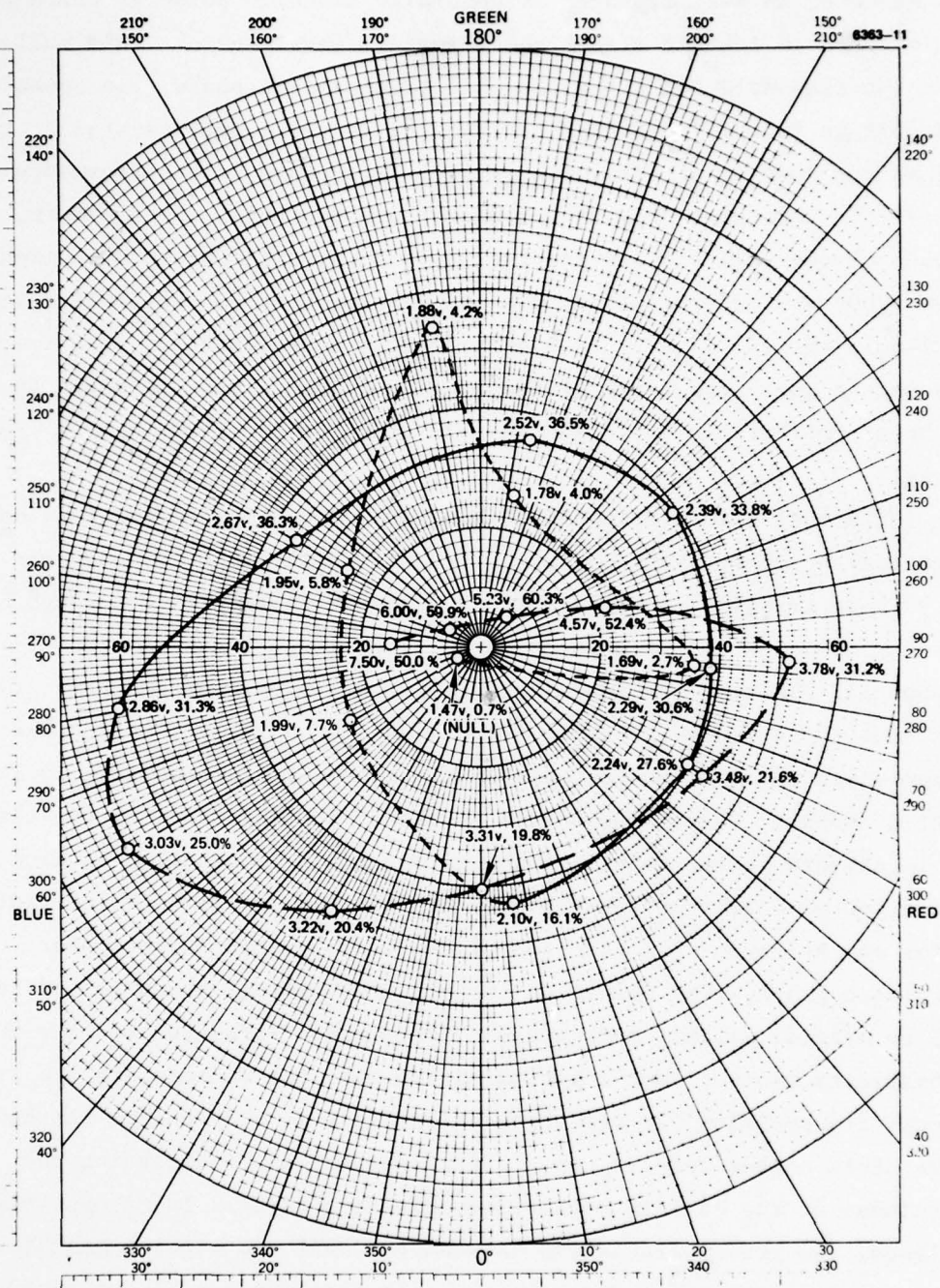
Figure 11. Chromaticity plot for a 0.5-mil HFE cell with 27.0° twist (derived from Figure 4).

20
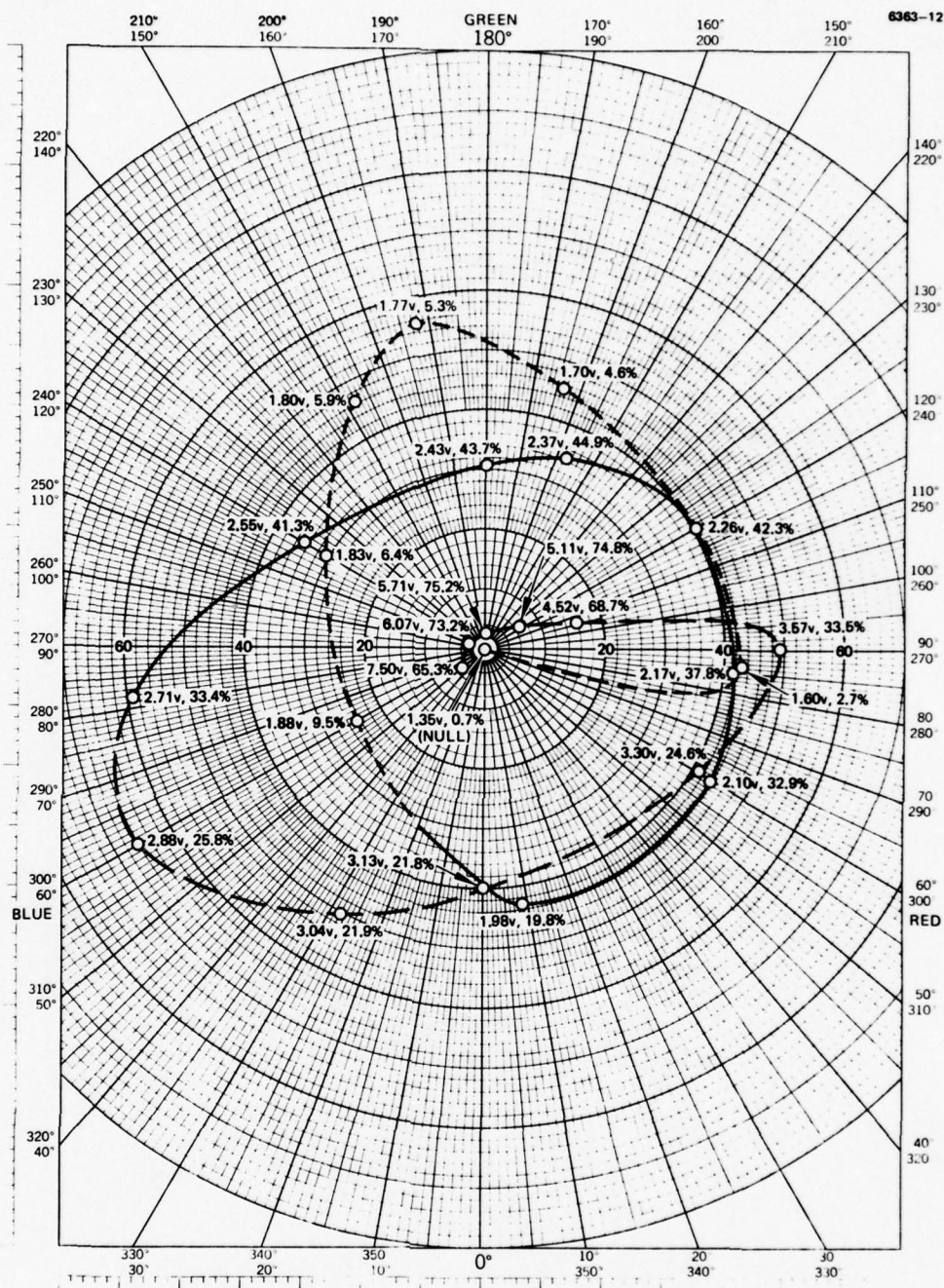
Figure 12.   Chromaticity plot for a 0.5-mil HFE cell with 45° twist (derived from Figure 5).
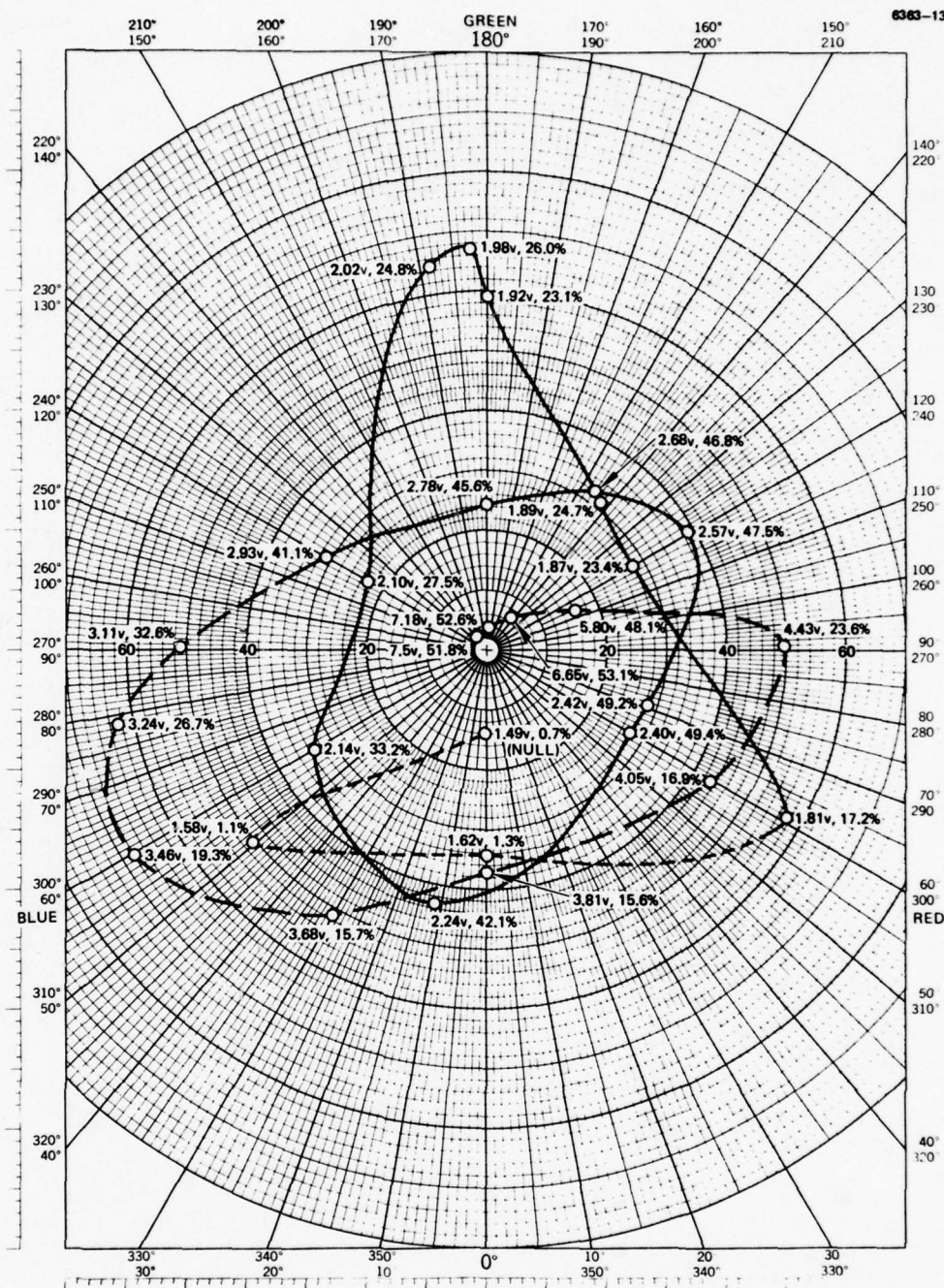
Figure 13. Chromaticity plot for a 0.5-mil HFE cell with 60° twist (derived from Figure 6).

Figure 14. Chromaticity plot for a 0.5-mil HFE cell with 73.1° twist (derived from Figure 7).
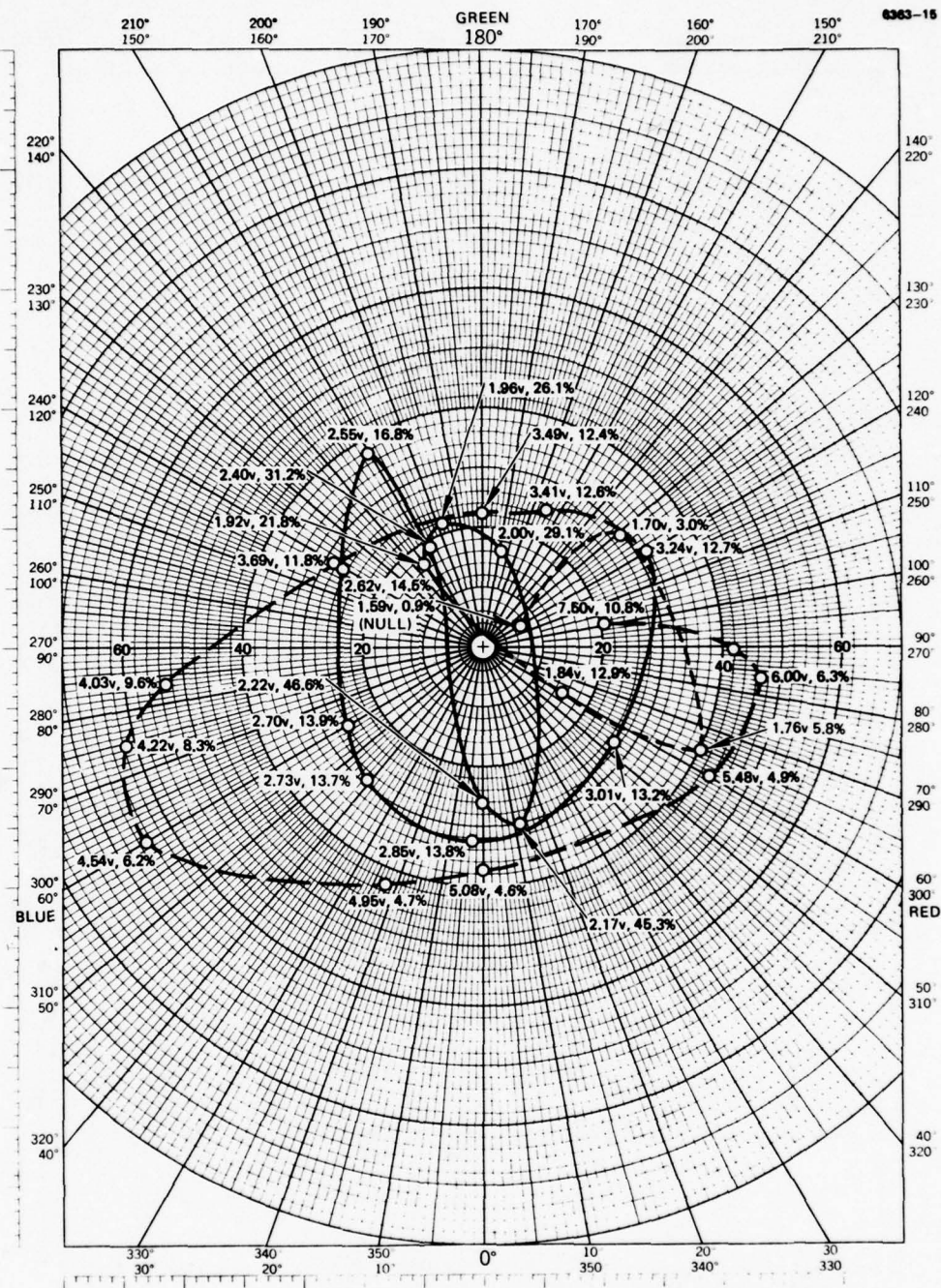
Figure 15. Chromaticity plot for a 0.5-mil HFE cell with 79.2° twist (derived from Figure 8).

24

in dashes; as mentioned above, this portion of the curve probably is not accessible in the ordinary light valve biased to the null point voltage.

Examination of the graphs reveals that although the transmission bands follow a rather predictable pattern, the systematic variation in the relative intensity of these bands causes the colors available for projection display to be substantially different at different twist angles. As a rule of thumb, we suggest that color purities of about 40% are desirable for the primary wavelenghts; intermediate wavelenghts may be acceptable at slightly lower values. Using this as a guide, we conclude that the cells with a 27° twist (Figure 11) and 45° twist (Figure 12) can provide magenta, some red, yellow, and blue-green to blue, but lack a good green. The 60° twist cell (Figure 13) supplies a fairly low intensity red, excellent green, magenta, yellow, and a bluish blue-green and has an excellent blue just slightly beyond the normally accessible range. The 73° twist cell (Figure 14) has a narrow red, good green, magenta, and yellow; a poor blue-green and an excellent blue are well out of range of a two-fold switching ratio. The 79° cell has poor color purity or low intensity at almost all accessible wavelenghts. On balance, it appears that optimum symbology should be obtained with a twist of about 60° for the 0.5-mil cells.

Voltage transmission curves of the type given in Figures 2 through 8 were also obtained for sixteen 0.25-mil HFE cells with twists ranging from 10.3^o to 82.5^o. Again, the percent transmission at each transmission peak was plotted as a function of the twist in alignment. Highly regular plots were obtained for the blue, green, and red peaks of the first order, but there was considerable scatter in the data for the peaks of the second order, and tremendous scatter for the peaks of the third order. This is illustrated in Figures 16 through 18 for the blue peaks of each order. The peaks of the fourth order are all very small, almost imperceptible in some cases. This was distinctly different from the curves for the 0.5-mil cells, in which the fourth-order peaks were quite large at the higher twist angles, and in which even the fifth-order peaks were significant. As noted for the 0.5-mil cells, the intensity at a given transmission peak increased as the twist angle increased, then passed
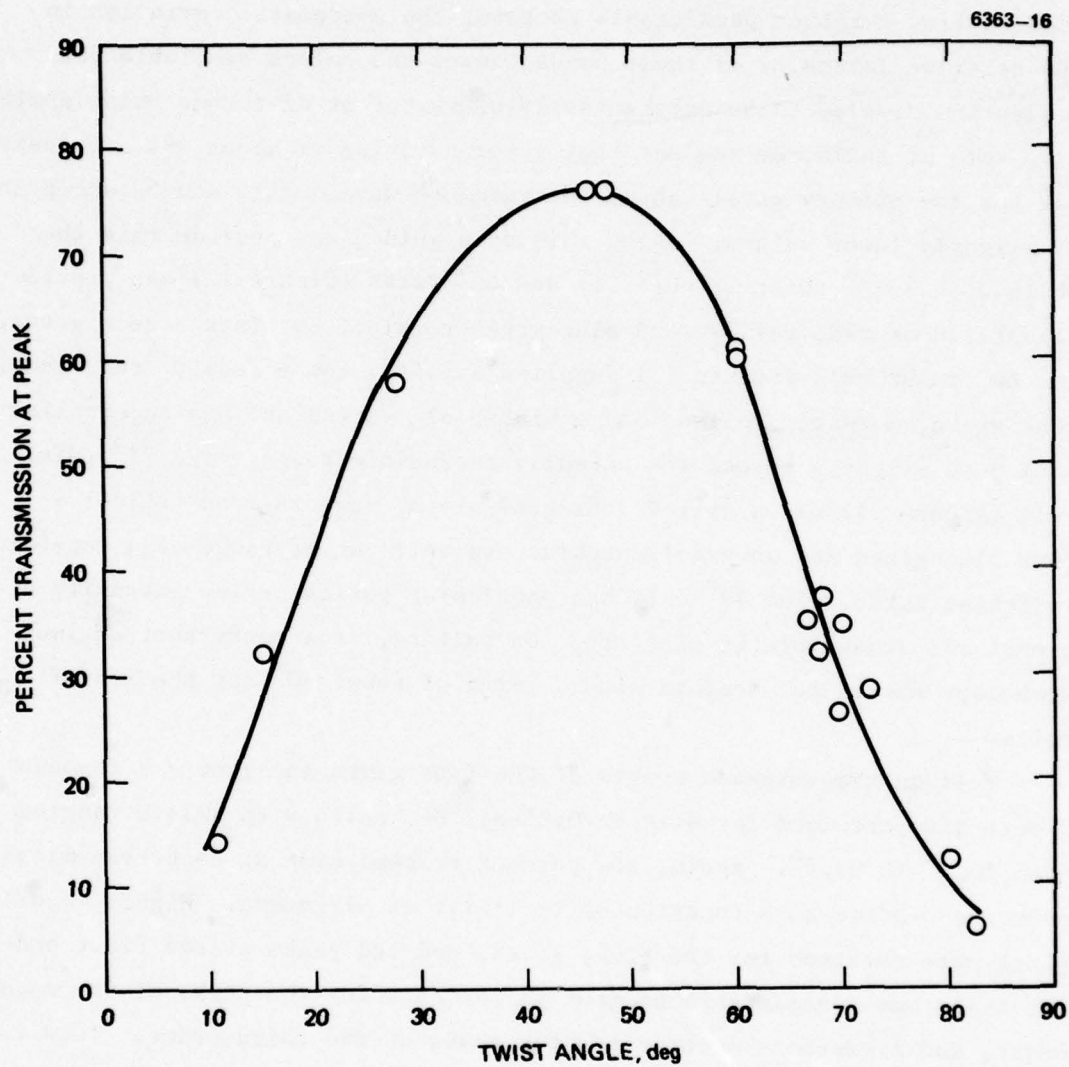
Figure 16. Intensity of the first order blue transmission
peak in 0.25-mil HFE cells as a function of
the twist angle.
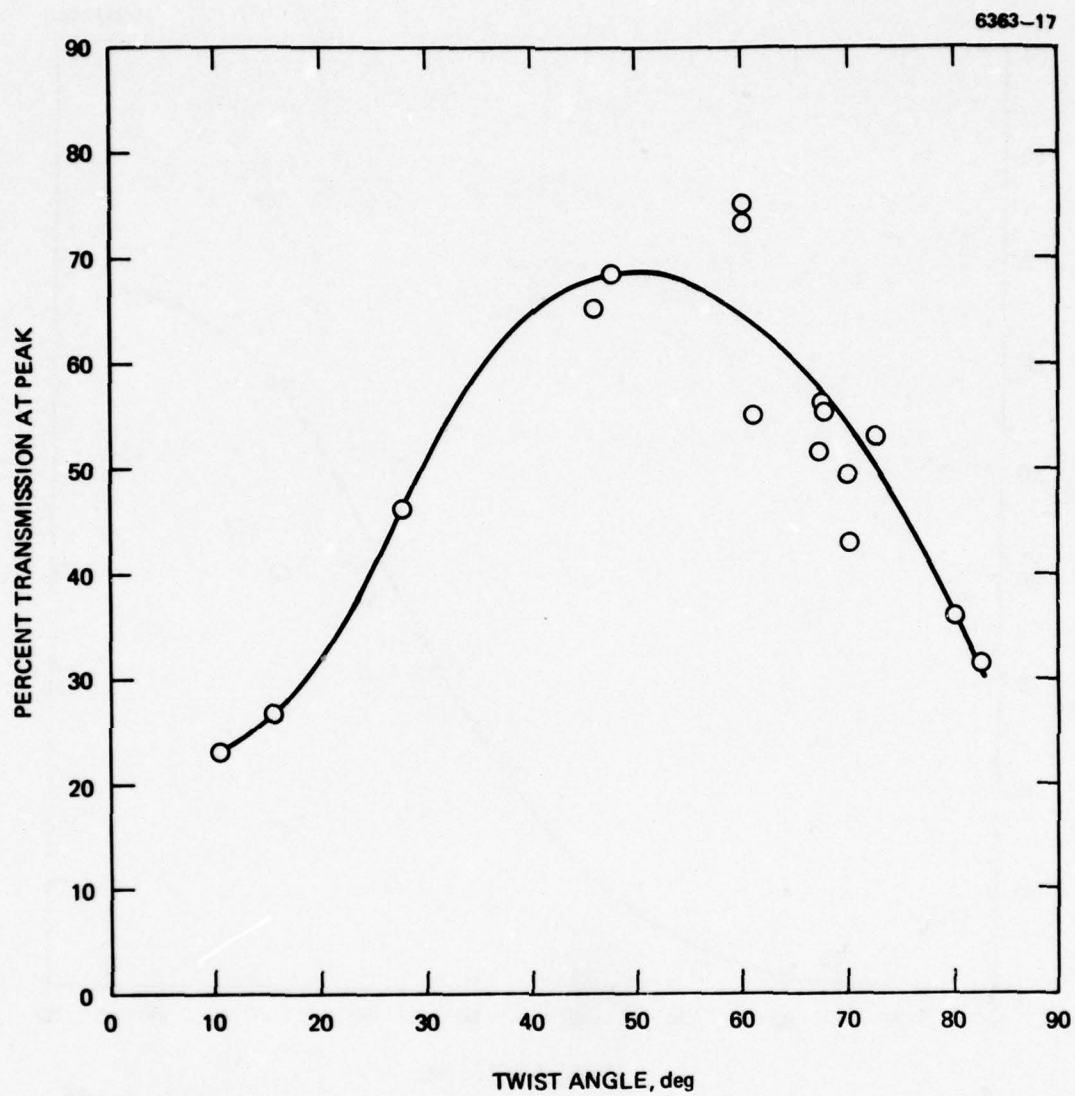
Figure 17. Intensity of the second order blue transmission
peak in 0.25-mil HFE cells as a function of the
twist angle.
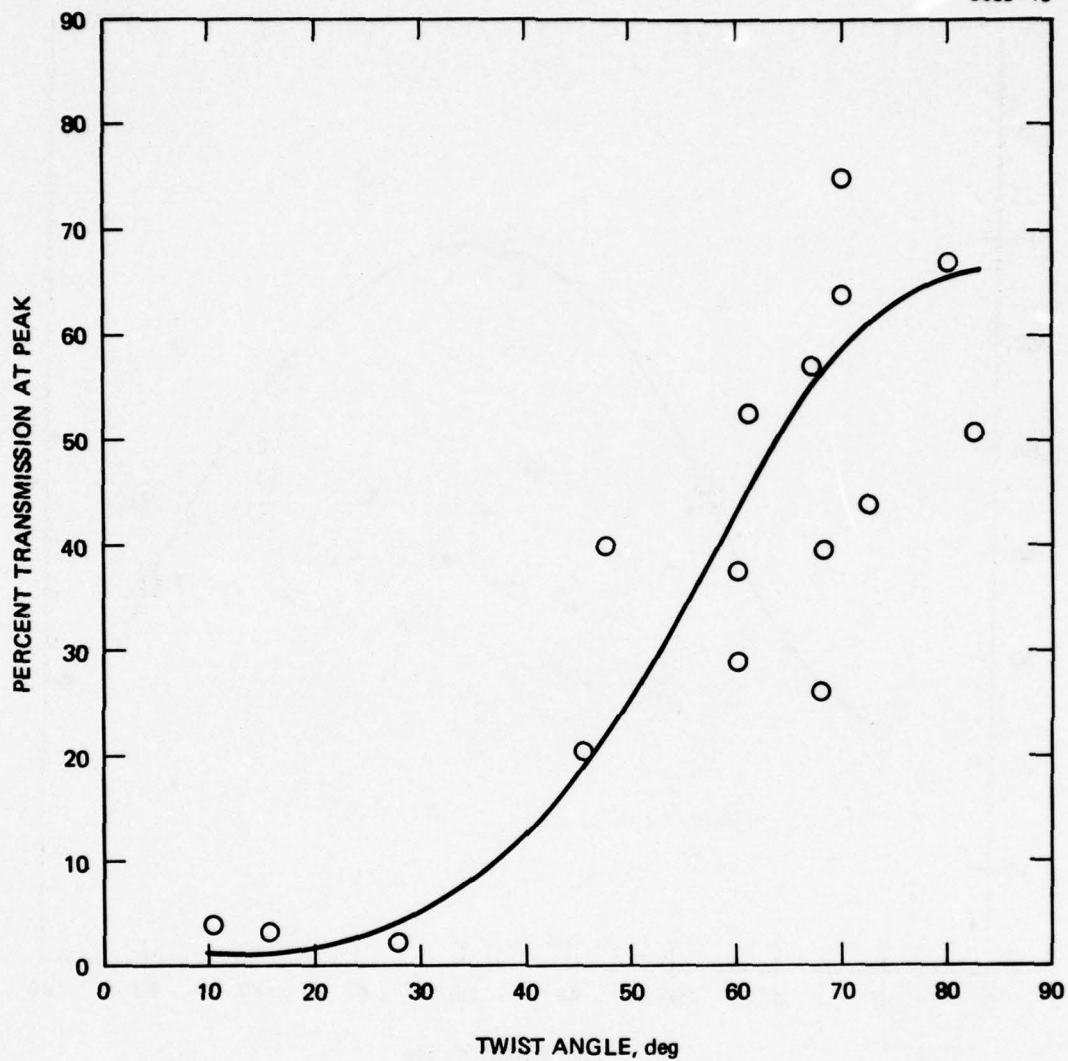
Figure 18. Intensity of the third order blue transmission peak in 0.25-mil HFE cells as a function of the twist angle.

through a maximum and decreased at higher twist angles. The approximate positions of these maxima are given in Table 1. The maxima are all at about 45° for the peaks of the first order and the blue peaks of the second order, for both 0.5- and 0.25-mil cells. However, the maxima of subsequent peaks are shifted farther toward higher twist angles for 0.25-mil cells than for 0.5-mil cells.

Table 1. Positions of the Maxima in the Plots of Peak
Transmission as a Function of the Alignment
Twist Angle

Order	Color of Interference Circle	Twist Angle at Maximum	
		0.5 mil	0.25 mil
First	Blue (466 nm)	--	45
	Green (545 nm)	44	46
	Red (623 nm)	45	47
Second	Blue	44	48
	Green	50	65
	Red	60	74
Third	Blue	62	(>82.5)
	Green	72	(>82.5)
	Red	78	(>82.5)

Γ 6101

29

Chromaticity plots of five of the 0.25 mil HFE cells are presented in Figures 19 through 23. The plots in Figures 19 through 22 are considered typical for the 0.25-mil cells; that in Figure 23 is considered atypical but is included to illustrate the scatter in the data. The dotted portions of the curve describe the behavior between the null and the point where the transmitted intensity exceeds 15%; the dashed portions define the behavior at voltages more than twice the null voltage.

A consideration of the chromaticity plots of both 0.25-mil and 0.5-mil cells shows some general trends. As one traces the plots backwards from the high voltage end where the transmitted light is almost white, the purest colors that are obtained are, in order, orange, magenta, blue, blue-green, yellow, magenta, green, and red. This series omits intermediate colors, which usually are not obtained in good quality. If one considers only the accessible, high-intensity portion of the spectrum (shown by the solid line in the chromaticity plots), this portion proceeds backwards from the white, high-voltage end as the twist increases. It also proceeds backwards from the high-voltage end as the thickness increases for a given twist angle. The position at which the purest colors appear is indicated by arrows above the voltage-transmission curves given in Figure 6.

Unavoidable differences in thickness were probably the major cause for scatter in the data. When Mylar spacers are used to control the thickness, there is a thin film of liquid crystal on both sides of the spacer, and the thickness of the liquid crystal layer depends on how much pressure is applied in tightening the screws on the cell holder. The 0.125-in. glass electrodes can also be bowed by applying pressure. These thickness differences were considered to be negligible when the data were collected, since we expected them to be small relative to the difference between 0.5-mil and 0.25-mil cells. However, the chromaticity plot shown in Figure 23 for the atypical 0.25-mil cell looks more nearly like that of a 0.5-mil cell.

The voltage at which a given transmission peak was found varied widely and unsystematically for the 0.25-mil cells. Any systematic influence of the twist angle was totally obscured by variations in the resistivity of the coated electrodes.

30
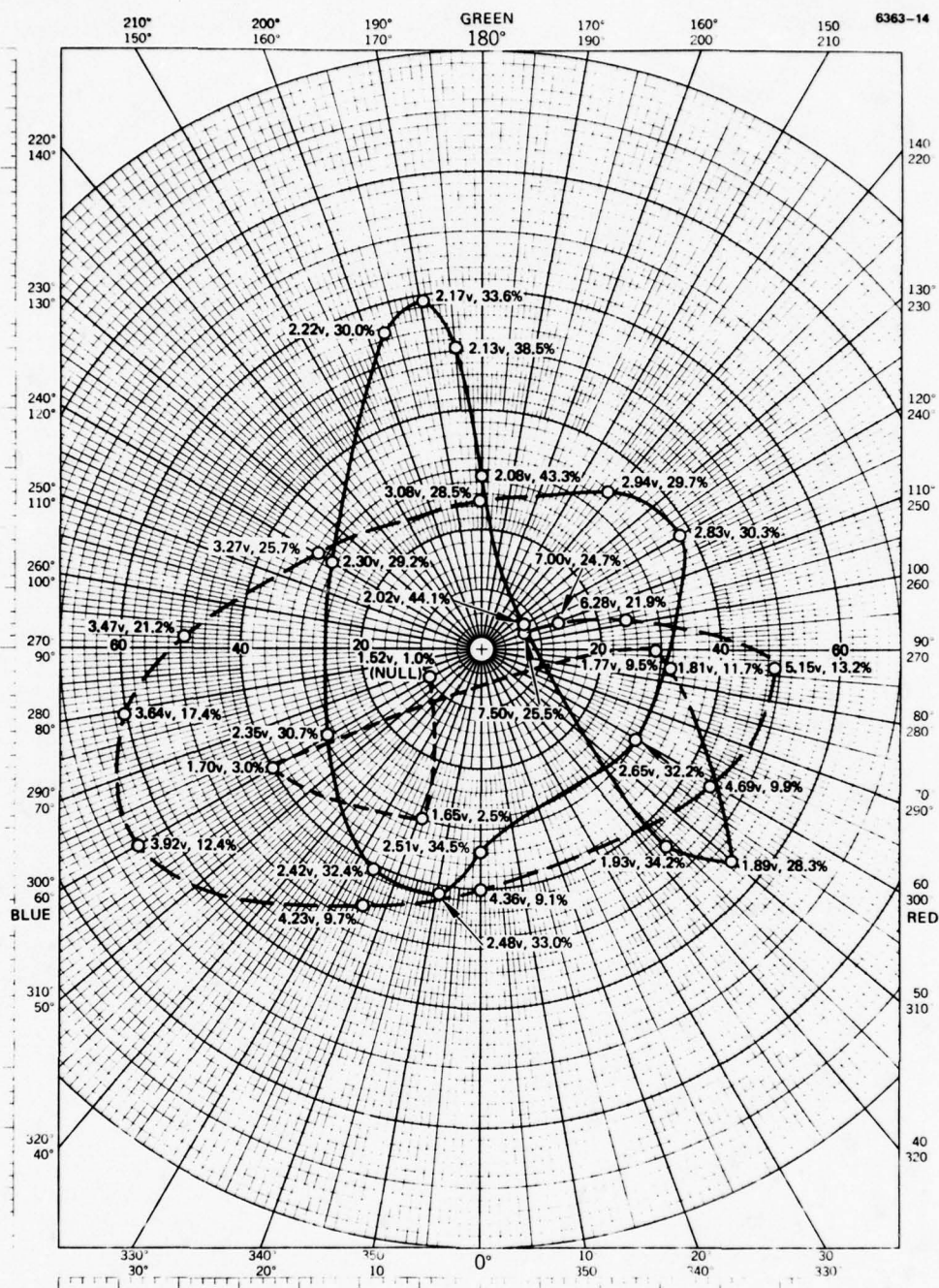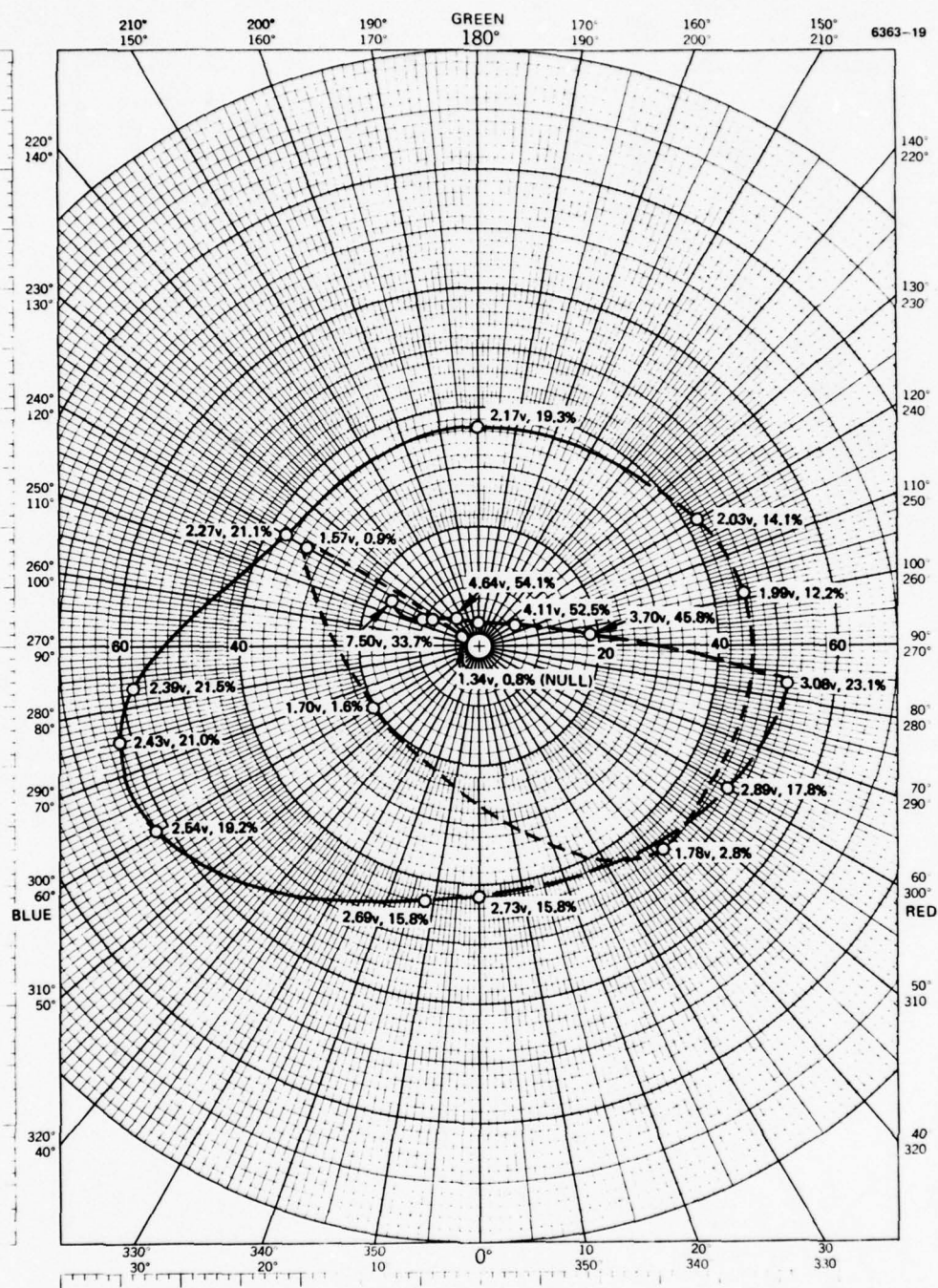
Figure 19. Chromaticity plot for a 0.25-mil HFE cell with 27.7° twist.

31
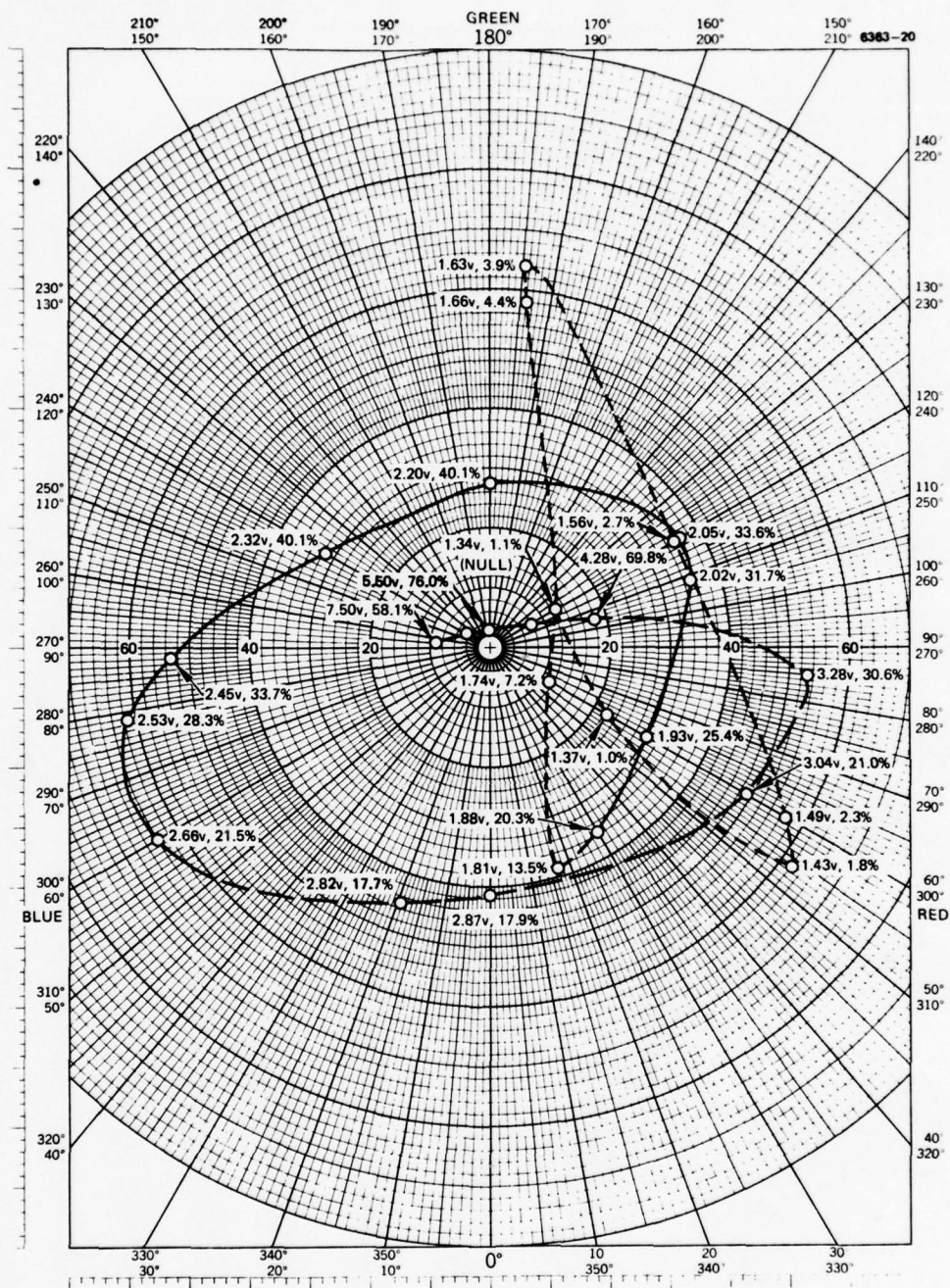
Figure 20. Chromaticity plot for a 0.25-mil HFE cell with 45.8° twist.

32
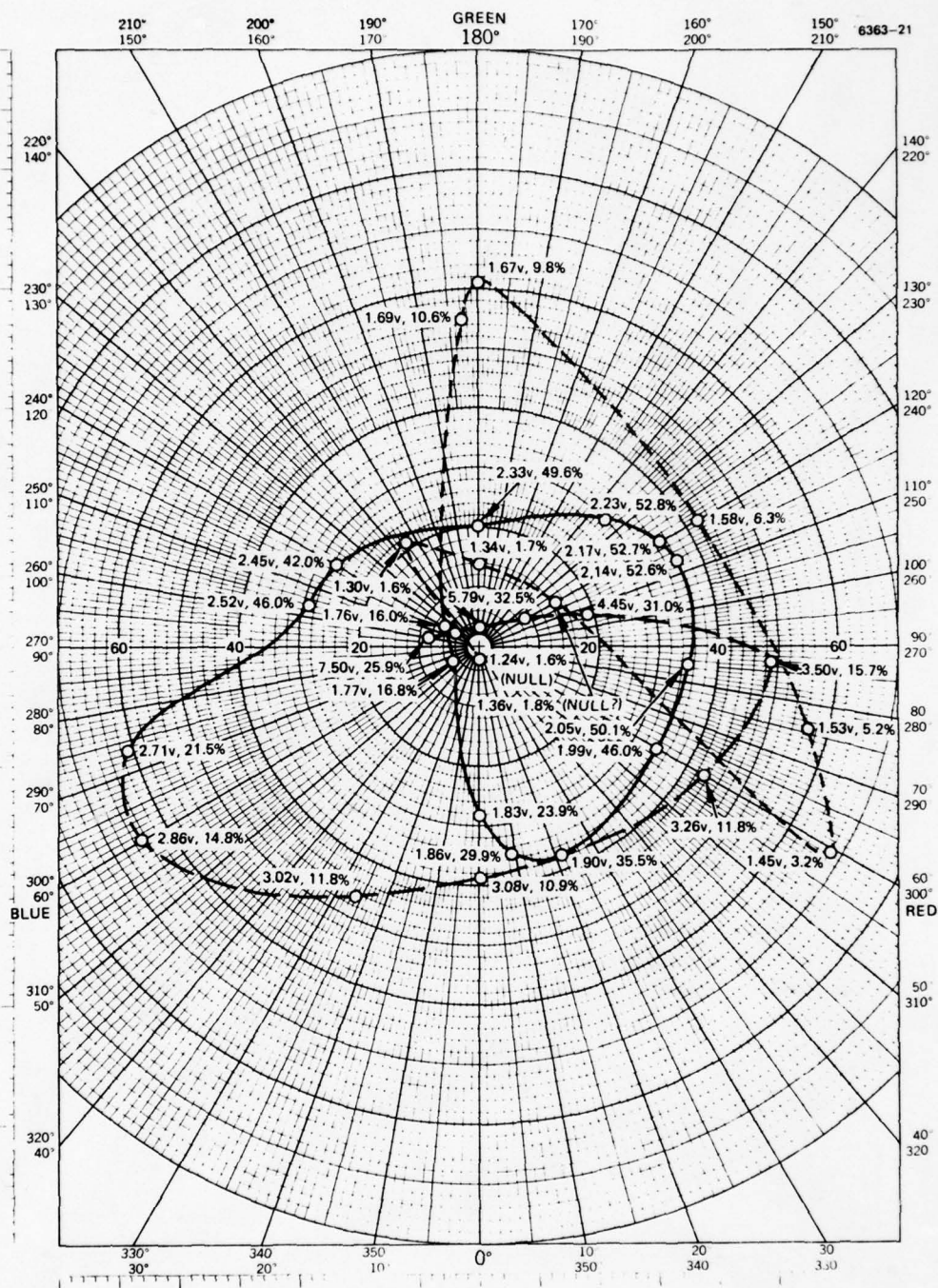
Figure 21. Chromaticity plot for a 0.25-mil HFE cell with 68.3° twist.
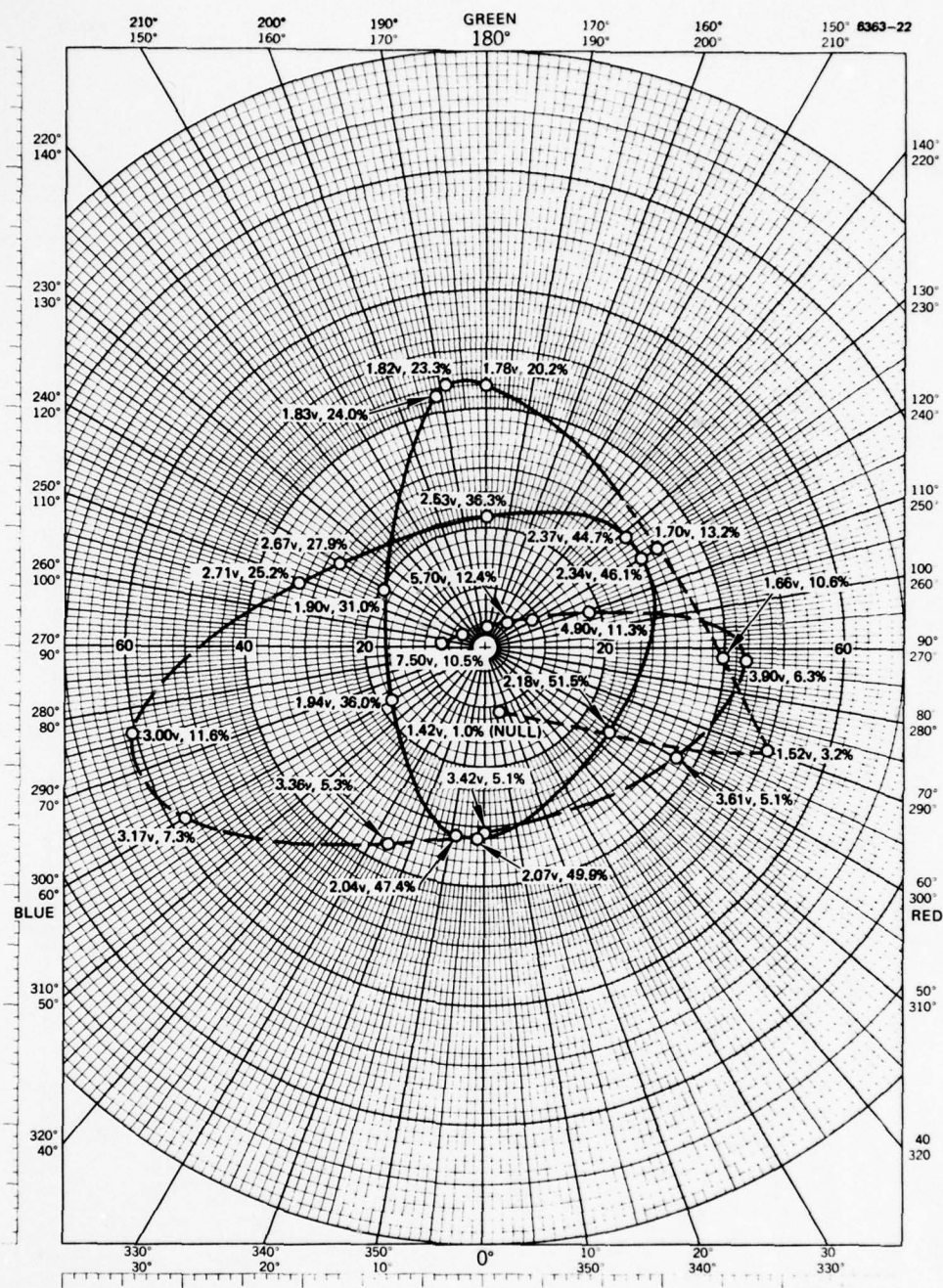
Figure 22. Chromaticity plot for a 0.25-mil HFE cell with 80° twist.

34
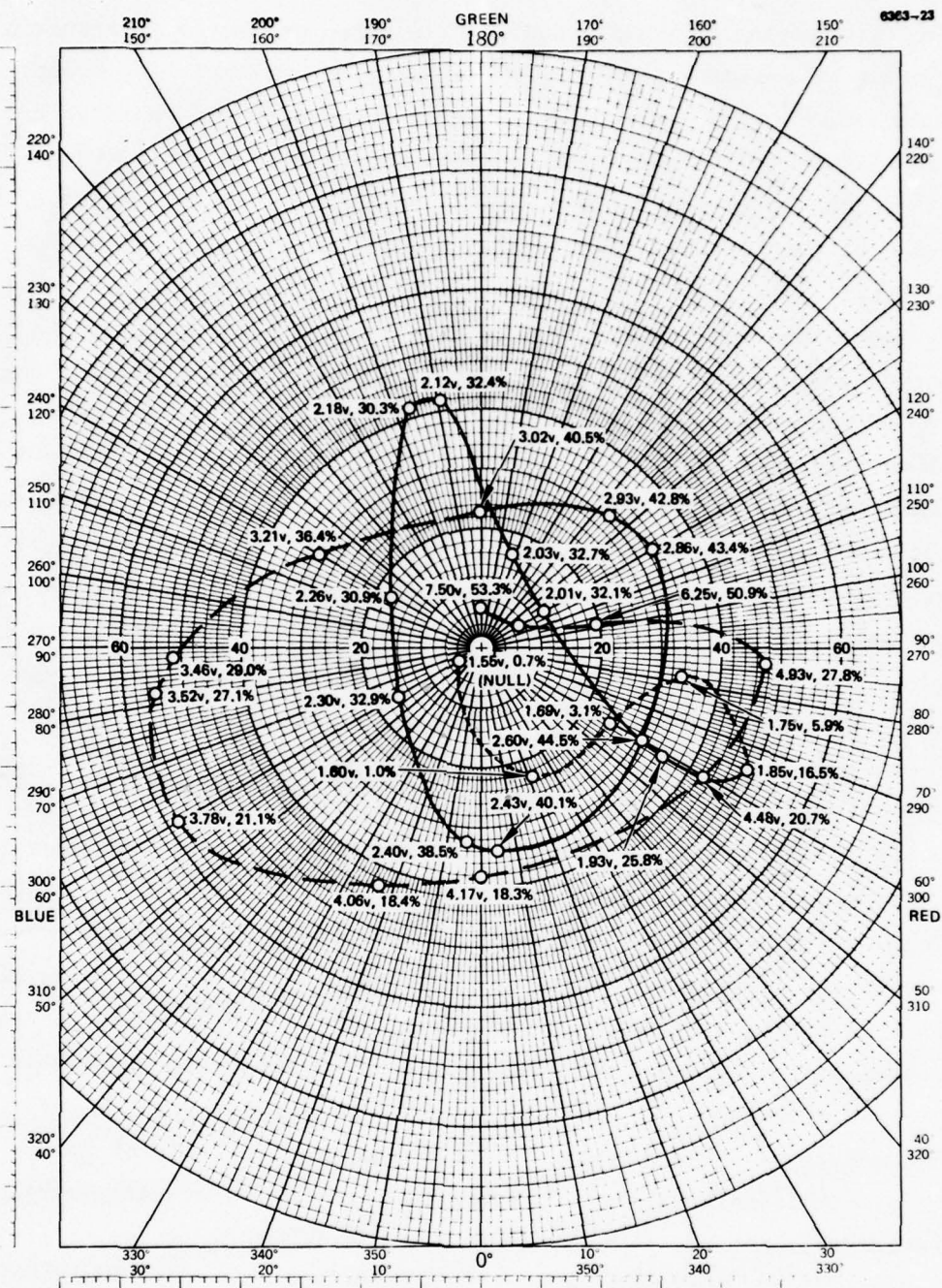
Figure 23. Chromaticity plot for a 0.25-mil HFE cell with 61° twist. This cell was considered to be atypical for a cell of this thickness and twist.

35

The third variable investigated was the match or degree of mismatch in the plane of polarization and the alignment direction at the front electrode, which was of particular interest because of the inevitable splay in alignment. This splay in alignment varies with the etching conditions, but it is generally about 5° per inch. It is caused by divergence of the ion beam, and it always follows a pattern consistent with a picture in which the beam originates from a virtual point source, as illustrated in Figure 24. If the plane of polarization is matched with the alignment direction at the center of the cell, there will be a mismatch with a positive angle on one side and a negative angle on the other side. If this mismatch modifies the voltage-transmission curves, there will be nonuniformities; these have indeed been observed in light valve displays and are a matter of continuing concern. They are particularly evident when the voltage is set to transmit a "narrow" color band to the screen. For example, in the curves given for the 0.5-mil, 60°-twist cell in Figures 6 and 13, at 2.42 V there is a peak in the second-order red band and red should predominate. However, the red is not very pure, and there is a rapid transition from magenta to yellow. The intermediate red is therefore very narrow, and, if red is transmitted to the two edges, the narrowness of the band and nonuniformity of the light valve will make this color-band almost useless. The magenta and yellow on either side extend over broader ranges, and the nonuniformity is much less noticeable when these bands are being used. Of course, nonuniformities in thickness and imperfect collimation of the projection beam may also be factors in the nonuniformity of the display, but we believe that the primary cause is the splay in alignment.

The effect of splay was first examined with a 0.25-mil, 68°-twist cell by determining the voltage-transmission curves for a small sampling beam reflected, in turn, from the center and from the two sides of the cell. Significant differences were observed. When the cell was characterized at one side, the peaks were shifted to higher voltages and the cell appeared to have a larger twist angle than at the center of the cell. At the opposite side, the peaks appeared at lower voltages and the behavior

36
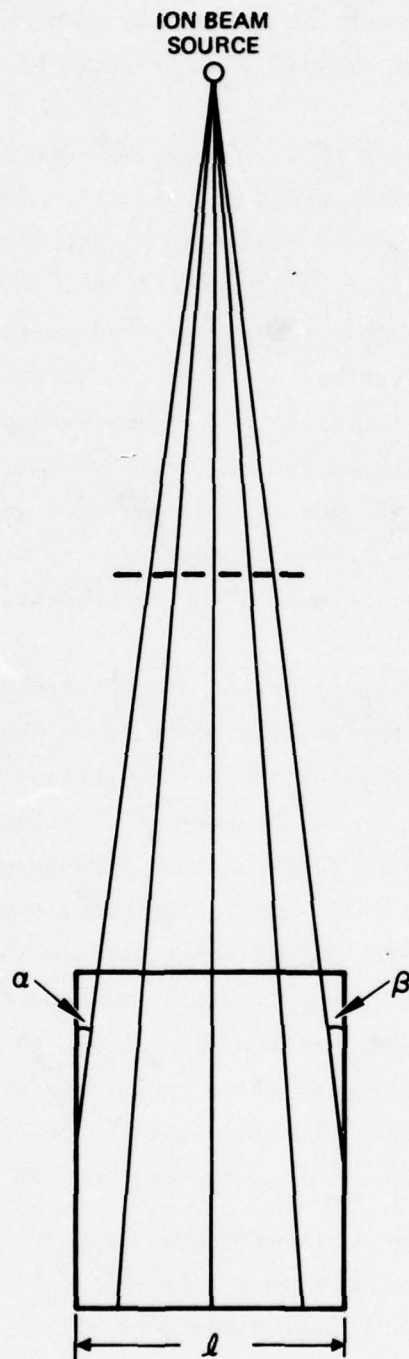
**ION BEAM
SOURCE**

Figure 24.
Diagram of the splay in
alignment on an ion-beam-
etched electrode surface.
Splay is given by $\alpha + \beta/\ell$.

was characteristic of a smaller twist angle. When a large spot at the center was compared with a small spot, the main effect was that the peaks of the curves for the larger spot were lower and the minima were higher. This was as expected since the large spot sampled a wider range of alignment angles.

A similar experiment was carried out with a 0.5-mil, 45°-twist cell using nine spots to characterize the various areas of the cell. Significant differences were again observed, but they could not be attributed to any single factor. Splay in alignment at the front electrode caused mismatch with the polarization plane; but this same splay, coupled with splay in alignment at the back of the electrode, also caused differences in the twist angle. In addition, 0.125-in. glass electrodes were used, and there was no assurance that the thickness was exactly the same throughout the cell. The alignment directions and the twist angle were measured for each spot in the cell, but this approach was dropped because neither of these could be correlated with the variations in the voltage-transmission curves.

The effect of mismatch in polarization plane and alignment direction was isolated from other factors by keeping the beam of light in the same place in the center of the cell and determining the voltage-transmission curves for different degrees of mismatch. The thickness did not vary in this series of measurements, since the same cell was used throughout. Moreover, the cell was made with 0.5-in.-thick glass electrodes and incompressible SiO_x spacer pads; therefore, it was quite uniform in thickness and not subject to inadvertent changes. Since the same cell was used, the voltage drop across the liquid crystal was always the same fraction of the applied voltage. The alignment twist angle also remained constant because all of the data came from the same spot in the cell. The cell was merely rotated in a plane parallel to the face of the cell.

The voltage and percent transmission at the transmission peaks are given in Table 2 for mismatch angles ranging from +2° to -2°. This is actually a very narrow range of mismatch angles; mismatches of +5° to -5° would be anticipated for a 2-in.-diameter light valve. However, even within this narrow range, significant differences were found. The null

38

Table 2. The Effect of Mismatch of the Plane of Polarization and the Front Surface Alignment on the Voltage-Transmission Characteristics of a 6-μm HFE cell.

Angle of Mismatch,[a] deg	Null Point[b]	Third Order Peak Blue		Second Order Peaks						First Order Peaks					
				Red		Green		Blue		Red		Green		Blue	
	V_{rms}	V_{rms}	%T	V_{rms}	%T	V_{rms}	%T	V_{rms}	%T	V_{rms}	%T	V_{rms}	%T	V_{rms}	%T
+2	1.59	1.78	5.3	2.21	14.2	2.37	26.2	2.61	47.4	4.12	97.2	4.76	93.0	5.70	89.6
+1	1.57	1.75	4.7	2.19	16.9	2.39	27.9	2.62	52.7	4.03	99.7	4.67	89.3	5.58	94.5
0	1.54	1.73	3.7	2.20	19.8	2.39	29.3	2.64	47.3	3.92	96.2	4.67	84.1	5.58	81.0
-1	1.52	1.70	3.7	2.19	23.3	2.40	33.5	2.65	48.6	3.88	97.4	4.57	85.5	5.50	78.8
-2	1.48	1.66	4.1	2.19	26.1	2.41	36.0	2.67	56.9	3.85	94.2	4.49	82.7	5.32	85.1

[a] A positive angle of mismatch was obtained by rotating the cell counterclockwise when viewed from the front side, while the plane of polarization was kept unchanged.

[b] Located between the blue and green peaks of the third order.

T2166

point, the third-order blue peak, and all three first-order peaks were systematically shifted to lower voltages on passing from a mismatch of $+2^{\circ}$ to -2°. In contrast, the second-order red peak remained essentially at a constant voltage and the second-order green and blue peaks increased substantially on passing from positive to negative mismatches; any systematic effect on the intensities of the second-order blue and first-order red, green, and blue peaks appears to have been obscured by scatter in the data. For a 6-μm cell, the effects on the peaks of the second order and the red peak of the first order are most important, since these peaks define the behavior of the cell in the region of accessible voltages and useful light intensities.

The effect of mismatch is unsymmetrical about the perfectly matched position. Imperfect matching may have been a factor in causing scatter in the data describing behavior as a function of twist. In fact, optimum performance may be achieved with the cell placed deliberately in a mismatched position. In a practical light valve display system, the user can easily determine by trial and error the cell position that delivers the optimum combination of colors.

When we attempted to apply the information derived from test cells to the construction of light valves, the major problem involved the uncertainty in the thickness of the liquid crystal layer. The voltage-transmission characteristics of light valves were determined in a manner similar to that used for test cells, except that the photoconductive substrate was illuminated with light of saturation intensity, and the external aluminum mirror was replaced by the internal dielectric mirror. The light valves were evaluated for twist angles of 50° to 85° and for four different thicknesses ranging from 6 to 15 μm. The 6-μm cells in this experiment were made with two different CdS substrates, opposing electrodes, and spacers. Therefore, their comparative liquid crystal thicknesses may vary slightly from those specified. The 9-μm, 12-μm, and 15-μm data were taken from the same substrate and opposing electrodes. The various twist angles in these cells were produced by rotating the

opposing electrode with respect to the CdS substrate without disassembling
the cell. The comparative results of cells of the same thickness can
therefore be viewed as quite reliable. However, absolute thickness values
may vary somewhat from those specified. Liquid crystal thickness was
assumed to be the thickness of the spacer or the sum of the thicknesses
of several spacers. The original light valves had 6-μm-thick SiO_x spacer
pads (measured with a Dektak) separated by spaces through which the
excess liquid crystal could freely escape. To this was added one or two
Mylar spacers with nominal thicknesses of 3.6 μm and 6.35 μm.
Results of the entire experiment are illustrated in the curves shown
in Figures 25 through 37.

The effect of varying the twist angle at a given thickness was
similar to that already described for the test cells. However, when the
voltage-transmission curves were compared with those of the test cells,
the nominal thickness of the light valves was relatively less than would
be expected on the basis of the test cells. This conclusion was based
on curves such as those shown in Figure 38 for cells with a 60° twist
angle. In this figure, the percent transmission at the peaks of the
second and third order were plotted against the nominal thickness of the
liquid crystal layer. Although the data are too sparse to clearly define
the relationship, there appears to be a tendency for the transmission of
a given color peak to pass through a maximum as cell thickness is
increased. Moreover, the thickness at which this maximum occurs seems
to be less for the peaks of the lower orders and for the shorter wave-
lengths within each order. When the data for the 0.25-mil and 0.5-mil
test cells are compared with these plots, they seem to correspond to
relatively thicker cells than would be expected on the basis of the
spacer thicknesses. Unfortunately, we have no reliable method for
accurately measuring the cell thickness directly in this thickness range.

In the 6-μm light valves, the peak heights for the transmission
peaks of the third order increased in going from blue to green to red.
This was the opposite of what was expected for cells of this thickness.

41
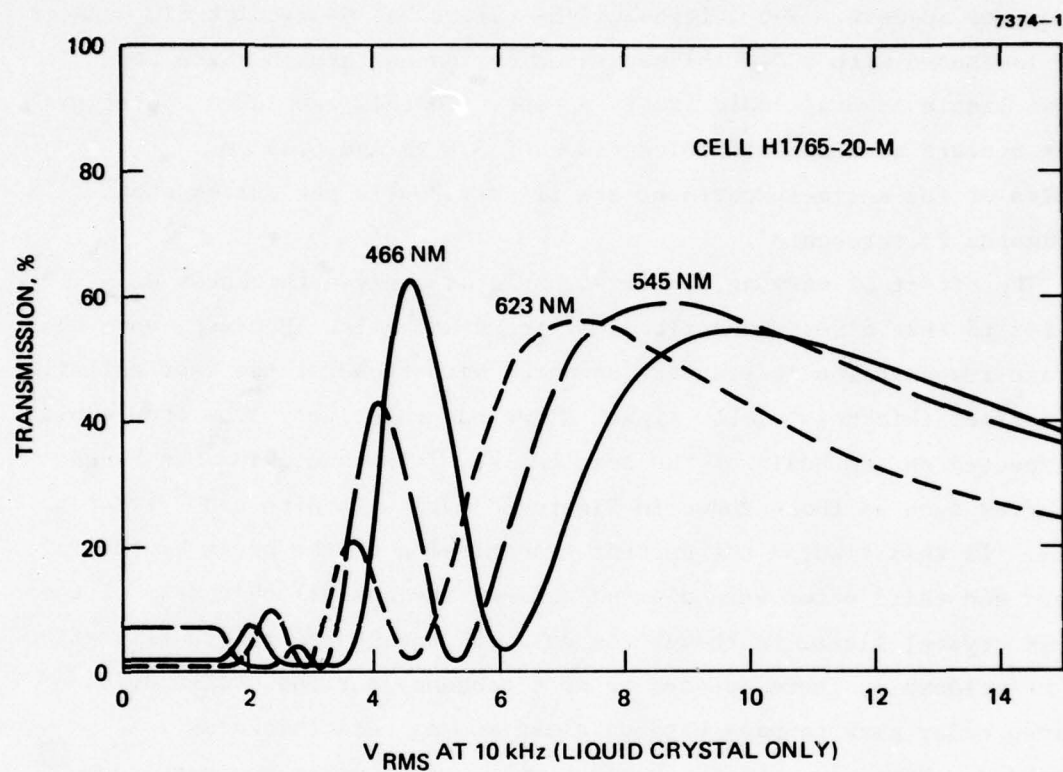
Figure 25. Voltage-transmission curves for a 6 μm LCLV with a 60° twist.
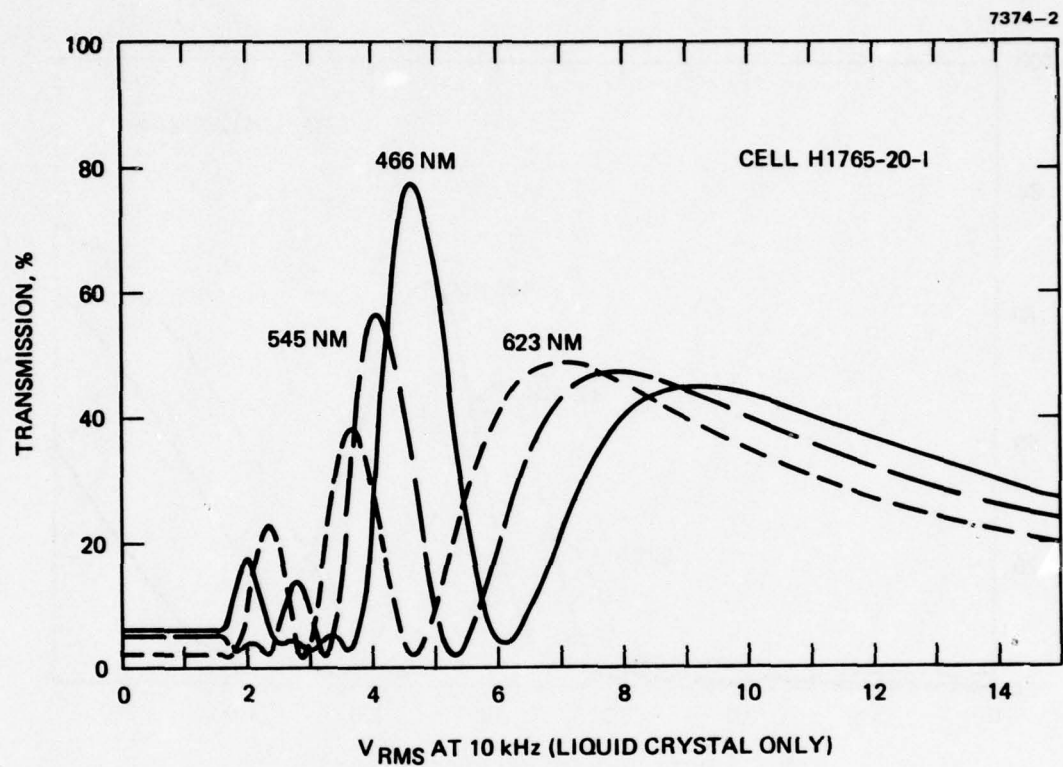
Figure 26. Voltage-transmission curves for a 6 µm LCLV with a 70° twist.

43
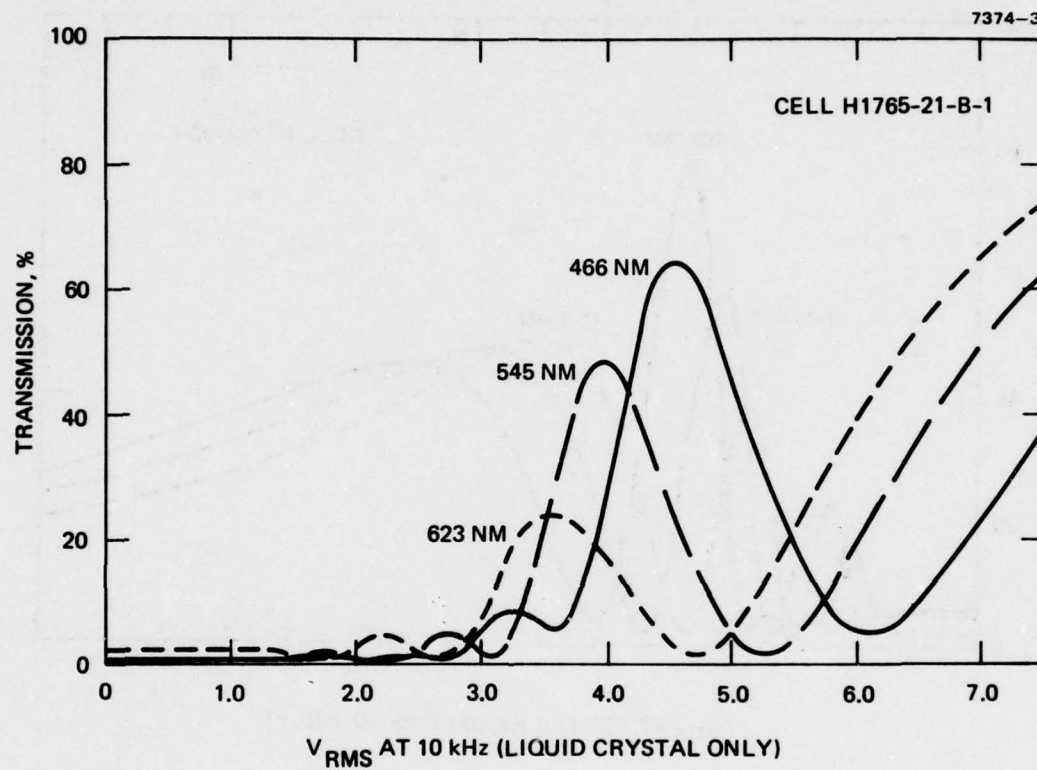
Figure 27. Voltage-transmission curves for a 9 μm LCLV with a 50° twist.

44
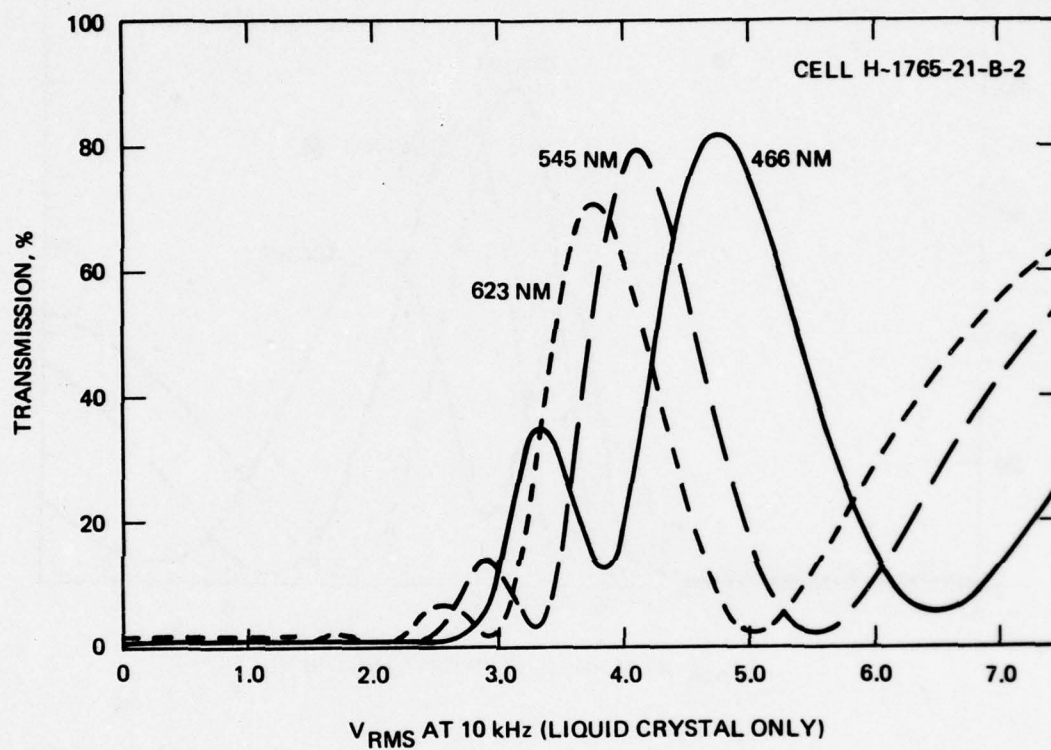
Figure 28. Voltage-transmission curves for a 9 μm LCLV with a 60° twist.

45
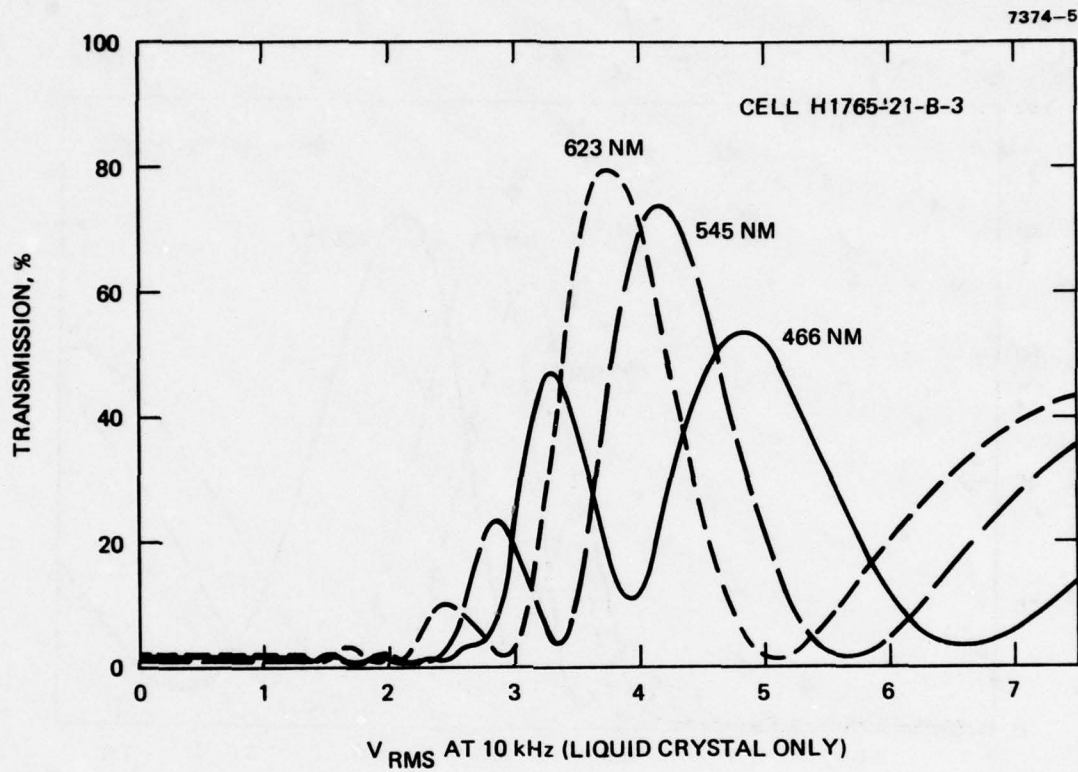
Figure 29. Voltage-transmission curves for a 9 μm LCLV with a 70° twist.
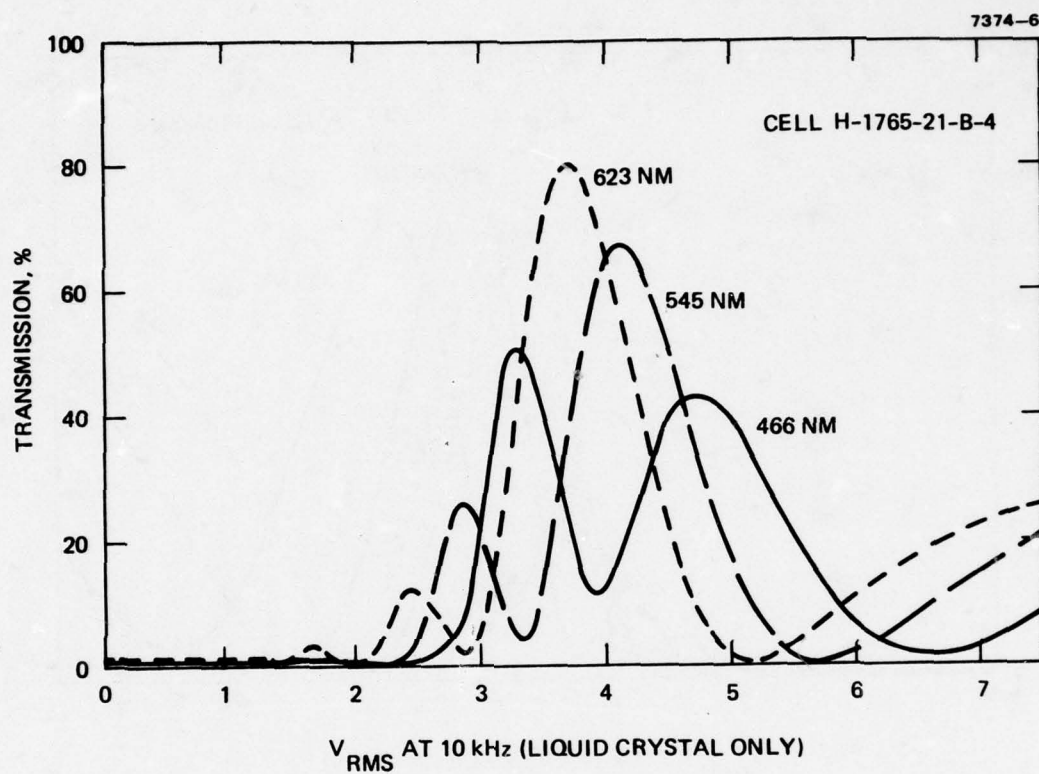
Figure 30. Voltage-transmission curves for a 9 μm LCLV with a 80° twist.
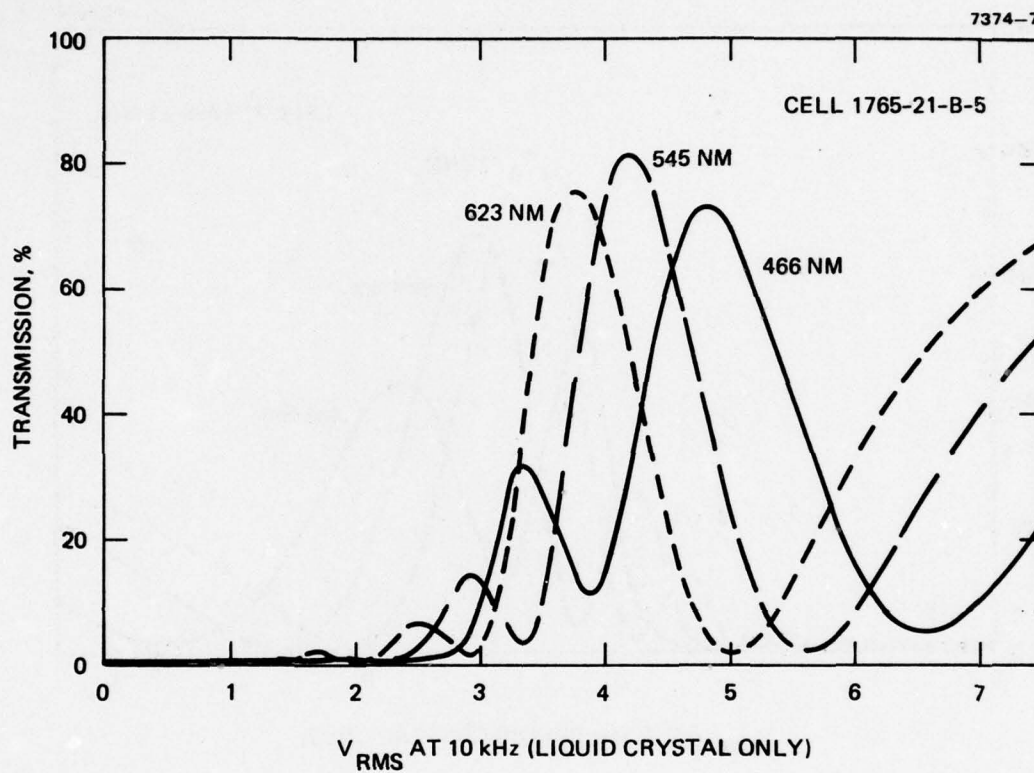
Figure 31. Voltage-transmission curves for a 12 μm LCLV with a 60° twist.
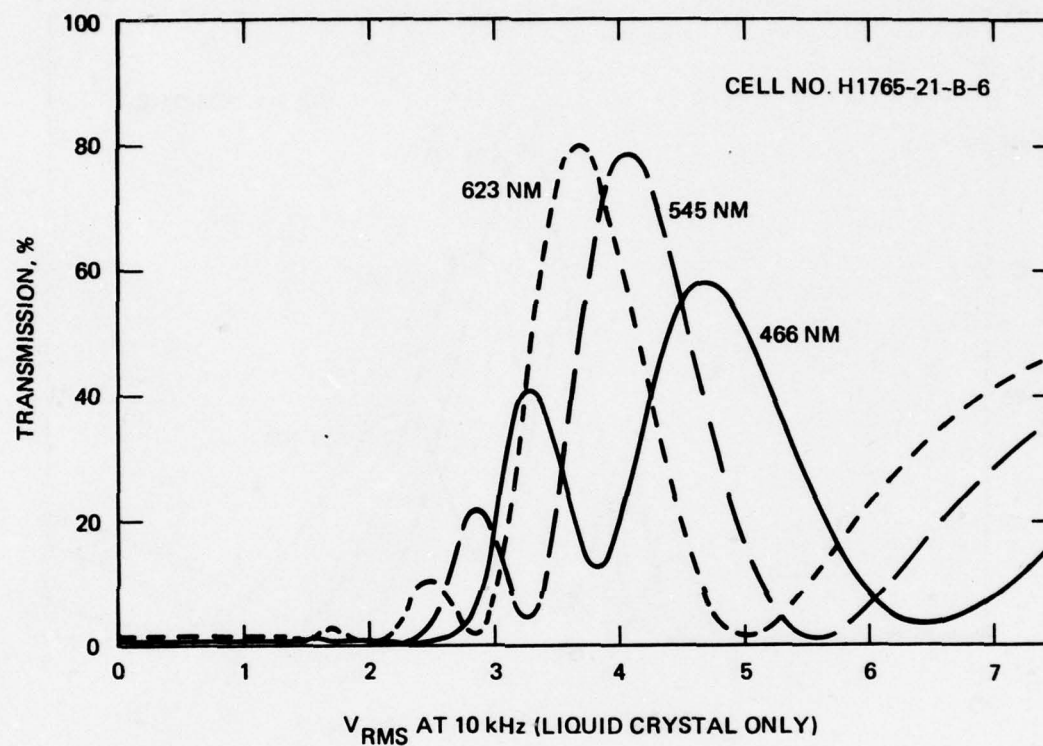
Figure 32.   Voltage-transmission curves for a 12 μm LCLV with a
70° twist.
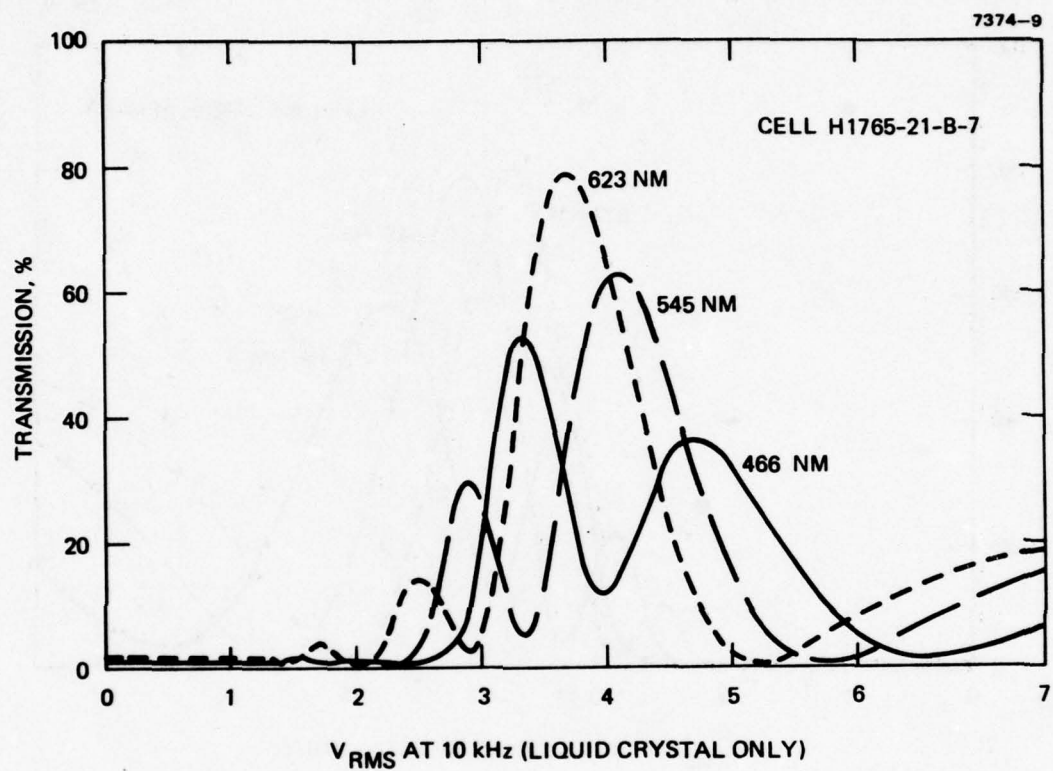
Figure 33. Voltage-transmission curves for a 12 μm LCLV with a 80° twist.

50
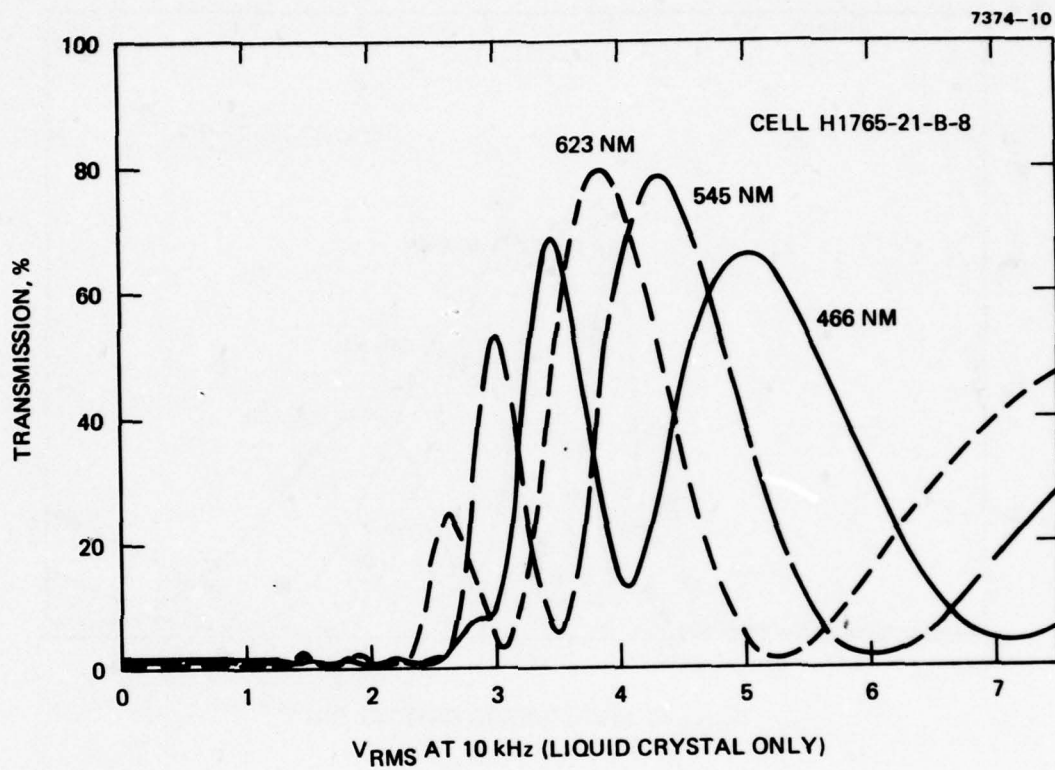
Figure 34.   Voltage-transmission curves for a 15 μm LCLV with a 60° twist.
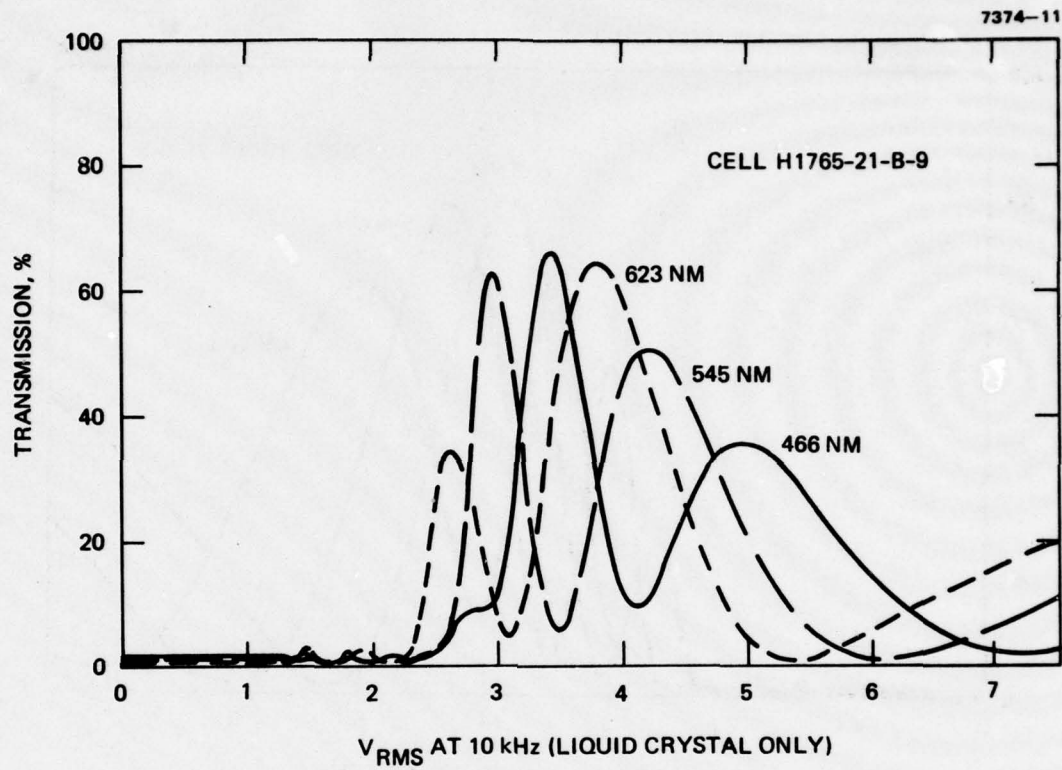
Figure 35. Voltage-transmission curves for a 15 μm LCLV with a 70° twist.
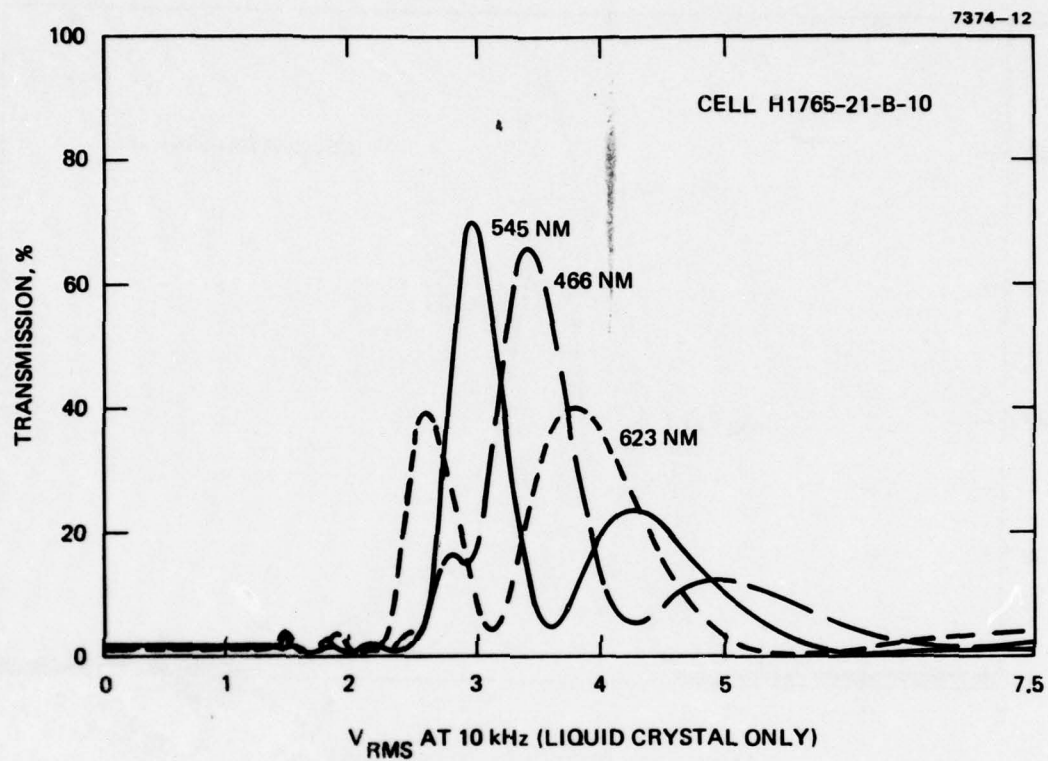
Figure 36. Voltage-transmission curves for a 15 μm LCLV with a 80° twist.
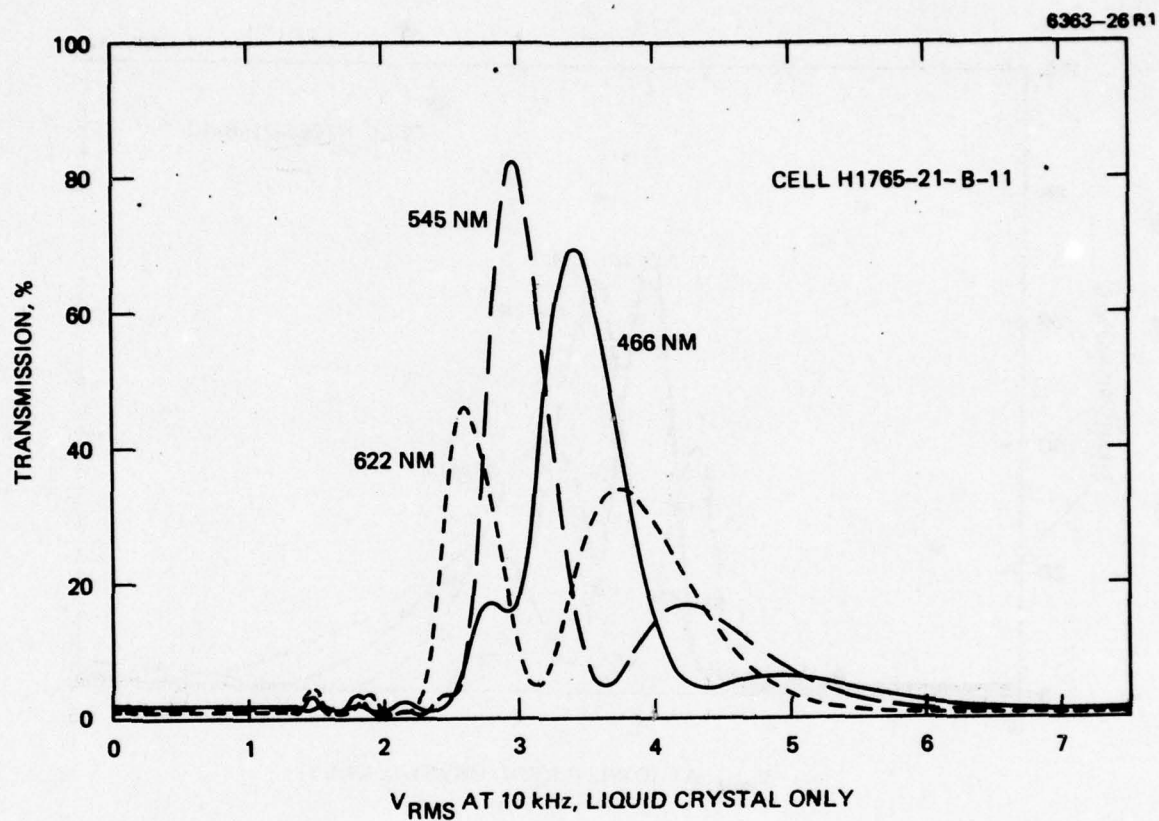
Figure 37. Voltage-transmission curves for a 15 µm LCLV with a 85° twist.
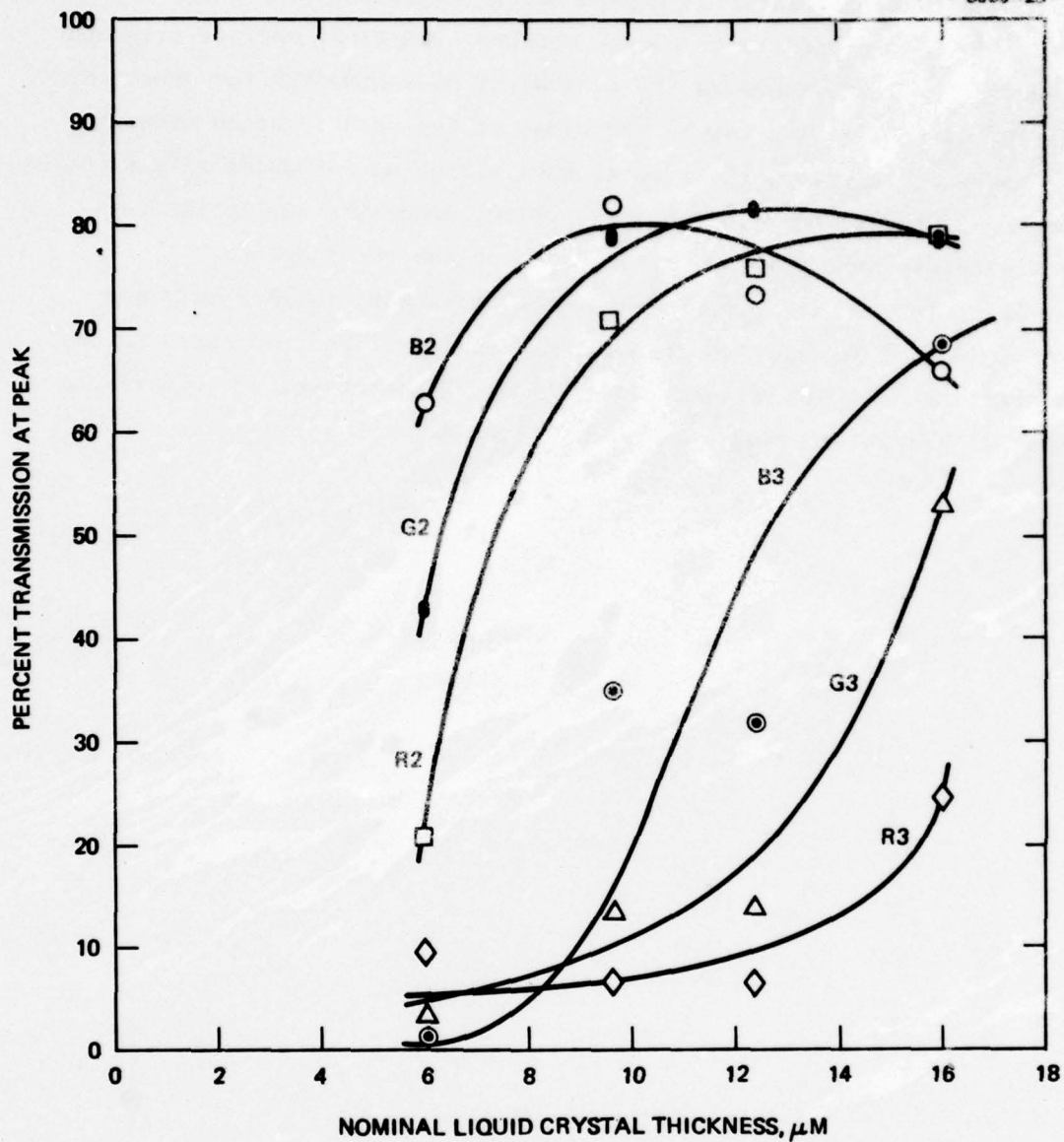
Figure 38. Peak intensity as a function of thickness for the blue, green, and red transmission peaks of the second and third orders in HFE light valves with 60° twist.

In thin cells (about 6 μm or less), the angle of rotation of polarized light by a twisted nematic is dependent on the wavelength of the light.[3] Since the plane of polarization was matched with front surface alignment using 545 nm light, there is the equivalent of a mismatch for other wavelengths. This mismatch may be the cause of the unanticipated order in peak heights. However, these peaks have almost no influence on the colors that can be projected with the light valve, since the null point is located between the blue and green peaks of the third order.

This study of the properties of HFE cells has provided only the bare minimum of information required for an intelligent approach in the construction of light valves with suitable characteristics. Clearly, a detailed theoretical study would be desirable.

SECTION 3
LCLV MULTIMODE OPERATION

A. REVIEW OF THE MULTIMODE CONCEPT

The original multimode (simultaneous b/w television and color symbology) operation of the light valve was based on the tilted perpendicular liquid crystal alignment. With this configuration, the multimode capability was a logical extension of the earlier monochromatic and color symbology light valves. (See the Final Technical Report, Contract Number N00024-75-C-7187.) Along with the dark off-state, which is below the negative anisotropy liquid crystal threshold, a low dispersion black/white gray-scale region was obtained at low voltage and then, with progressively higher voltages, the distinct birefringent color peaks were selected (see Figure 39).

The program to achieve complete multimode operation centered on two major developmental efforts:

- The development of a high-switching-ratio, fast-response photosensor film to allow image light switching from the dark off-state through the range of birefringent color peaks

- The formulation of a new high-birefringent, low-viscosity, negative-anisotropy liquid crystal material so that a thin liquid crystal layer, capable of television rates, would have enough birefringence to exhibit the color peaks.

In addition, the continuing problem of alignment tilt angle drift required solution.

During the program, it became clear that a solution to the tilt angle instability condition would require a major long-term research program. Thus, the main thrust of the program was directed toward adapting the HFE mode (originally developed for optical data processing applications) for use in graphics/symbology projection displays. An extension to color symbology operation was developed using a dark off-state null found in the liquid crystal characteristic above the threshold (see Figure 40). From this point, the liquid crystal could be switched to the birefringent color peaks found in the 6 to 15 μm biphenyl materials.

57

3259-3
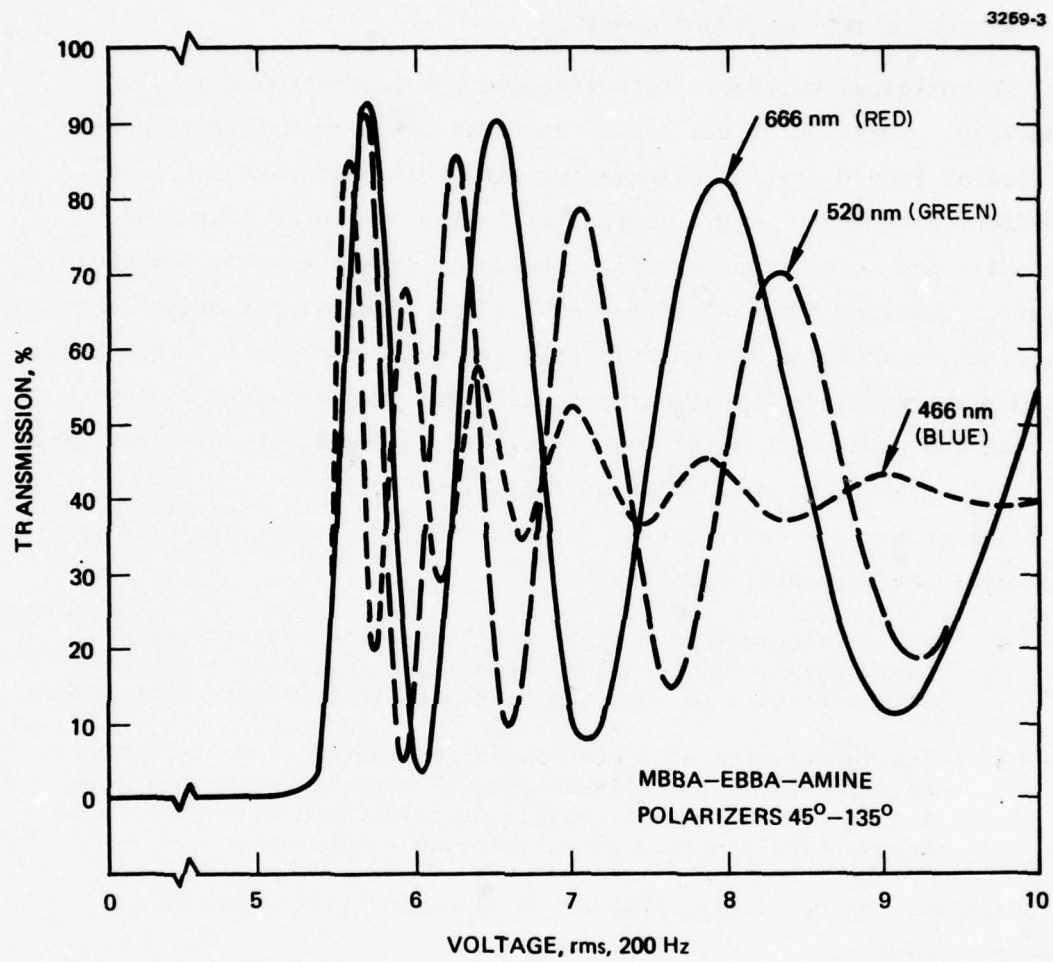
Figure 39. Birefringent liquid crystal response characteristic.

58
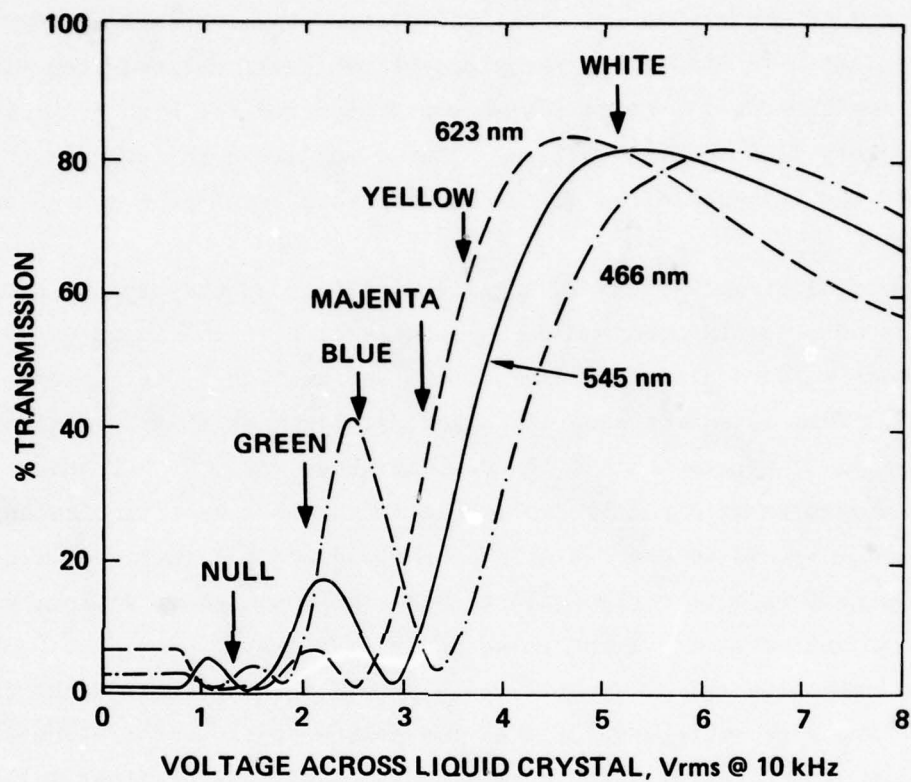
Figure 40. 45°-twist HFE mode: liquid crystal thickness = 6.0 μm.

Further investigation indicated that there was no direct extension to multimode operation. To achieve a black/white gray-scale region with a twisted (or parallel) nematic liquid crystal alignment, it is necessary to switch to the region of low birefringence that occurs at the high voltage end of the transmission versus voltage characteristic. However, as is indicated in Figure 41, the slope of the curve to zero transmission is very low and the low transmission state required for high contrast-ratio imagery lies at high voltages. Thus, to switch through the color peaks and the gray-scale region to the off-state requires a switching ratio* of ≥ 15.

A switching ratio of 15 is significantly beyond the capabilities of the cadmium sulfide photosensor presently used in the light valve. The highest value achieved in thick films (see Section 5) is approximately 5. This is approaching the practical limit of this type of photosensor. Thus, the thin-film CdS LCLV, used with the HFE mode, did not appear to be directly applicable to the multimode requirement. However, the second generation silicon photosensor has the capability of very high switching ratios with the fast response times necessary to demonstrate multimode light valve configurations.

The only true multimode operations possible both required the fast response and high switching ratio of the silicon photosensor. The CdS light valve would be possible to use in dual mode, where either television or color symbology could be selected, or in color symbology/color monochrome television mode, where shades of red television could be superimposed with multi-color symbology.

*The switching ratio is defined as the ratio of light valve current with uniform input illumination to the current at dark. This ratio depends on the light intensity, and, if not specified, it relates to 100 $\mu W/cm^2$. The current ratio approximately equals the voltage ratio across the liquid crystal, and it determines the dynamic range, or the part of liquid crystal characteristic that actually is used in a light valve.
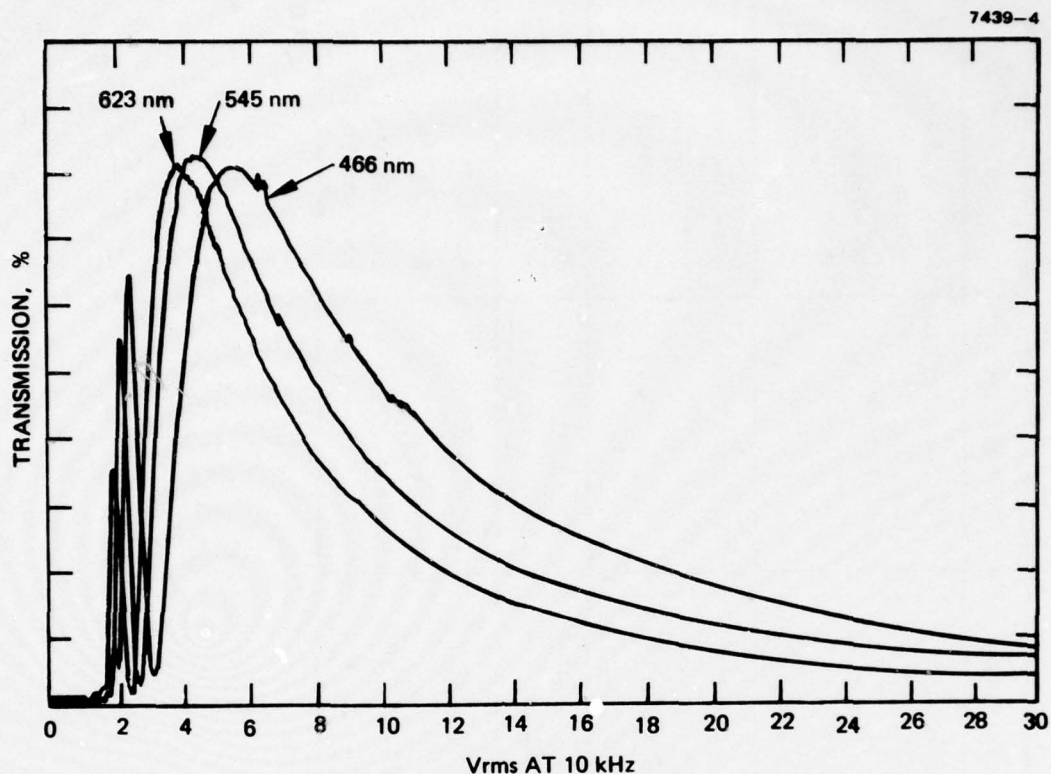
Figure 41. Transmission characteristic of a 45° HFE-mode
liquid-crystal cell at high voltages.

A comparison of possible HFE multimode light valve configurations
is given in Table 3. Although the silicon photosensor is clearly the
choice for true multimode operation, the liquid crystal mode had not
been defined precisely. In fact, the results with the HFE mode reported
in Section 2 indicate that thick liquid crystal layers (6 to 15 µm)
with concomitantly long response times may be necessary to achieve good
birefringent color peaks.

61

Table 3. Comparison of HFE MMLV Configurations

Configuration	Advantages	Requirements	Probability	Problems
Back slope TV	True multimode	High switching ratio (>15:1) High contrast in back slope Fast time response	Silicon: good (CdS not applicable)	Gray scale region; LC response time
Time sequential frame	True multimode	Very fast time response (15 m) High contrast in back slope	Silicon: good CdS: poor	Gray scale region; LC response time
Switched dual mode	Multi-function	High contrast in back slope	Silicon: good CdS: possible	Gray scale
3 + 1 color TV	Multimode	High power narrow band Projection light sources	Very good	Red TV; Gray scale; Intensity of projection light

T6101

62

B. MULTIMODE FIELD EFFECT

To achieve true television rates and reduce the requirement of very high switching ratios for the black state in the television mode, we initiated a study of the orientational effects of thin, fast, twisted nematic liquid crystal layers with respect to the projection light polarization direction. This program was carried out at the Industrial Products Division of the Hughes Aircraft Company and was directly supported by company funds.

This program demonstrated a novel liquid crystal electro-optic configuration that allows a single LCLV to project television-rate monochrome blue-black/white television along with superimposed birefringent color graphics/symbology ("multimode" operation).

The configuration results from the use of a twisted nematic liquid crystal cell placed in a novel orientation with respect to a crossed polarizer/analyzer combination. The effect works in the region of the electro-optic curve where the birefringence is decreasing as the positive dielectric anisotropy liquid crystal molecules line up with the electric field. The shape of the transmission versus voltage curves shown in Figure 42 for a nominal 45° twisted nematic liquid crystal layer operated in the HFE mode and the multimode field effect. The curves are for reflective mode operation with a return pass through the liquid crystal after reflection from a broadband dielectric or metal mirror. In the case of the HFE mode, the incoming polarization direction is placed along one of the two surface alignment directions. This allows a dark off-state for a particular color to be achieved at the low voltage end of the transmission curve. For high voltages, the three color curves decrease to low transmission only at very high voltages. For the multimode field effect, the incoming polarization direction is placed at some angle with respect to the cell alignment direction. In Figure 43, this mode is compared with the HFE mode. This polarization direction causes a broad spectral width null, or dark state, to appear at higher voltages (above the transmission maxima). However, as illustrated in Figure 42, this null has very low transmission and occurs at much lower voltages than the low transmission state found at high voltage in the HFE mode.

63
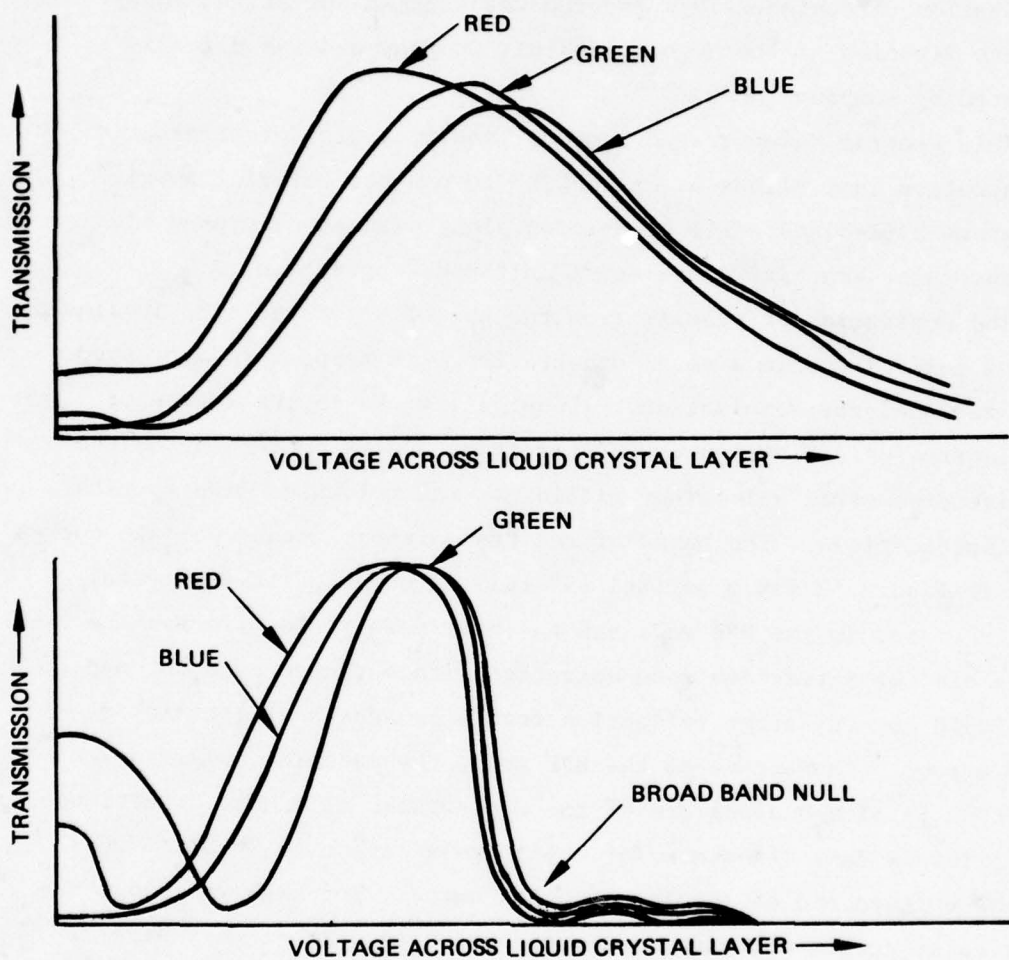
Figure 42. Transmission vs voltage for hybrid and multimode
field effect.

INCOMING LIGHT POLARIZATION DIRECTION

F

ANALYZER
DIRECTION

45°

F ARROWS
INDICATE LIQUID
CRYSTAL LAYER
SURFACE
ALIGNMENT
DIRECTIONS

HYBRID FIELD EFFECT

INCOMING LIGHT POLARIZATION DIRECTION

F θ_A θ_B

ANALYZER
DIRECTION

$0^\circ < \theta_A + \theta_B < 90^\circ$

$\theta_A \neq 0, \theta_B \neq 0$

MULTI—MODE FIELD EFFECT
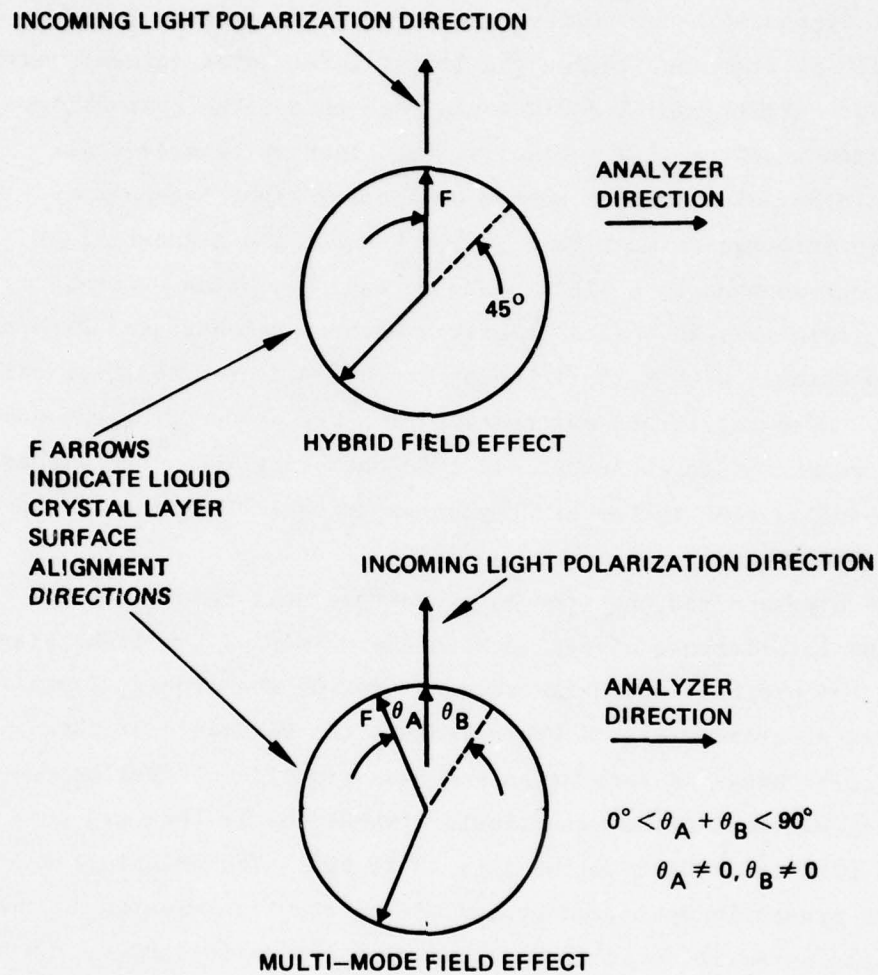
Figure 43. Surface alignment for hybrid and multimode field
effect.

65

The importance of this lower voltage null is that it makes high contrast black/white gray-scale imagery possible with low-voltage switching capabilities. Also, multimode operation can be achieved by switching to the lower voltage color peaks. Thus, image light activation of color graphics and symbology would occur according to the level diagram of Figure 44. The voltage bias of the light valve would be set so that with no light activation the lowest level color (green) would be selected. Light level 1 and 2 would then select the next higher colors (magenta and yellow). Finally, the black/white gray-scale region would be selected by a region of imaging light intensities. The black/white information must be inverted because the highest light intensity corresponds to a black state on the projection screen. Presently, more than 10 shades of gray have been demonstrated with magenta and yellow symbols with a static input image. Measured contrast ratio is >120:1. Somewhat larger switching ratios are needed from the substrate to reach the green level. In this operating mode, the liquid crystal response time in the b/w region is suitable for video frame rates without smearing.

It is hypothesized that the lower voltage null results from a destructive interference effect between the phases of the light traveling along the ordinary and extraordinary axes of the liquid crystal. The null is of broad spectral width because the bandwidth of the separate color peaks is very broad and thus significant overlap occurs. This effect has been noted with liquid crystal layers from 2.3 to 6 μm thick and with cell twist angles from 45 to 90°. The orientational angles are presently optimized by minimizing the transmission in the null and can be varied over a small range of angles to achieve the best conditions. For a 90° twist angle cell, a full compensation of the birefringence occurs, providing an absolute null; however, the on state becomes up dominant.

The b/w television mode of operation has also been used with color filters to simulate operation in an additive color television projection system. A higher contrast ratio is achieved with broader spectral width filters than with the thickness tuned hybrid field effect mode. Also, unlike the HFE mode, the precise thickness for low-thickness cells is not

66
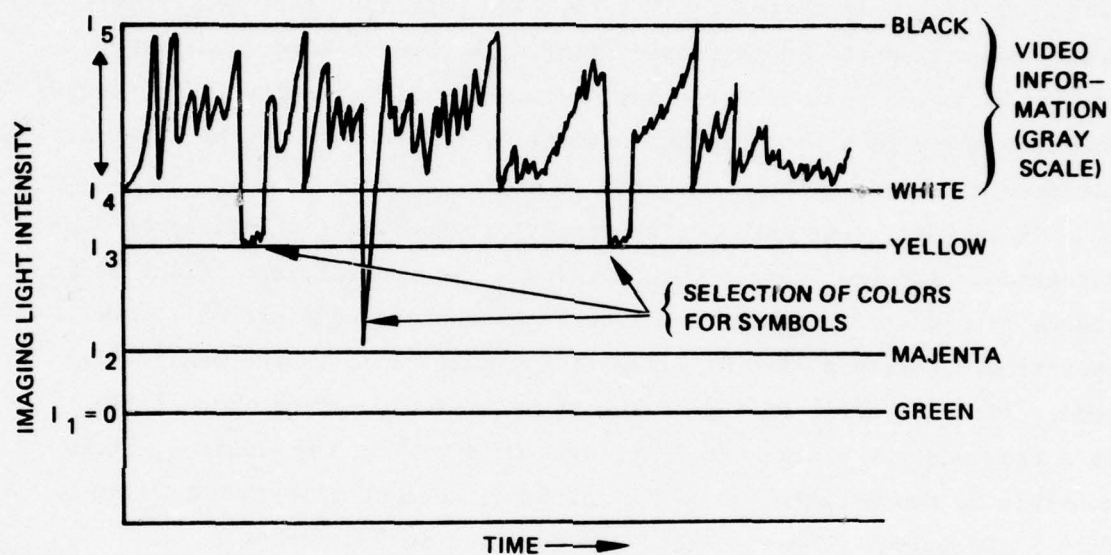
Figure 44. Imaging light activation of color graphics and symbology.

crucial in achieving a dark off-state; therefore, a TV rate operating liquid crystal birefringent layer is easily achieved, which can operate either as a b/w or as a single chromatic channel light valve.

In Table 4 the results of an experimental study of a 2.5-μm, 45°-twist, liquid crystal layer of birefringence $\Delta n = 0.21$ are presented. The data is presented for three different orientations of the etch directions (shown in Figure 45) with respect to the projection light polorization direction. The table shows that, with a maximum switching ratio of <9:1 (Orientation 1) TV rate, high contrast black/white gray-scale television can be presented along with three colors. Only the green peak needs further optimization in terms of intensity. The magenta peak intensity in a photopic measurement is low because of the spectral mismatch of the color band with the photopic response.

In two different angles with respect to the light polarization direction, different results are obtained. In general, the effect is to reduce the switching ratio requirements to achieve complete multimode operation but with a loss of ultimate contrast ratio in the black/white mode. Also the color of the off-state becomes blue-black in contrast to a true neutral black. In fact, with Orientation 3 of Table 4, it is possible to demonstrate the basic multimode concept with the CdS thin-film light valve. These results are reported in Section 4.

68

Table 4. Present Measured Single LCLV Multimode Performance

Mode	Orientation 1			Orientation 2			Orientation 3		
	Intensity	CR	SW.R.	Intensity	CR	SW.R.	Intensity	CR	SW.R.
B/W gray-scale television	73	127:1	2.5	80	35:1	2	83	15:1	1.5
Yellow	82	150:1	3.9	94	41:1	3	105	24:1	2
Magenta	30	49:1	6	44	19:1	4	51	12:1	3:1
Green	19	35:1	8.7	34	15:1	6.8	40	9:1	4.6

T6101

69
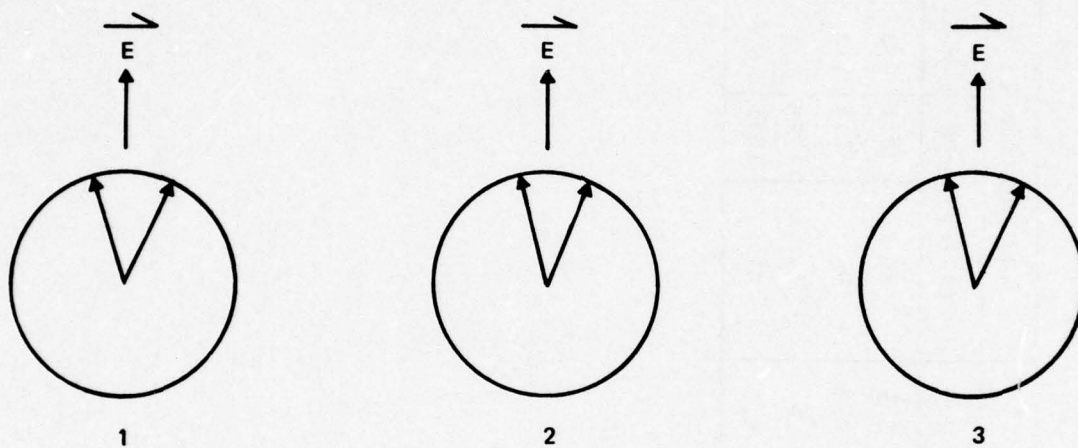
Figure 45.   Multimode orientations for Table 4.

SECTION 4

LIQUID CRYSTAL PHOTOCHEMICAL STABILITY STUDIES

A. INTRODUCTION

The objectives of this study were to determine the extent to which
the photochemical stability of the liquid crystal, E7, limited the life-
time of the HFE light valve and to identify the major factors affecting
photochemical stability. A complementary study of the thermal stability
of the liquid crystal was carried out concurrently on a Hughes-supported
research and development program.

For this study, the technical approach was to monitor the changes
in the electro-optical effect and to analyze and identify compounds pro-
duced by light and heat. All light irradiation experiments were carried
out on cells that were unsealed and that permitted air to diffuse into
the liquid crystal at the edges. Results indicate that access to oxygen
is an extremely important factor affecting the lifetime of the light
valve. The thermal stability studies also indicated that oxygen tremen-
dously accelerated the decomposition of the liquid crystal at 80 to 100°C.
Moreover, the major products of the photochemical decomposition were
also formed by thermal decomposition. One of these decomposition
products was isolated from a mixture obtained by allowing K21, one of
the components of E7, to decompose thermally in air. It was identified
as 4-cyano-4'-heptanoylbiphenyl (I), an oxidation product of K21.

7439-10
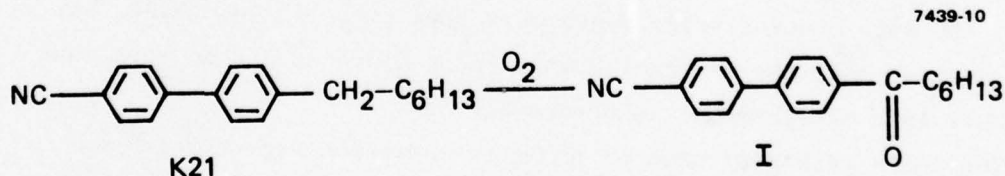
The identity of I was verified by an independent synthesis performed on
this program.

Some of the experiments were designed to determine the effect of I
on the lifetime of an HFE cell. Other experiments demonstrated the

71

influence of the wavelength and the intensity of the light. Experimental details are presented in the following section.

B.   EXPERIMENTS AND RESULTS

The results of the photochemical lifetime tests on HFE cells are summarized in Table 5. The liquid crystal used was E7 (BDH Chemicals, Ltd., Poole, Dorset, England BH12 4NN), which is a four-component mixture consisting of three cyanobiphenyls and a cyanoterphenyl (Table 6). The liquid crystal was used without further purification, and Figure 46 shows the extent of impurities present.

Two xenon short-arc lamps were used in this study: a Christie 900 W and an Optical Radiation (Orcon) 1600 W run at 1000 W. Figure 47 illustrates the spectral distribution of these lamps. Figure 48 shows the physical placement of filters and lenses used in the experiments. For the cutoff wavelength of 420 nm, a Corning CS3-73 sharp cut filter was used. Wavelength cutoffs at 385 nm (Orcon) and 360 nm (Christie) were controlled by the hot mirrors used in each system, and no other filters were used.

All cells had a 1 in.^{2} aperture that was completely filled with the exposing beam. In all cases, except with the light valve, an external, first-surface aluminum mirror was used. Temperatures were measured by taping a thermocouple to the back side of the mirror. With 1/8 in. glass, control experiments showed that the measured temperature outside of the cell was no more than 1°C lower than the internal temperature. No such control experiments were made with 1/2 in. glass, but it is assumed that the externally measured temperature is no more than 5°C lower than the internal temperature.

The cells were monitored by their transmission versus voltage response at 623, 545, and 466 nm between 0 and 7.5 V (the light valve was measured between 0 and 30 V). Initially, measurements were taken daily for about a week and every 2 to 4 days thereafter. Cell failure was manifested in the transmission versus voltage curves by a decrease of transmission and resolution of the second and third order peaks

72

Table 5. Photochemical Lifetime Tests on 45° Twist HFE Cells

Cell	Type	Liquid Crystal Thickness	Liquid Crystal	Xenon Lamp Intensity, mW/cm²	Temperature °C	Short Wavelength Cutoff, nm	Lifetime, hr	Exposure Life, W-Hr/cm²	Calculated Lifetime in System[a]
H2882-32[e]	Test[a]	¼ mil[g]	E7	418	30-33	420	1839	769	3076
H2882-34[e]	LV[b]	4 μm[h]	E7	408	35-37	385	145	59	236
H2882-50[e]	Test	2.2 μm[h]	E7	427 1345[c]	32-39	420	774	486	1944
H2882-60[f]	Test[a]	¼ mil[g]	E7K[d]	508	30	360	43	22	88
H2882-61[f]	Test[a]	¼ mil[g]	E7K[d]	409	30-32	420	876	358	1432

[a] These cells are made from 1/8" thick glass coated with indium-tin oxide ("Nesatron," PPG). The substrates were overcoated with SiO_2 and shallow angle ion beam etched, one at 45° with respect to the other.

[b] Light valve. See Ref. 1.

[c] This cell was exposed at 1345 mW/cm² for 169 hr.

[d] The liquid crystal, E7, was doped with 0.37% of 4-cyano-4'-heptanoylbiphenyl (I).

[e] Liquid crystal batch 508128.

[f] Liquid crystal batch 508231.

[g] Mylar spacers were used.

[h] Spacers were pads of $(SiO)_x$.

[i] Calculated lifetime for an operating system with a lamp intensity of 250 mW/cm² (GSC Type).

T6101

73

Table 6. Composition of Liquid Crystal E7

COMPOUND	STRUCTURE	VENDOR DESIG- NATION	7439-8 %
4–CYANO–4'–HEPTYLBIPHENYL	NC–⬡–⬡–C_7H_{15}	K21	25
4–CYANO–4'–PENTYLBIPHENYL	NC–⬡–⬡–C_5H_{11}	K15	51
4–CYANO–4'–OCTYLOXYBIPHENYL	NC–⬡–⬡–O–C_8H_{17}	M24	16
4–CYANO–4'–PENTYLTERPHENYL	NC–⬡–⬡–⬡–C_5H_{11}	T15	8

74
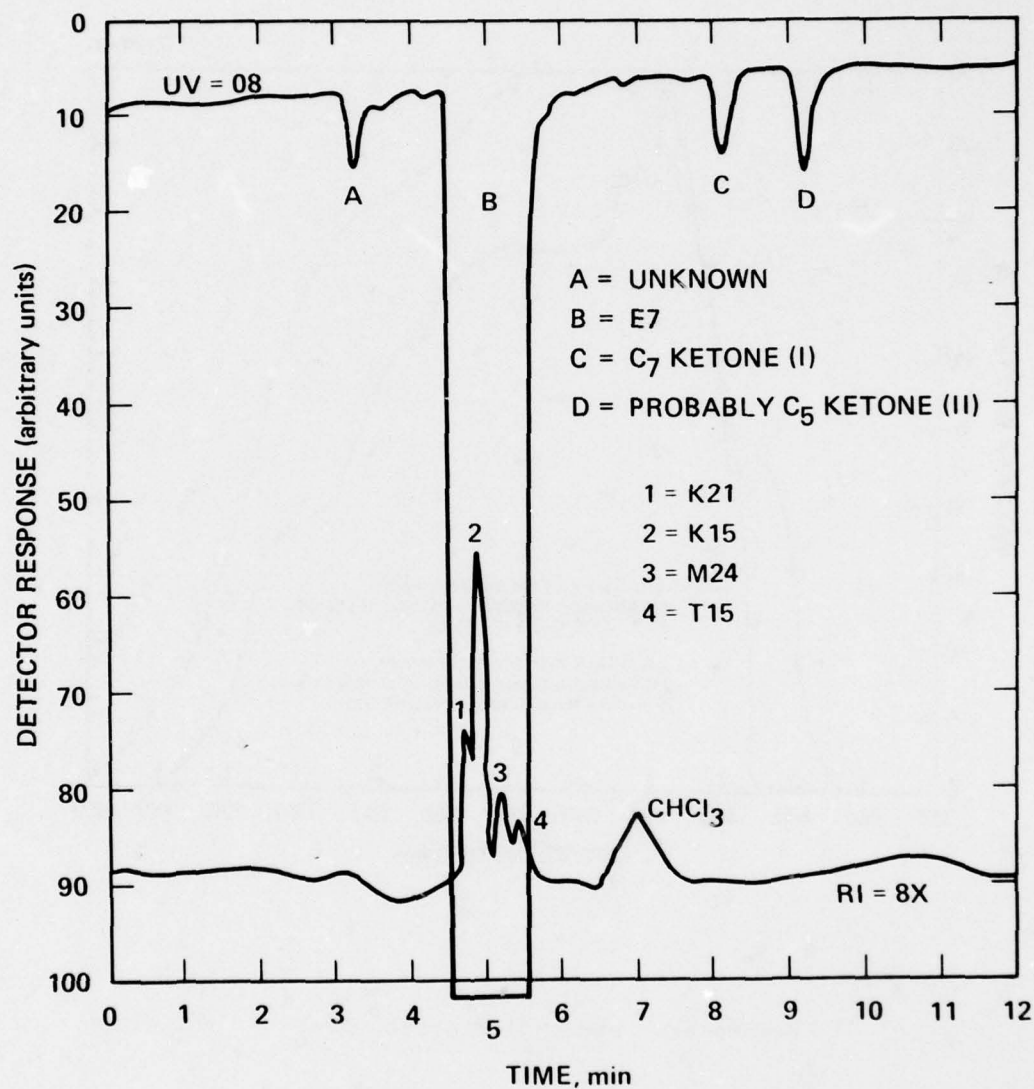
Figure 46. Liquid chromatogram of E7 as received. Upper trace is from a uv detector at high sensitivity; the lower trace is from a refractive index detector. (Liquid crystal batch 508128).

75
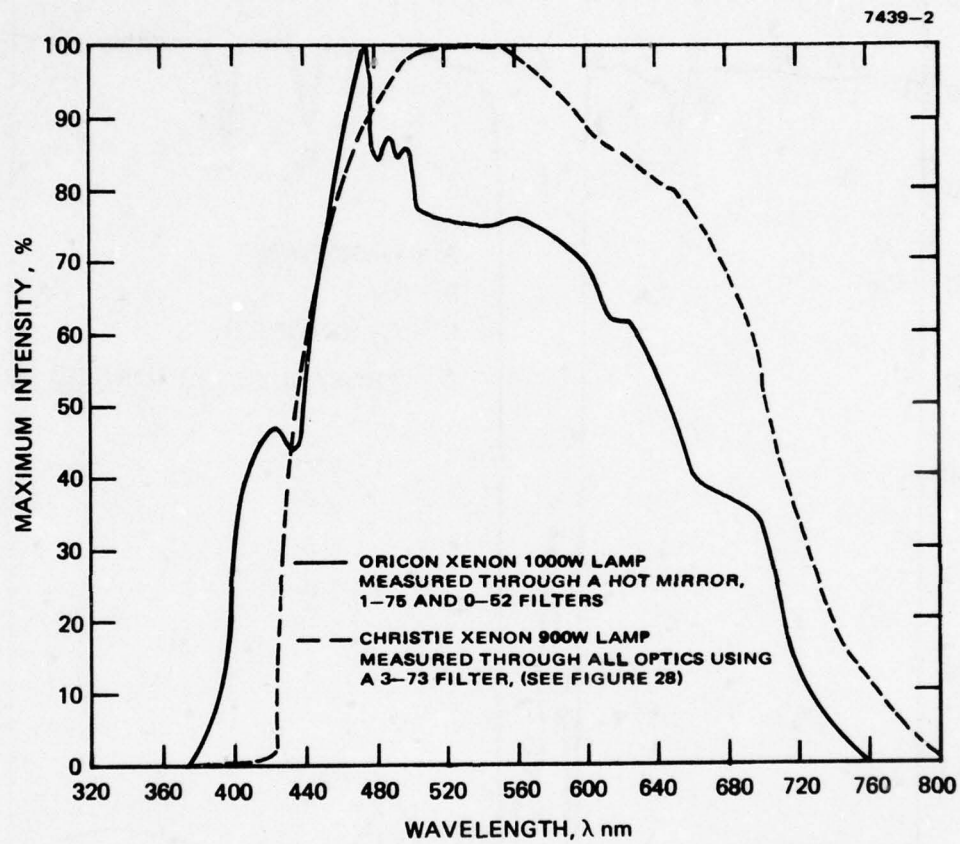
Figure 47. Spectral distribution.

(a)

(b)
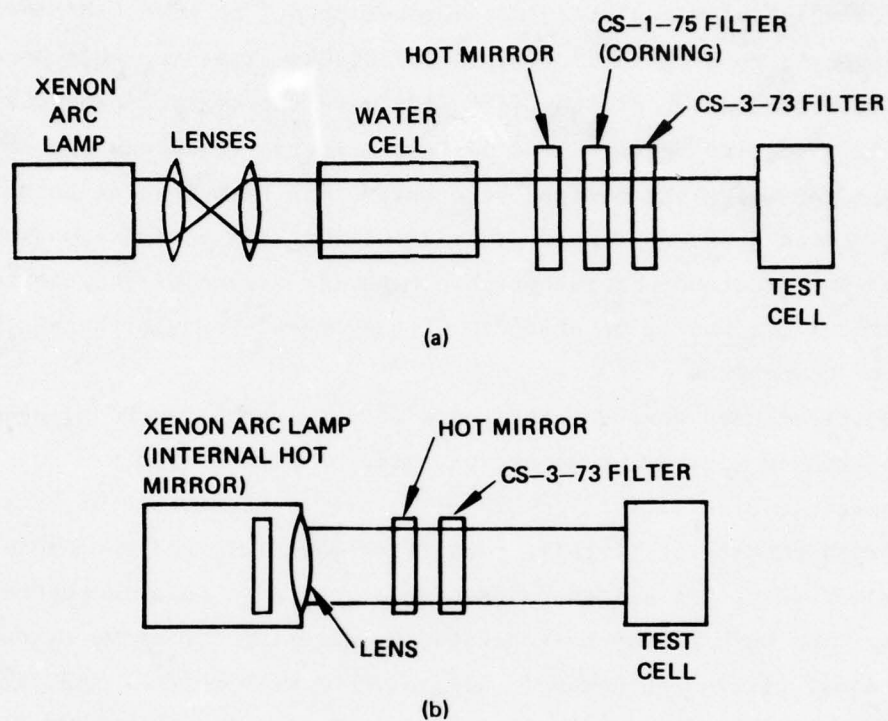
Figure 48.   Arrangement of filters for photochemical stability studies:
(a) Christie 900 W xenon lamp; (b) Optical radiation 1600 W
xenon lamp.

(2 to 4 V). Additionally, formation of a cloudy spot or streak was concurrently noticed. Figures 49 and 50 are an example of transmission versus voltage curves at the start and end of a lifetime test.

The preparation of 4-cyano-4'-heptanoylbiphenyl (I) was carried out by the Friedel-Crafts acylation of 4-bromobiphenyl to give 4-bromo-4'-heptylbiphenyl, mp 89.2-95.7°C (lit.[4] 99-100-C). Treating this product with cuprous cyanide in dimethylformamide gave the desired product, mp 79.5-82.5°C. Its infrared and nuclear magnetic resonance spectra were consistent with the desired structure. Its high-resolution mass spectrum showed a parent ion at $m/e = 291.165$. This material showed identical spectral and chromatographic behavior as one of the thermal and photochemical decomposition products of 4-cyano-4'-heptylbiphenyl (K21), one of the components of E7.

Analytical data were obtained on a Waters Associates Model M6000 high-performance liquid chromatograph equipped with a 4 mm x 3 cm μ-Porasil (10 μm particle size silics) column using a solvent mixture of hexane/chloroform/acetonitrile (19:4:1, respectively). This solvent elutes E7 as two major peaks but allows separation of the more polar decomposition products. The bulk E7 may be separated by diluting the above mixture with an equal portion of hexane. All solvents were Burdick and Jackson "distilled in glass" spectrograde. They were filtered through Millipore 0.45 μm Teflon filters and degassed in an ultrasonic generator prior to use. Quantification was done by calibrating with pure known components and measuring peak heights. Figure 51 shows a chromatogram of E7 and decomposition products following exposure. The content of the ketone 1 in the original sample was 0.025 to 0.050%, and it increased to 0.104 to 0.209% on cell failure.

Light intensity measurements were made with a Hewlett-Packard Model 8330A radiant flux meter equipped with a Model 8334A radiant flux detector. The instrument was factory-calibrated (traceable to NBS standards). Measurements were made through a Balzers neutral density

78
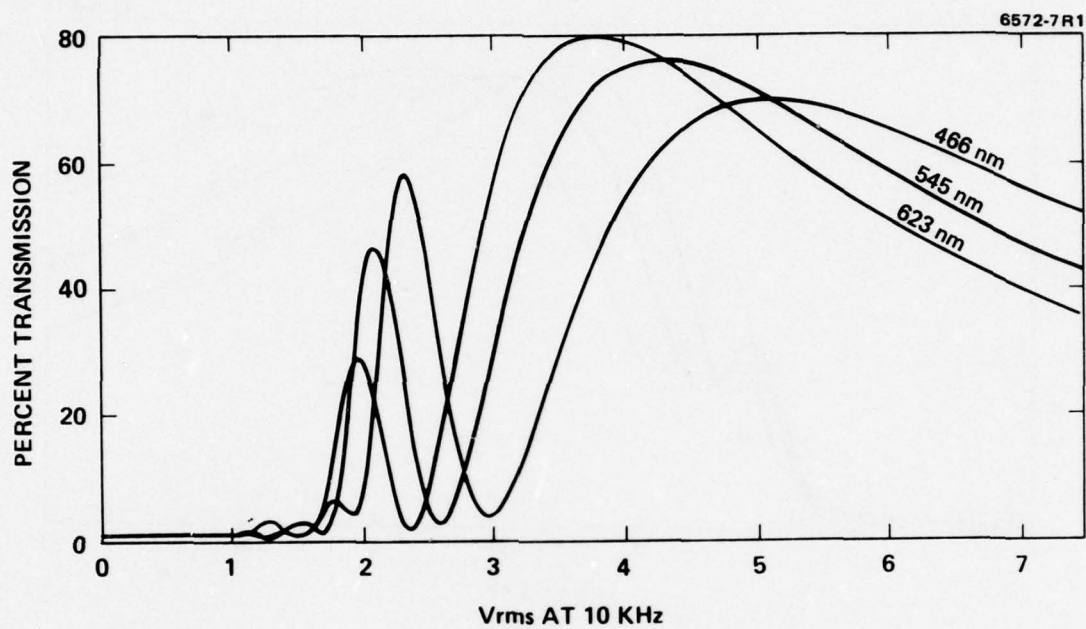
Figure 49. Transmission versus voltage response of a 6.4 μm, 45° twist cell before exposure (cell 2, Table 4).
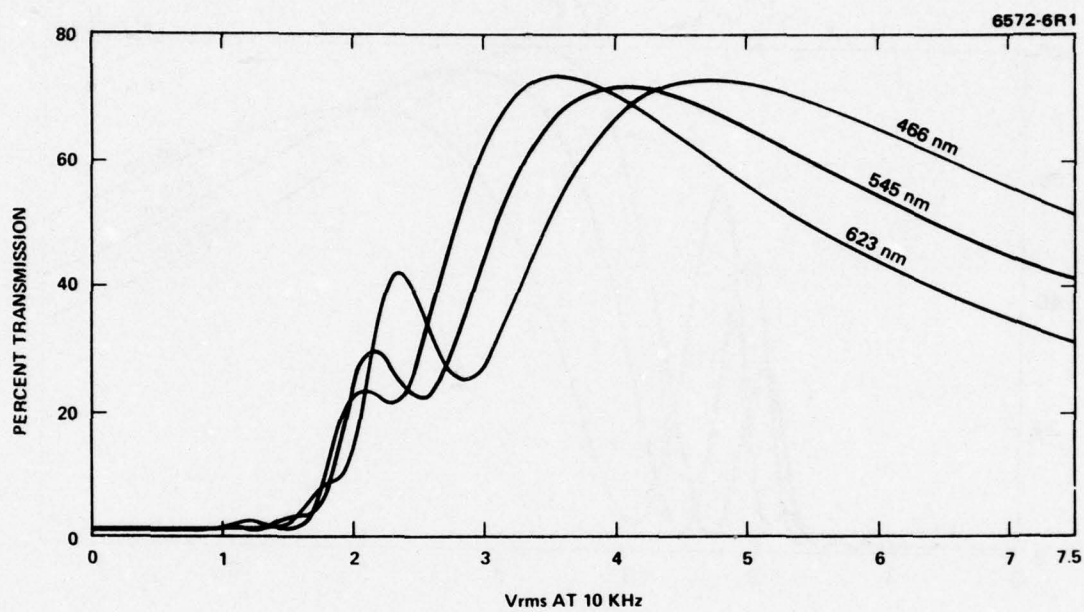
Figure 50. Transmission versus voltage response of 6.4 μm, 45° twist cell at the failure point following exposure (cell 2, Table 4).
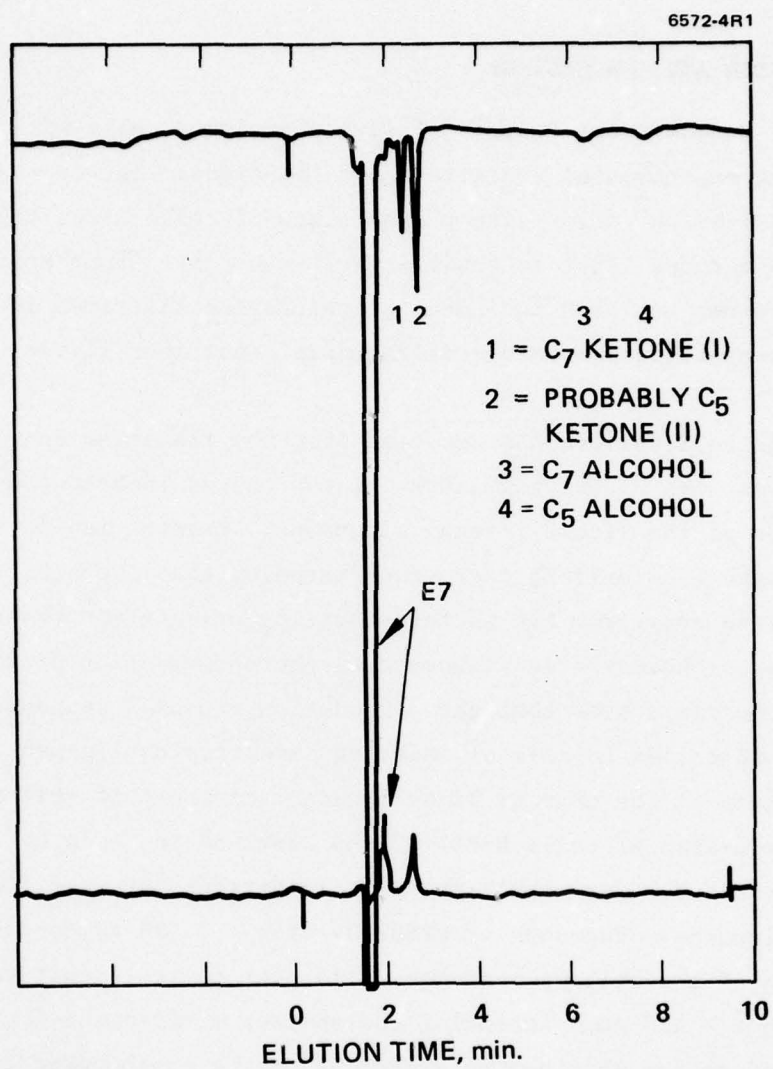
Figure 51. Liquid chromatogram of E7 following cell failure due to photochemical decomposition.

81

filter with 1.1% transmission. Intensities are reported without regard to spectral distribution of the lamp, and it is assumed that the filter is uniform throughout the spectrum of interest.

C. DISCUSSION AND CONCLUSIONS

Table 5 presents the results of five photolyzed cells with their corresponding experimental conditions and lifetimes. The exposure lines expressed as $W\text{-}hr/cm^2$ allow direct comparison of cells since this takes into account varying light intensities for each test. Furthermore, an additional column has been included for calculated lifetimes in a practical LCLV projection system operating under conditions listed for each cell.

Although cell failure was detected from the transmission versus voltage curves, the underlying cause for the change in behavior was a reorientation of the liquid crystal alignment. Examination of the test cells with a polarizing microscope revealed that the nematic director tilted away from the surface-parallel orientation toward the perpendicular or homeotropic alignment as photodegradation progressed. Therefore, one can assume that the degradation produces compounds with surfactant properties capable of inducing homeotropic alignment.

The effect of the near uv light incident on the test cell is shown by comparison of cells H2882-32 and H2882-34 in Table 5. These cells were exposed under nearly the same conditions but at different cutoff wavelengths. Exposure of H2882-34 with $\lambda > 385$ nm decreased the lifetime of the cell by a factor of 13 over the cell that was exposed with $\lambda > 420$ nm. Including the shorter wavelengths increases the amount of energy absorbed by either E7 or its photodegradation products in their absorption tails. A 420-nm filter was selected to eliminate as much of the near uv light as possible while retaining most of the blue region of the visible.

82

Light intensity appears to have a nonlinear effect on cell lifetime. Increasing the intensity during an experiment with cell H2882-50 caused a dramatic decrease in exposure life, relative to that of cell H2882-32, which was illuminated with the same wavelengths but at a lower intensity throughout the lifetime of the cell.

Although the presence of ketone I did not noticeably affect the initial alignment, it significantly decreased the photochemical stability of the alignment. This behavior was demonstrated by lifetime tests on cells using E7 doped with additional I to bring its concentration to 0.37%. The effect of the added ketone was to reduce the useful exposure life to less than half, as can be seen from the results for cells H2882-61 and H2882-32, using $\lambda > 420$ nm. A more drastic reduction in exposure life occurred for cell H2882-60, which contained the added ketone and was irradiated with $\lambda > 360$ nm. The combined effects of higher ketone concentration, shorter wavelengths, and slightly higher intensity reduced the exposure life of this cell to less than 3% of that of H2882-32.

The major photochemical decomposition product of E7 is indicated by peak 2 in the chromatogram shown in Figure 51. It is also present as a contaminant in the starting material (peak D in Figure 46), and it is the major thermal decomposition product of K15. We assume that it is 4-cyano-4'-pentanoylbiphenyl (II), a ketone derived by oxidation of K15 in reactions analogous to those producing I:

7439-9

$$NC-\langle\bigcirc\rangle-\langle\bigcirc\rangle-\underset{\underset{O}{\parallel}}{C}-C_4H_9$$

II
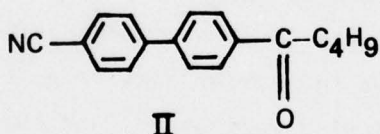
Its presence in the liquid crystal will have deleterious effects similar to those found for I.

We believe that the components of E7 decompose primarily by auto-oxidation, particularly those components that have benzylic hydrogen (K15, K21, and T15). Reactions typical of such auto-oxidations are

shown in Figure 52. Although these equations are written for the photochemical degradation, a similar series of reactions is expected to characterize the thermal degradation as well.

The ketones ($\underset{\sim}{7}$), which have significant light absorption tails at 420 nm, can accelerate the decomposition by entering the mechanism at photosensitizers:

$$\underset{\sim}{7} \xrightarrow{\text{h}\nu} R'-\overset{\overset{\displaystyle O'}{|}}{\underset{\underset{\displaystyle \underset{\sim}{8}}{|}}{C}}-R''$$

$$\underset{\sim}{8} + \underset{\sim}{L} \longrightarrow \underset{\sim}{5b} + \underset{\sim}{2}$$
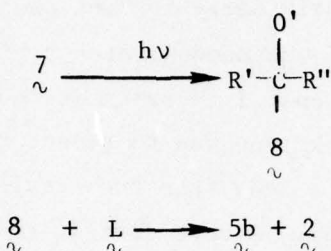
The glycol $\underset{\sim}{9}$ has not yet been detected, but we expect that it will be surface-active and may be involved in reorienting the liquid crystal toward homeotropic alignment. Since $\underset{\sim}{9}$ is formed by a reaction of two radicals, it would be formed at a rate proportional to the square of the light intensity. This can explain the nonlinear relationship between lifetime and light intensity noted above.

Since oxygen-containing species are involved in nearly all of the proposed reactions, alignment stability should be greatly enhanced by eliminating them from the starting material and preventing contact with molecular oxygen, particularly at high temperatures or under intense illumination. Eliminating molecular oxygen without careful purification of the liquid crystal to eliminate ketones could possibly accelerate the realignment, however, since the surface-active glycol 9 is formed from the ketone by a free-radical dimerization, and the dimerization actually may be retarded by molecular oxygen. Further experiments are necessary to clarify the role of oxygen. Filtering the projection light to eliminate more of the short wavelength radiation would undoubtedly increase the lifetime of the light valve even without other measures to promote chemical stability. But the 3000 hr life time with a 420 nm filter in the present systems is an impressive achievement.

84

$$RH \xrightarrow{h\nu} R^\bullet + {}^\bullet H \qquad \text{WHERE } R^\bullet = \text{AN UNSPECIFIED RADICAL}$$

$$R^\bullet + R' - CH_2 R'' \longrightarrow RH + R' - \overset{\bullet}{C}H - R'' \qquad \text{WHERE } R' = NC -\!\!\!\langle \text{biphenyl} \rangle\!\!\!-$$

$$\underset{\underset{\sim}{1}}{} \qquad\qquad \underset{\underset{\sim}{2}}{} \qquad\qquad R'' = C_6 H_{13}; \; C_4 H_9$$

$$\underset{\sim}{2} + O_2 \longrightarrow \overset{\overset{O-O^\bullet}{|}}{R' - CH - R''}$$
$$\underset{\sim}{3}$$

$$\underset{\sim}{3} + \underset{\sim}{1} \longrightarrow \overset{\overset{O-OH}{|}}{R' - CH - R''} + \underset{\sim}{2}$$
$$\underset{\sim}{4}$$

$$\underset{\sim}{4} \longrightarrow \overset{\overset{O^\bullet}{|}}{R' - CH - R''} + {}^\bullet OH$$
$$\underset{\sim}{5a}$$

$$\underset{\sim}{5a} + \underset{\sim}{1} \longrightarrow \overset{\overset{OH}{|}}{R' - CH - R''} + \underset{\sim}{2}$$
$$\underset{\sim}{6}$$

$$\underset{\sim}{6} + R^\bullet \longrightarrow \overset{\overset{OH}{|}}{\underset{\underset{\bullet}{}}{R' - CH - R''}} + RH$$
$$\underset{\sim}{5b}$$

$$5a \text{ OR } 5b \longrightarrow \overset{\overset{O}{\|}}{R' - C - R''} + H^\bullet$$
$$\underset{\sim}{7}$$

$$^\bullet OH + \underset{\sim}{1} \longrightarrow \underset{\sim}{2} + H_2 O$$

$$\underset{\sim}{3} + \underset{\sim}{5b} \longrightarrow \underset{\sim}{4} + 7$$

$$2\,\underset{\sim}{3} \longrightarrow 2\,\underset{\sim}{5a} + O_2$$

$$2\,\underset{\sim}{2} \longrightarrow \overset{}{\underset{\overset{|\quad\;|}{R''\;\;R''}}{R' - CH - CH - R'}}$$
$$\underset{\sim}{8}$$

$$2\,\underset{\sim}{5b} \longrightarrow \overset{\overset{OH\;\;OH}{|\quad\;|}}{\underset{\overset{|\quad\;|}{R''\;\;R''}}{R' - C - C - R'}}$$
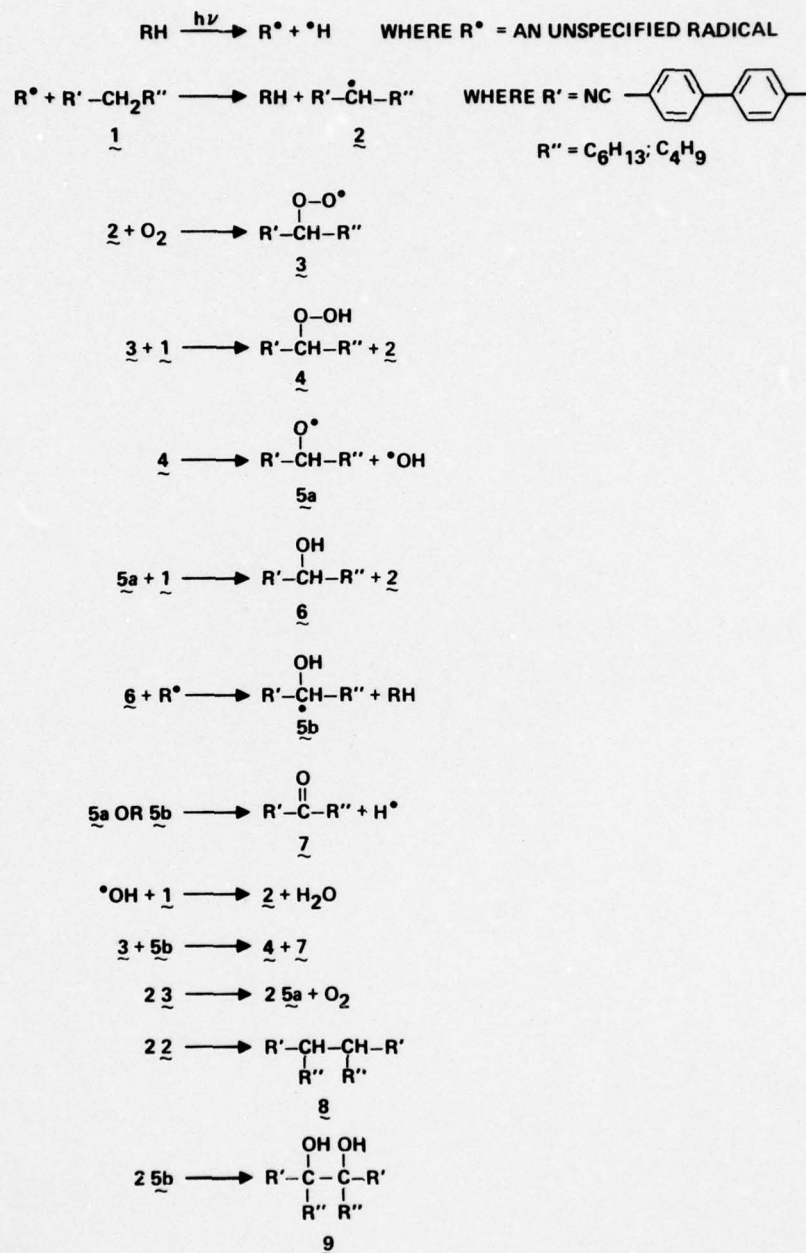$$\underset{\sim}{9}$$

Figure 52. Possible auto-oxidation mechanism of alkyl cyanobiphenyl components of E7.

85

SECTION 5

CdS PHOTOSENSOR DEVELOPMENT

A.   INTRODUCTION

We have identified the following photosensor characteristics where significant improvement is necessary to achieve a practical multi-mode color symbology/monochrome television light valve device:

- Switching ratio and linearity of the gamma transfer characteristics curve

- Photosensitivity and response time

- Device resolution

- Negative memory effects.

In this section, the above characteristics are discussed in more detail.

A higher switching ratio is required to reduce the project symbol edge width found in present light valves. The principal cause of this edge effect is the nonlinear nature of the CdS photosensor response. The CdS response is proportionately greater at low imaging light levels. Thus the edge intensity of the Gaussian-shaped CRT spot used to write the imput image is amplified by the photosensor. This causes the liquid crystal to be driven above the threshold at the edge of a symbol creating a symbol border consisting of the lower order liquid crystal color peaks. The optimum solution to this problem is to linearize the CdS photosensor response. This can be achieved by increasing the available switching ratio of the film so that a smaller region of the curve can be used to drive the liquid crystal through the required voltage range. The repsonse over the smaller region will be more linear and a significant improvement in the magnitude of edge effect will result. This has been discussed in more detail in the Final Technical Report, Contract N00024-75-C-7187, p. 17.

Two approaches to achieving a higher switching ratio in the photosensor film were pursued. The first approach consisted of a three layer, graded bandgap composite structure of CdZnS, CdS, and CdSSe

87

films deposited sequentially. However, the composite photosensor had the following problems:

- The chemo-mechanical polishing process developed for CdS was not suitable for the CdSSe film used in the composite photosensor

- Extremely slow response times were observed

- The thick films necessary for high switching ratio showed image granularity

- The complex processing necessary lowered the run-to-run reproducibility.

The second approach to achieving a higher switching ratio was to use a thick layer of CdS. This approach was attractive because the ac capacitance of the CdS layer determines the dark impedance and thus the ultimate switching ratio. In addition, Hughes has developed considerable experience in fabricating thin CdS layers for monochrome television light valve devices. There were, however, specific problems associated with thick CdS layers. The main problem was that although thick CdS films exhibit higher switching ratios, device resolution is significantly reduced. This results from the conditions in the rf diode sputtering process, which cause the film to grow as tapered crystallites (inverted cones) from a limited number of nuclei at the ITO-CdS interface. The film structure contained significant longitudinal porosity because of the low atom mobility at the growing film surface. The net result was that the crystallite diameter increased with film thickness, thereby limiting device resolution for thick, high switching ratio CdS films.

To solve this problem we have increased the film nucleation density and adatom mobility so that true columnar structure is obtained without the lateral crystallite growth that limits device resolution. We were able to achieve this by increasing the kinetic energy of the arriving species to the substrate and enhancing the surface diffusion. In preliminary experiments, we have inhibited the growth of the crystallites in the thick films by using a combination of high deposition

rates and enhanced film ion bombardment. The results of this investigation are presented in the next section.

B.   RESULTS

Scanning electron microscopy (SEM) is a useful tool in studying the surface morphology and cross-sectional structure of CdS films. Figure 53 shows a typical SEM micrograph of thin CdS film (15 µm) deposited under normal conditions before the present program began. The film grows as tapered crystallites, where crystallite diameter increases rapidly with film thickness. For a thick film (50 µm), this mode of film growth reduces device resolution to an unacceptable level. Therefore, to be useful, thick CdS films must be produced in a manner that inhibits lateral crystallite growth.

Figure 54 shows a SEM micrograph of typical surface morphology and cross-sectional structure of thick CdS film produced under new conditions. The film consists of vertical columnar crystallites that are densely packed and show very little lateral growth. This feature allows us to fabricate the thick layers of CdS required for high switching ratio and, simultaneously, to maintain good device resolution.

In addition to high switching ratio and good resolution, the CdS photosensor film required for a multimode light valve device must also have fast response time characteristics. Table 7 lists a few typical examples of CdS film characteristics obtained in recent experimental runs. We generally observe the following:

- Higher film thickness results in a higher switching ratio. The relationship may not be linear beyond a certain film thickness when only moderate gain in switching ratio is obtained.

- Films with higher photosensitivity give higher switching ratios but tend to give slower response times. On the other hand, certain processing techniques (e.g. nitrogen doping) that result in fast response time characteristics give lower photosensitivity and switching ratio.

89

Figure 53. Typical SEM micrograph of tapered crystallite
cross-sectional microstructure of CdS films.
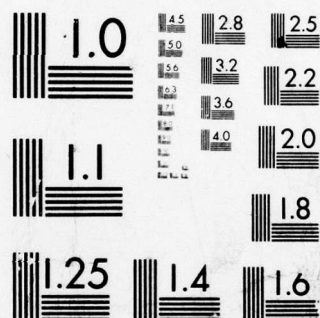
MICROCOPY RESOLUTION TEST CHART

NATIONAL BUREAU OF STANDARDS-1963-A

Table 7. Typical Characteristics of
Improved CdS Films

| CdS Film Specimen No.	Film Thickness, μm	Switching Ratio at 100 μW/cm^2 Input Light Intensity	Response Time at 100 μW/cm^2 Input Light, msec	
			Rise	Decay
12577	55	5.4	30	150
12677	45	4.2	30	100
121277	35	2.5	20	20
10677	50	4.0	20	50

T6101

Since multimode operation requires both color symbology and monochrome television capability, it is apparent that both high switching ratio and TV rate response time must be obtained in the CdS photosensor film. Although we have demonstrated high switching ratio and TV rate response time in two different types of CdS films, combining these in one film remains a challenging task. The next section summarizes the remaining problems to be addressed to optimize photosensor performance for a true multimode light valve operation.

C.   REMAINING PROBLEMS

- The main problem, as mentioned before, is to optimize the process parameters such that both high switching ratio and fast response time are obtained in the same CdS film. At present, we are able to obtain either high switching ratio or fast response time but not both.

- Another problem is related to the high deposition rates required to inhibit tapered crystallite formation in thick CdS films. High deposition rates give rise to nodule growth in thick films due to source particle incorporation (see Figure 55). These modules may form visible defects in the final image on the screen. Further process optimization is needed to eliminate nodule growth in thick CdS films.

- Post-processing degradation of CdS caused by polishing and the subsequent thin films deposition (CdTe, dielectric

92

├─┤ 10 μm
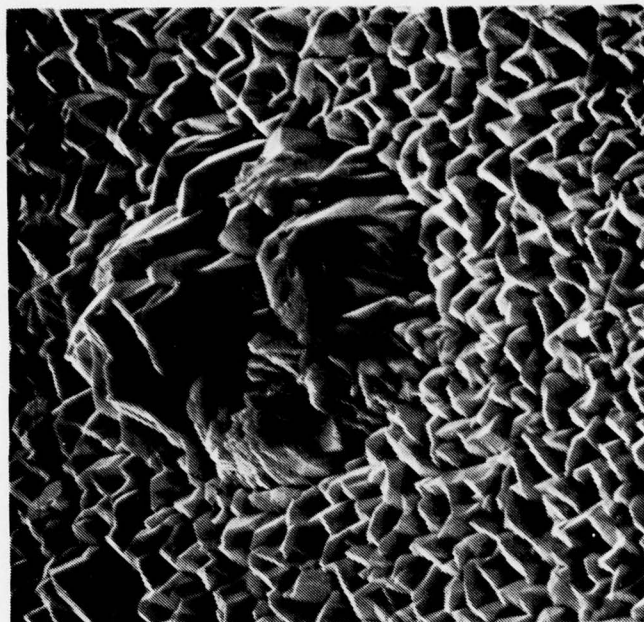
├─┤ 50 μm

Figure 55. Typical module defects in thick CdS films.

93

mirror) must be investigated to ensure good performance at the completion of the device.

- We have observed that thick CdS films necessary for high switching ratio show negative memory effects. Further photosensor development work is required to eliminate the negative memory in thick CdS films.

Table 8. Response Times of Final LCLV Devices

Color	Input Imaging Light Power, $\mu W/cm^2$		Response Time, msec			
			(a)		(b)	
	(a)	(b)	Rise*	Decay**	Rise	Decay
Magenta	89	150	110	400	200	350
Blue	25	88	200	400	250	350
Green	17	50	250	400	300	350
Red	5	10	400	400	400	400

*0 to 90%

**100 to 10%

T6101

The voltage transmission curves for both cells (a and b) are shown in Figures 56 and 57 with the substrates illuminated with light of saturation intensity. The operating voltage indicated on the figures is that required to bias the cell to the transmission null in the absence of input illumination.

B. LCLV H4053

Cell Specification

Cell designation:	H4053, S/N 10101
Liquid crystal:	BDH biphenyl nematic E7
Liquid crystal alignment:	45° twisted nematic
Aperture size:	2 in. diameter
Input image peak: (photosensitivity)	525 nm (P-1 Phosphor)
Operating voltage range:	<20 V_{rms}
Operating frequency range:	20 kHz

Measured Performance

Operating conditions:	15.7 V_{rms} at 2 kHz (O.E. tab at 8 o'clock)
Sensitivity:	Maximum extinction at 120 $\mu W/cm^2$. Full on at 10 $\mu W/cm^2$ at operating conditions.
Contrast ratio:	11:1
Limiting resolution:	45 lines/mm at 100 $\mu W/cm^2$

Time response at 100 $\mu m/cm^2$

Rise (to 90% of max.)	10 ms
Decay (to 10% of max.)	20 ms

Cell Construction

Substrate:	Sputtered CdS with SiO_2/TiO_2 sputtered mirror.
Cell design:	Sealed

The voltage-transmission curves of the multimode light valve are shown in Figure 58. The region of back slope operation is approximately between 8 and 16 V.
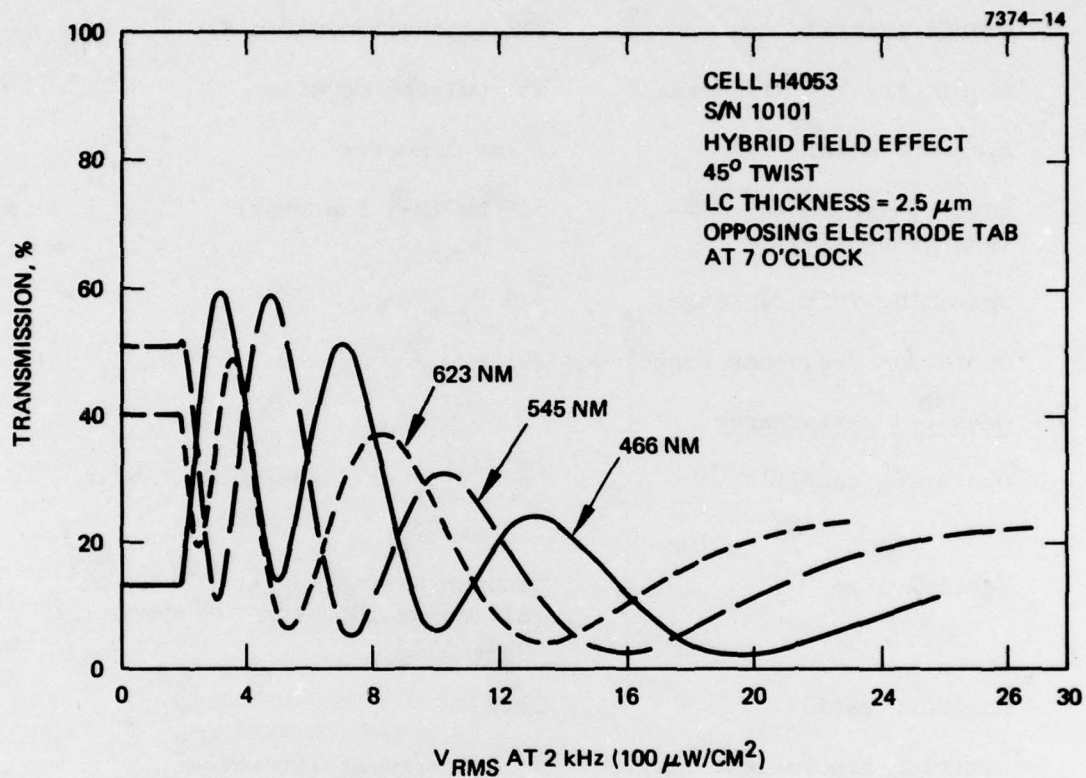
Figure 58. Voltage-transmission curves for LCLV H 4053.

100

SECTION 7

RECAPITULATION AND CONCLUSIONS

In summary, during this phase of the program, stable, long-lifetime high-valve operation was achieved and an improved CdS photoconductor was demonstrated. Improved color-symbology light valves were fabricated and delivered for the Navy's evaluation, and a promising multimode liquid-crystal effect was invented. In spite of these achievements, additional development is required. The multimode operation demands a further increase in the photoconductor switching ratio. To minimize the outline effect, photoconductor linearity should be improved, and, to achieve good TV display, the response time should be reduced and the image retention effect eliminated.

In the liquid-crystal area, the back slope operation should be evaluated for the multimode light valve and, if it is good, should be developed. If it is not, the present approach should be optimized.

REFERENCES

1. A.D. Jacobson and W.P. Bleha, "Development of a Color Symbology AC Liquid Crystal Light Valve," Final Technical Report, Contract N00024-75-C-7187, April 1977.

2. A.D. Jacobson, "Development of a Reflective Mode Liquid Crystal Light Valve," Final Technical Report, Contract N00024-73-C-1185, May 1975.

3. J. Grinberg and A.D. Jacobson, J. Opt. Soc. Am. <u>66</u>, 1003 (1976).

4. G.W. Gray, K.J. Harrison, J.A. Nash, J. Constant, D.S. Hulme, J. Kirton, and E.P. Raynes, <u>Liquid Crystals and Ordered Fluids</u>, Vol. 2, J.F. Johnson and R.S. Porter, eds. (Plenun Press. New York, 1973), p. 617.